Miniaturizable Ion-Selective Electrode System: Solid Contact Electrode and Liquid Junction Free Reference Electrode

A DISSERTATION

SUBMITTED TO THE FACULTY OF THE GRADUATE SCHOOL

OF THE UNIVERSITY OF MINNESOTA BY

Xu Zou

IN PARTIAL FULFILLMENT OF THE REQUIREMENTS

FOR THE DEGREE OF

DOCTOR OF PHILOSOPHY

Philippe Bühlmann, Adviser

May, 2014

© Xu Zou 2014

Acknowledgement

I would like to thank the following people for their contributions to the work described in this thesis and throughout graduate school:

I would express my sincere gratitude to my adviser Dr. Philippe Bühlmann. His passion for science and broad knowledge base have been truly helpful for my research progress. His continuous guidance, support and encouragement has turned my graduate school experience into a wonderful journey and assisted both my professional and personal development.

Dr. Li Chen and Dr. Chunze Lai for helping me get started my research and special acknowledgement for Li's contribution to cyanide-selective electrode.

Dr Wenjie Lan who was a collaborator in paper-based ion sensing project.

Jia H. Cheong and Brandon Taitt who were undergraduate researchers I worked with, for their contribution to developing solid contact ion-selective electrodes.

Koichi Nishimura for his work on cyanide-selective electrode and Shogo Ogawara for his contribution on FAB based electrode.

Prof. Steve Kass and Dr. Evgeny Beletskiy for synthesizing and supplying compounds as chloride and phosphate ionophores, and for their help during the collaborations.

The members of the Bühlmann group for their friendship, support, discussion, and for making this group a great place to work at.

Prof. Pete Carr, Prof. Edgar Arriaga, Prof. Aaron Massari, Prof. William Smyrl and Prof. Philippe Bühlmann for being a part of my preliminary exams committee and thesis defense committee and/or reviewing this thesis, and their advice and help in my graduate studies.

Special thanks for the support and encouragement from my family and friends.

Dedication

To

Aaron David Humble

Abstract

Ion-selective electrodes are widely used as important analytical tools to determine the concentration of a wide range of ions for clinical, environmental, and chemical process analysis. Conventional ion-selective electrodes have an interior solution that forms a liquid contact with the selective membrane. However, complications due to evaporation and freezing in certain circumstances lead to irreproducibility and instability of the signals and shortened life expectancy. In addition, miniaturization is an obstacle for this type of electrodes since a liquid reservoir is always required. Solid contact ion-selective electrodes emerged in order to meet all the requirements that conventional electrodes could not fulfill. They are superior as they do not require maintenance, are durable and contains the potential for miniaturization for portable and implantable devices. They replace the conventional interior solution with a solid conducting material as a transduction layer, which provides electron transfer instead of ions as charger carriers at the interface.

For an electrochemical sensor like an ion-selective electrode system, the working electrode generates signals based on sample components. Another critical part is the reference electrode, which must maintain a constant potential over long periods of continuous measurements. The vast majority of all electro-analytical measurements are performed with reference electrodes separated from samples by salt bridges. Unfortunately, salt bridges have several disadvantages. Used in real life samples, they clog with proteins and lipids, suffer from contamination by sample components, and because there are large ion fluxes from the electrode into samples, they can considerably contaminate small volume samples. In a routine laboratory setting, such problems can be

counteracted by frequent flushing of reference electrodes with cleaning solutions, free flowing liquid junctions, and regular replenishing of salt bridge solutions. These options are cumbersome enough in a laboratory setting, and they are also very difficult to implement in many real life scenarios, such as in intensive care units at hospitals or at remote environmental monitoring stations.

My work involves developing a universal method for a solid contact electrode that is calibration-free, durable, reproducible, and inexpensive to fabricate. One of the most critical things for a solid contact electrode is the transducer layer between the gold or carbon substrate and an ion-selective membrane because it needs to reliably provide stable and reproducible interfacial potentials. This potential is determined by the redox components of this layer, which can be compared to a pH buffer solution. The pH of a buffer solution will be stable despite a slight change of the components in the solution. Similarly, a redox buffer can stabilize interfacial potentials with a redox couple doped into a polymer layer. This layer serves as both a conducting layer and resistive layer to the slight changes within the membrane. A poly(vinylchloride) plasticized with nitrophenyl octyl ether doped with cobalt(2+)tris(1,10-phenanthroline) tetrakispentafluorophenylborate and cobalt(3+)tris(1,10-phenanthroline) tetrakispentafluorophenylborate has been developed as a transducer layer. This layer has shown very reproducible potential in potassium chloride solutions with a potential of standard deviation of 0.5 mV and response slope of 61mV / decade to varying concentrations which is consistent with theoretical value. A redox buffer platform based on the more lipophilic redox buffer consisting of the Co(III) and Co(II) complexes of 4,4'-dinonyl-2,2'-bipyridyl was developed and applied to K^+, Na^+, Ca_2^+, H^+, and CO_3^{2-}

with emf values of an electrode-to-electrode standard deviation as low as 0.7 mV (2% error in concentration)

As for reference electrodes, we are able to successfully eliminate the liquid junction, which greatly contributes to the shortened life and instability of signals. A new method of operating reference electrodes with hydrophobic ion-doped polymeric membranes has been developed. It involves the application of a current pulse to a hydrophobic ion-doped membrane, thereby controlling transmembrane ion fluxes to obtain a sample independent reference electrode potential. The potential of the membrane will be determined by the ions released from the membrane by the current. It is the external current that controls the constant potential. Thus, if the same current is applied to the membrane every time, a constant potential independent of the sample should be obtained. The concept has been proven with a simple poly(vinylchloride) plasticized with nitrophenyl octyl ether doped with tetrabutylammonium tetrakis(4-chlorophenylborate). Tetrabutylammoniums are released to the interface, which determine the potential of the membrane that is independent of the sample. The concentration of the ions released into the sample depends on the current amplitude and length and can be explained quantitatively by the diffusion theory. The good stability of the potential exhibited in this study by reference electrodes exposed to serum is particularly promising in view of biological and medical applications that require long term monitoring. This operating mechanism is not limited to ion exchanger membranes and may be applied to ionophore doped membranes. This suggests a high level of flexibility in the design of reference electrodes optimized for specific applications.

Table of Contents

List of Tables

List of Figures

CHAPTER ONE

CHAPTER TWO

CHAPTER THREE

CHAPTER FOUR

CHAPTER FIVE

CHAPTER SIX

CHAPTER SEVEN

CHAPTER EIGHT

List of Symbols and Abbreviations

a	activity
Baytron P or PEDOT/PSS	poly(3,4-ethylenedioxythiophene) and poly(styrenesulfonate)
C_9,C_9-bipy	4,4'-dinonyl-2,2'-bipyridyl
([C_8mim^+][C1C1N^-])	1-methyl-3-octylimidazolium bis(trifluoromethylsulfonyl)imid
CN^-	cyanide
CP	conducting polymer
CV	cyclic voltammograms
DOS	dioctyl sebacate
Econst	sum of all constant potentials
EC	electronic conductor
EMF/emf	electromotive force
ESI	electron spray ionization
ETH500	tetradodecylammonium tetrakis(4-chlorophenyl)borate
EPB	phase boundary potential
F	faraday constant
FeCN	hexacyanoferrate(II)
FIM	fixed interference method

GC	glass carbon
i	current,
I^{z-}	primary ion
IL	ionic liquid
ISE	ion-selective electrode
ISM	ion-selective membrane
J^{-}	interference ion
K	association constant
K_{IJ}	equilibrium constant for the exchange of I and J between the membrane and the sample phase
KTpClPB	potassium tetrakis[4-chlorophenyl]borate
$K_{I,J}^{\text{pot}}$	potentiometric selectivity coefficient for ion I over ion J
LiOAc	lithium acetate
MMA/DMA	poly(methyl methacrylate)/poly(decyl methacrylate)
MWCNT	multiwalled carbon nanotube
o-NPOE	o-nitrophenyl octyl ether
OCP	open circuit potential
PCA	principle component analysis
PEDOT	poly(3,4-ethylenedioxythiophene
phen	1,10-phenanthroline

PPy	poly(pyrrole)
PSS	poly(styrenesulfonate)
POT	poly(3-octylthiophene)
PVC	poly(vinyl chloride)
R	the molar gas constant or resistance
SAM	self-assembled monolayer
SHE	standard hydrogen electrode
SSM	separate solution method
SWCNT	single wall carbon nanotube
S-PG	screen-printed graphite layer
T	temperature
Tg	glass transition temperature
TBA	tetrabutylammonium
TmClPB	tetrakis(3-chlorophenyl)borate
TDDMACl	tridodecylmethylammonium chloride
THF	tetrahydrofuran
TPFPB	tetrakis(pentafluorophenyl)borate
UV-visible	ultra violet-visible
z	charge
3DOM carbon	three-dimensionally ordered macroporous carbon

Publications

Selected publications most relevant to this dissertation:
Current Pulse Based Reference Electrodes Without Liquid Junctions **Xu U. Zou** and Philippe Bühlmann. *Analytical Chemistry* **2013**, 127(25), 8958-8959

Solid Contact Ion-Selective Electrodes With a Well- Controlled Co(II)/Co(III) Redox Buffer Layer **Xu U. Zou**, Jia H. Cheong, Brandon J. Taitt, and Philippe Bühlmann. *Analytical Chemistry* **2013**, 85(19), 9350-9355.

Calibration Free Ionophore Based Solid Contact Ion-Selective Electrodes With a Co(II)/Co(III) Redox Couple **Xu U. Zou**, Xue Zhen, Jia H. Cheong and Philippe Bühlmann Manuscript in preparation

Ionic Liquid Reference Electrodes With a Well- Controlled Co(II)/Co(III) Redox Buffer as Solid Contacts **Xu U. Zou**,[§] Li D. Chen[§] Chun-Ze Lai, [§] and Philippe Bühlmann Manuscript in preparation § These authors contributed equally to this work.

Use of an Electrically Neutral Axial Ligand to Improve the Selectivity of a Cyanide-Selective Electrode, Koichi Nishimura, **Xu U. Zou** and Philippe Bühlmann manuscript in preparation

Additional publications for graduate works:
Cyanide-selective electrode based on Zn(II) tetraphenylporphyrin as ionophore Li D Chen, **Xu U. Zou**, Philippe Buhlmann, *Analytical Chemistry* **2012**, 84, 9192–9198

Ion-Selective Electrodes with Colloid-Imprinted Mesoporous Carbon as Solid Contact, Jinbo Hu, **Xu U. Zou**, Andreas Stein and Philippe Bühlmann Submitted

Paper-based potentiometric ion sensing Wen-Jie Lan, **Xu U. Zou**, Mahiar Hamedia, Jinbo Hu, E. Jane Maxwell, Philippe Bühlmann, and George M. Whitesides Manuscript in preparation

Paper-based reference electrode and potentiometric ion sensing Wen-Jie Lan, **Xu U. Zou**, Mahiar Hamedia, Jinbo Hu, E. Jane Maxwell, Philippe Bühlmannb, and George M. Whitesides U.S. Provisional Patent Application, 2014

CHAPTER ONE

Introduction

1.1 Chapter Overview

In this chapter, the background of this thesis is presented, following a discussion of the underlying theory. Since the majority of the work discusses ion-selective electrode systems, this chapter begins with an introduction to ion-selective electrodes and their fundamentals (1.2). Ion-selective electrode system consists of two major parts: a working electrode and a reference electrode. To meet the goal of miniaturization, Chapter 1.3 introduces the basic concepts and the current state of the art of solid contact ion-selective electrodes. Chapter 1.4 addresses reference electrodes, summarizing their history and requirements. Chapter 1.5 briefly addresses the advancement of calibration-free ion-selective electrodes.

The contents of this chapter do not cover a complete introduction of all the topics discussed in this thesis. In each of the following chapters, a more detailed background specifically addressing each project is provided.

1.2 Ion-Selective Electrode

1.2.1 Background and Theory

An ISE is a potentiometric sensor that responds to the activity of ions in a sample solution. The set-up usually consists of an ISE, a potentiometer and an external reference electrode (Figure 1).

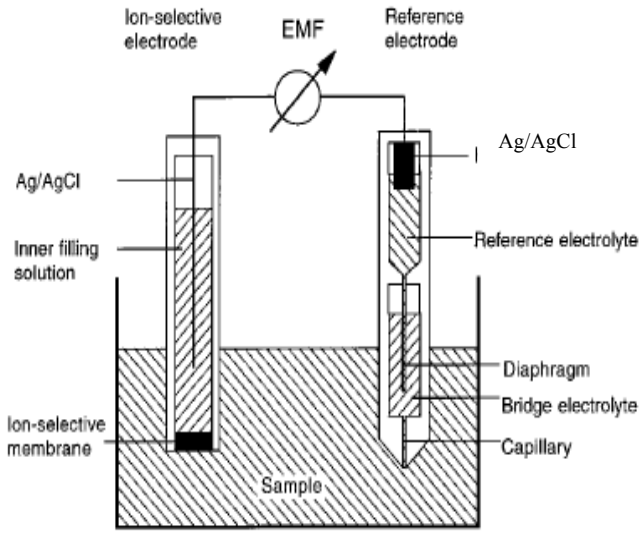

Figure 1. Diagram of a typical experiment setup with ion-selective electrode[1]

The potential across the cell can be depicted as follows:

Ag |AgCl | inner filling solution | membrane | sample | salt bridge | KCl (satd) | AgCl | Ag

E_5 E_4 E_M E_J E_3 E_2 E_1

ion-selective membrane electrode reference electrode system

The electromotive force (*emf*) across the cell is a combination of potentials at all interfaces and can be measured by the potentiometer. It can be described as[1]

$$emf = (E_1 + E_2 + E_3 + E_4 + E_5) + E_M + E_J = E_{const} + E_M + E_J \quad (1)$$

E_1 to E_5 are all sample independent so they together can be replaced by E_{const}. The *emf* is only determined by the membrane potential (E_M) and the liquid junction potential at the interface between the salt bridge and the sample (E_J). E_J can be kept small or constant by using concentrated electrolyte solutions with cations and anions of similar mobilities or estimated by the Henderson equation.[2] Hence, E_M is the main contribution to the *emf* change due to samples and can be divided into three parts: the phase boundary potential at the sample/membrane interface, the diffusion potential within the membrane and the phase boundary potential at the membrane/inner filling solution interface. Usually, the phase boundary potential at the membrane/inner filling solution interface can be seen as independent of the sample solution and the diffusion potential is zero if there is no concentration gradient within the membrane. In sum, the potential can be described by the following equation

$$E_M = E_{const} + E_{PB} \quad (2)$$

where E_{PB} is the phase boundary potential at the sample/membrane interface which can be derived from basic thermodynamic theory. The electrochemical potential of ion I ($\mu_I'(aq)$) is

$$\mu_I'(aq) = \mu_I(aq) + z_I F\phi(aq) \quad (3)$$

where z_I is the charge of the ion of interest, $\phi(aq)$ is the electrical potential, F is Faraday constant and $\mu_I(aq)$ is the chemical potential of ion I in the aqueous phase. $\mu_I(aq)$ can be written as

$$\mu_I(aq) = \mu_I^{\,0}(aq) + RT\ln a_I(aq) \tag{4}$$

where R is the gas constant, T is the absolute temperature, $\mu_I^{\,0}$ is the standard state chemical potential, and a_I is the activity of the ion I in the aqueous phase. Insertion of eq (4) into eq (3) gives the electrochemical potential of the ion I in the aqueous phase:

$$\mu_I'(aq) = \mu_I^{\,0}(aq) + RT\ln a_I(aq) + z_I F\phi(aq) \tag{5}$$

Similarly, the electrochemical potential in the membrane phase of ion I is

$$\mu_I'(org) = \mu_I^{\,0}(org) + RT\ln a_I(org) + z_I F\phi(org) \tag{6}$$

Since $\mu_I'(aq)$ and $\mu_I'(org)$ are equal at equilibrium, the electrical potential difference between two phases can be calculated as:

$$E_{PB} = \phi(org) - \phi(aq) = -\frac{\mu_I^{\,0}(org) - \mu_I^{\,0}(aq)}{z_I F} + \frac{RT}{z_I F}\ln\frac{a_I(aq)}{a_I(org)} \tag{7}$$

Insertion of equation (7) into (2) gives

$$E_M = E_{const} - \frac{\mu_I^{\,0}(org) - \mu_I^{\,0}(aq)}{z_I F} + \frac{RT}{z_I F}\ln\frac{a_I(aq)}{a_I(org)} \tag{8}$$

Under the condition that all the sample independent potentials go into E^0 and the activity of ion I in organic phase stays constant, equation (8) can be simplified to

$$E_M = E^0 + \frac{RT}{zF}\ln a_I(aq) = E^0 + 2.303\frac{RT}{zF}\log a_I(aq) \tag{9}$$

This is called the Nernst equation. For example, at room temperature (T= 298K), for an ion of +1 charge, a change in *emf* with a slope of 59.16 mV will be observed per 10-fold change in the activity of ion I^+ in the sample solution.

1.2.2 Components of ISE Membranes

The key component of an ISE is a sensing membrane that mainly consists of four components: polymer support, plasticizer, ionic site, and lipophilic receptor (ionophore).[1]

The polymer matrix acts as a supporter for the membrane, providing the necessary physical properties like mechanical stability. A key factor for the choice of a polymer is its glass transition temperature (T_g), which should be below the sample temperature so that the membrane permits ionic species to be mobile enough to allow sufficient ionic conductivity for measurements, diffusion of membrane components and mechanical properties for routine industrial processes. As a result of its stability, the most widely used polymer is poly(vinyl chloride) (PVC). Unfortunately, PVC has a glass transition temperature of 80 $^{\circ}$C and therefore must be plasticized.

The plasticizers embed themselves between the chains of polymers, keeping them apart, thus lowering the T_g of the membrane, reducing the viscosity, increasing the mobility of the ions in the membrane, and decreasing the resistance. They can also contribute to the selectivity of the membrane due to their polarity. The plasticizer takes up most of the remaining mass of the membrane and must fit specific criteria. It must be physically compatible with the polymer in order to give a homogeneous organic phase and dissolve all the components. In addition, it should have a high boiling point to avoid evaporation.

The ionic site provides the membrane with the capability of ion exchange while decreasing the resistance. In the case of an ionophore-free membrane or a membrane doped with an electrically neutral ionophore, the ionic sites act as the counter ions of the primary ions in the membrane, which guarantee the perm-selectivity and prevent counter

ions from the bulk solution from entering the membrane. Moreover, the ionic site can optimize the membrane selectivity when chosen in an ideal the molar ratio of the ionic site and the ionophore complex.[3]

Lipophilic receptors, also known as ionophores determine the selectivity of an ISE. Ideally, ionophores need to be lipophilic to be able to dissolve in the plasticized polymer matrix and must strongly but reversibly bind with the ions of interest. An ISE exhibits selectivity because ionophores have a much larger free energy of complexation with the primary ion than the interfering ion.

1.2.3 Selectivity

Selectivity is one of the most important parameters to consider when designing sensors. In the case of ISEs, the selectivity describes the membrane's preference for the primary ions over the interfering ions. Two main factors contribute to the selectivity. One is the difference in solvation energy between the aqueous phase (sample solution) and the organic phase (membrane). This so-called single ion distribution coefficient can be formulated as $k_I = \exp\left(-\left\{\mu_I{}^0(org) - \mu_I{}^0(aq)\right\}/RT\right)$. Ions that have larger k_I values are more favored in the transfer process and thus enter the sensing membrane more readily. For example, the selectivity sequence of an ionophore-free cation-exchange electrode is $Cs^+ > Rb^+ > K^+ > Na^+ > Li^+$, which follows the Hofmeister series.[2] With ionophores in the membrane, the selectivity sequence will favor the ions having stronger binding strength with the ionophore and change the selectivity sequence (Figure 2).

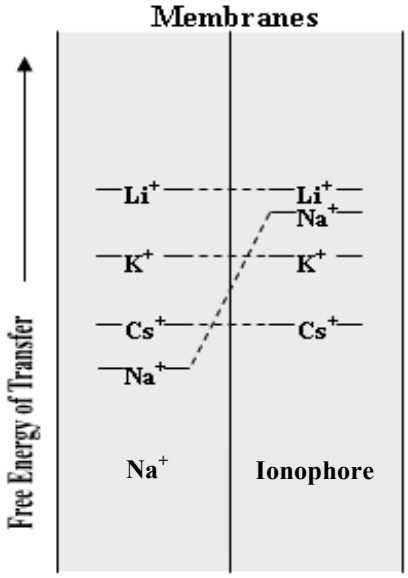

Figure 2. Depiction of the difference in free energy of transfer for monocations of a Na^+ ionophore–doped membrane and an ionophore-free membrane[2]

The selectivity is quantified by the selectivity coefficient, which can be solved by the semi-empirical Nicolsky-Eisenman equation:

$$E = E^0 + \frac{RT}{z_I F}\ln(a_I(IJ) + K_{I,J}^{pot} a_J(IJ)^{z_I/z_J}) \tag{10}$$

where $a_I(IJ)$ and $a_J(IJ)$ are activities of the ions I and J in a mixed solution.

This equation is now known inaccurate for ions with different charges. A more accurate definition of K_{IJ}^{POT} is

$$K_{IJ}^{POT} = \exp[\frac{(E_J^0 - E_I^0)z_I F}{RT}] \tag{11}$$

assuming that both primary ions and interfering ions have the same activities of 1 M, E^0 is the potential calculated by extrapolating the calibration curve to 1 M activity. Two ways are employed to assess selectivity coefficient. One is separate solution method (SSM) where calibration curves for ion I and ion J are measured respectively and E_J^0

and E_I^0 can be calculated by extrapolation of the calibration curve to 1 M activity. The selectivity can be obtained based on Equation 11. The other method is the fixed interference method (FIM) where the calibration curve for the primary ion I is obtained with a background of interfering ions J with constant concentration. The ISE responds to ion I at high primary ion concentrations but responds to ion J at low primary ion concentrations. $K_{I,J}^{pot}$ can be determined by

$$K_{I,J}^{pot} = a_I(DL)/a_J(BG)^{z_I/z_J} \qquad (12)$$

where a_I(DL) is the primary ion activity at the detection limit, and a_J(BG) is the interfering ion activity in the background.(Figure 3). Selectivities as determined by the SSM and FIM are theoretically numerically identical.

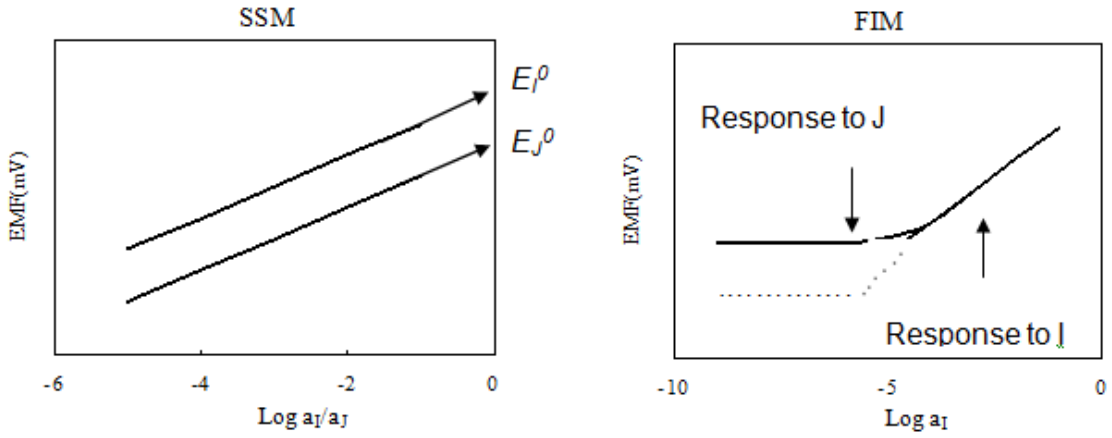

Figure 3. Representation of the separate solution method (SSM) and fixed interference method (FIM) under ideal condition.

1.3 Solid Contact Ion-Selective Electrode

The miniaturization of ion-selective electrode has drawn considerable interest in view of implantable devices, measurements in small volumes, and mass production. However, the internal electrolyte of conventional ISEs impedes miniaturization because of the difficulties of minimizing and stabilizing the volume and shape of the inner filling solution.[4-5] Consequently, solid contact electrodes with an ion-selective membrane directly attached onto a solid substrate have attracted considerable interest as a new generation of potentiometric ion sensors due to its obvious advantages: absence of a need for maintenance, robustness, cost-effective production and potential for miniaturization.[5-9]

1.3.1 Theory

A traditional ion-selective electrode contains an inner filling solution, which is in direct contact with the internal reference, such as Ag/AgCl. The measured potential is the sum of the potentials at all the interfaces. One important interface is the one between the inner filing solution and the membrane whose charge carrier is the ion common in both phases. In solid contact ion-selective electrodes the liquid reservoir is replaced with a solid substrate, with the electron carrying charge across the membrane/substrate interface (Figure 4).

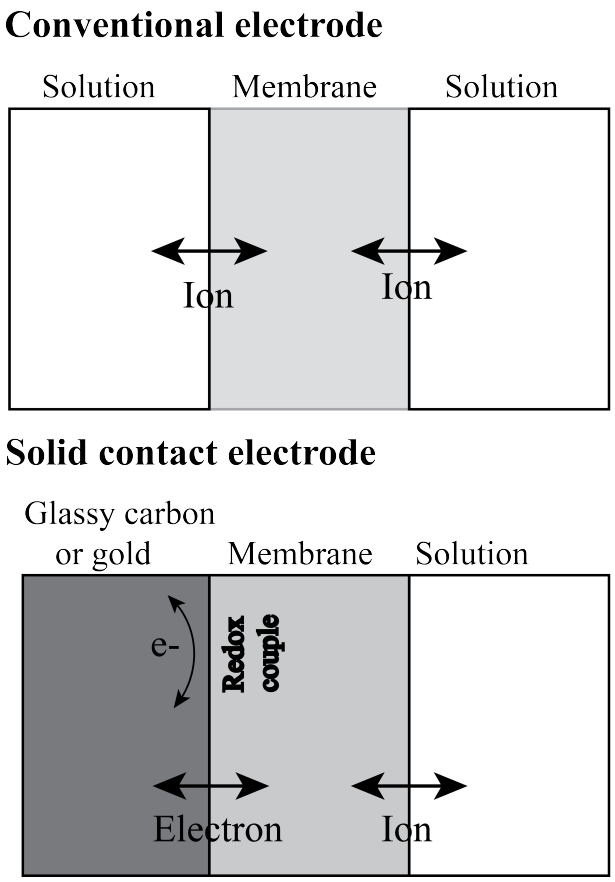

Figure 4. Configuration of solution/membrane/solution interfaces for conventional electrode and substrate/membrane/solution interfaces for solid contact electrode

As a conventional electrode has a well-defined inner filling solution/membrane interface, it should have a reliable and stable potential reading. However, evaporation of water in the inner filling solution causes changes of the concentration of the relevant ions, which affects the potential stability. Although the liquid reservoir could be miniaturized, the miniaturizability is limited due to the liquid and it could also exacerbate the potential instability since the concentration of small amount of solution is more affected by evaporation. Solid contact electrodes are free of the above disadvantages but still pose other challenges.[10-12] Random potential changes at the membrane/substrate interface are attributed to blocked thermodynamically ill-defined interfaces, which are formed when

an ion-selective membrane is attached to an electron conducting (substrate electrode) material.[13] Moreover, the potential can also be affected by formation of an oxygen half-cell[14] or the presence of a thin water layer between the contact and the membrane phase.[15-16]

1.3.2 Types of Solid Contact Ion-Selective Electrode

1.3.2.1 Coated Wire Ion-Selective Electrode

The initially proposed coated wire ion-selective electrode was very simple. A platinum wire coated with PVC based ion-selective membrane showed Nernstian response to calcium[6] and a variety of anions.[17] However, the potential of a platinum wire in a membrane phase not containing any redox couple will not respond in a definite and reproducible manner and will drift significantly in relatively short time period.[17] A system containing Ag^+ ionophore complexes on a silver epoxy substrate was designed to include redox capacity, which demonstrates its potential stability. Nevertheless, the extension of the $Ag^+/^0$ system to samples containing no Ag^+ or to ISE membranes doped with different ionophores has not been reported[18-19] and private communication from Prof. Mark Meyerhoff, University of Michigan, indicated that loss of Ag^+ into the sample solutions hampered the development of such systems.

1.3.2.2 Conducting Polymers as Transducer Layer

Conducting polymers (CP) are applicable as ion-to-electron transducers in solid-state ISEs for the following reasons:[4] (1) conducting polymers, as electronically conducting materials, can form an ohmic contact to materials such as carbon, gold and

platinum; (2) conducting polymers can be prepared with convenient methods: (a) electrodeposition on the electronic conductor by electrochemical polymerization of a variety of monomers, and (b) alternatively, several soluble conducting polymers can be deposited from solution; (3) conducting polymers possess electroactive properties with mixed electronic and ionic conductivity, which can transduce an ionic signal into an electronic one in the solid state. Figure 5 shows the working mechanism for conducting polymer based ion-selective electrode. The conducting polymer and ion-selective membrane are deposited on the electronic conductor sequentially. Electrons act as charge carriers across the electronic conductor/conducting polymer interface while cations or anions as the charge carriers across the CP/ISM interface depending on whether the ISE is anion-selective or cation-selective.

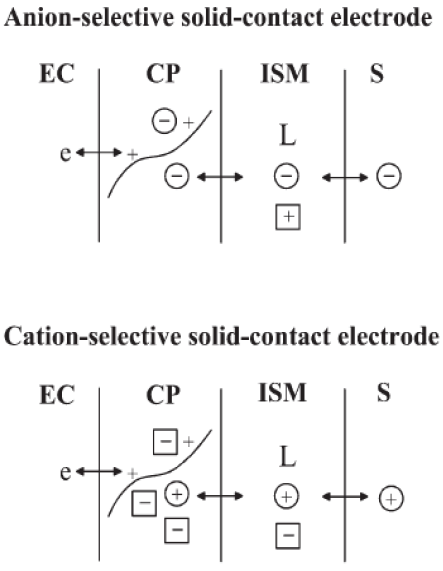

Figure 5. Working principle of solid-contact ISEs based on an oxidized (p-doped) conducting polymer as ion-to-electron transducer. EC: electronic conductor, CP: conducting polymer, ISM: ion-selective membrane, S: solution, e: electron, L: ion-recognition site. Primary ions are circled and counterions are squared.[4]

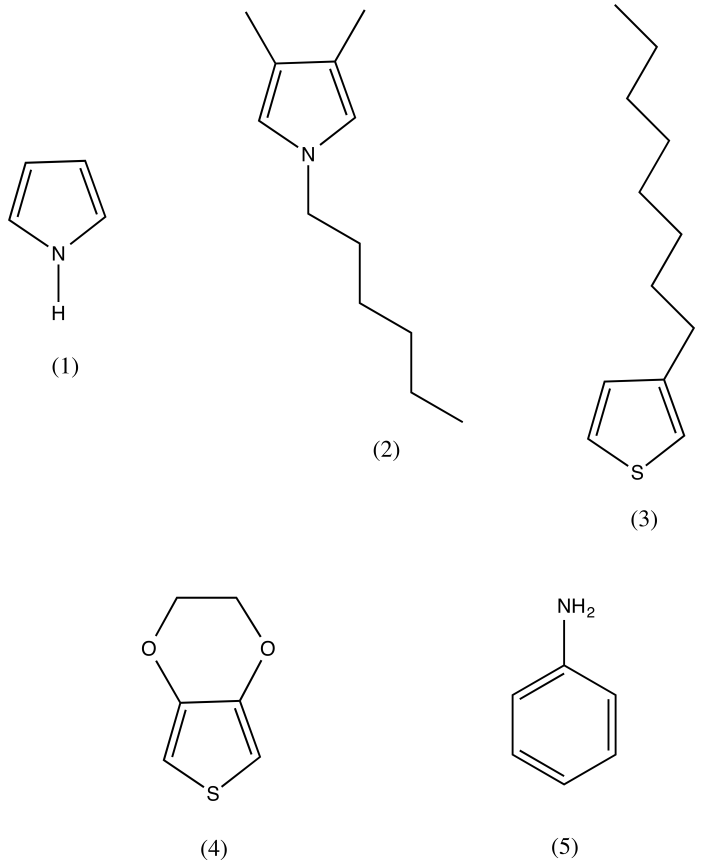

Figure 6. Monomer units of conducting polymers that have been applied as ion-to-electron transducers: (1) pyrrole, (2) 1-hexyl-3,4-dimethylpyrrole, (3) 3-octylthiophene, ,(4) 3,4-ethylenedioxythiophene, and (5) aniline.[4]

1.3.2.2.1 Polypyrrole-based Materials as Solid Contact[20-31]

Electrodes incorporating polypyrrole, synthesized by electropolymerization, as a solid contact between a platinum disk and a Na^+-selective PVC membrane showed improved performance over an electrode without the polypyrrole layer. The polypyrrole can provide a mediating layer having both ionic and electronic charge transfer and theoretically can act as a suitable transition layer for blocked electrodes such as coated wire electrodes.[32] Tetraphenylborate-doped polypyrrole with good electroactivity was

synthesized. The new polymer modified electrodes were explored to develop solid state Zn^{2+} sensor and K^+ sensor with good selectivity.[23] Zielinska et al applied a conducting poly(pyrrole) (PPy) film doped either with chloride ions (PPyCl) or hexacyanoferrate(II) ions (PPyFeCN) onto glassy carbon (GC) or a screen-printed graphite layer (S-PG) as an inner electric contact to fabricate Cl^- selective electrode. All the electrodes showed close to Nernstian responses, however, polypyrrole doped with hexacyanoferrate (PPy/FeCN) was found to result in Cl^--ISEs with longer lifetime than polypyrrole doped with chloride (PPy/Cl) due to detrimental effects of the organic components of the screen-printed graphite substrate.[20] Kaden et al.[28] and Vonau et al.[29] reported a composite of polypyrrole and Nafion as solid contact in pH electrodes based on glass membranes, showing that polypyrrole could successfully be applied as solid contact also for other types of membranes than polymer-based ion-selective membranes. Poly(1-hexyl-3,4-dimethylpyrrole) was used as solid contact in carbonate-selective ISEs based on a silicone rubber membrane by Kim et al.[30] and by Nam and Cha et al.[31]. The advantage is that poly(1-hexyl-3,4-dimethylpyrrole) is soluble in THF, which offers some additional flexibility in the electrode manufacturing process, as compared to electropolymerization.

1.3.2.2.2 Poly(thiophene) based Material as Solid Contact[33-44]

Bobacka et al. experimentally and theoretically demonstrated poly(3,4-ethylenedioxythiophene) (PEDOT) as a excellent solid contact material due to its sufficiently high bulk (redox) capacitance[45] and due to the potential of solid-state K^+-ISEs based on PEDOT as solid contact being less sensitive to O_2 and CO_2 (pH) compared to those based on PPy as solid contact.[37] The solid-contact conducting polymers were prepared by electropolymerization of the 3,4-ethylenedioxythiophene

monomer and by solution casting of the commercially available aqueous dispersion of PEDOT/PSS (Baytron P). Films of PEDOT/PSS (Baytron P) were cast to screen-printed gold substrates.[39] All-plastic, disposable, solid-state Ca^{2+}-ISEs and K^{+}-ISEs were prepared by Michalska and Maksymiuk via casting PEDOT/PSS(Baytron P) solution and plasticized PVC-based membranes on plastic substrates, in which the PEDOT/PSS worked both as ion-to-electron transducer and as the electronic contact.[40] The performances of solution-cast films of poly(3-octylthiophene) (POT) on screen-printed gold substrates and on platinum as solid contacts in miniature Cl^{-}-ISEs were comparable to those of traditional Cl^{-}-selective electrode with inner solution. Improved performances such as more stable potential and longer lifetime were observed by using an additional adhesive layer (3-aminopropyltriethoxysilane) between the screen-printed gold electrode and the POT film due to enhanced charge transfer ability.[43] Solid-state Pb^{2-}-ISEs with a detection limit of $10^{-9.3}$ M were successfully constructed by Bakker and Pretsch et al by using solution-cast POT as the solid contact and a Pb^{2+}-selective membrane based on poly(methyl methacrylate)/poly(decyl methacrylate) (MMA/DMA). This type of electrode showed a much faster response and a better detection limit.[44]

1.3.2.2.3 Polyaniline based Material as Solid Contact[46-49]

Electrosynthesized polyaniline doped with Cl^{-} was applied as solid contact in PVC-based pH electrodes for highly acidic solutions (down to pH 0.5). This electrode could be stored in a pH 7.47 Tris buffer solution, serum and hydrofluoric acid solution for one month without any loss of performance.[46] Lindfors and Iyaska found the partial conversion of polyaniline from its conducting emeraldine salt form to its nonconducting

emeraldine base form in solid contact K^+-ISEs based on plasticized PVC by using UV-visible spectroscopy. This conversion happened during long-term measurements (1 – 3 months) but not during short-term measurements (4 days).[47]

1.3.2.2.4 Conducting Polymers Dissolved in Ion-Selective Membrane[50-54]

Conducting polymers can be doped directly into the ion-selective membrane in solid-state ISEs. Such devices are often called single piece electrode. Solid-state Li^+-ISEs based on plasticized PVC containing 1% (w/w) polyaniline doped with bis(2-ethylhexyl) phosphoric acid showed the same dynamic response range as the corresponding liquid-contact ISE although the presence of polyaniline increased the H^+ interference, due to the pH sensitivity of polyaniline.[51] Miniaturized solid-state K^+-ISEs were prepared using plasticized PVC membranes containing 2% (w/w) polypyrrole, polyaniline or poly(*o*-anisidine) doped with diesters of sulfosuccinic acid. The membranes were solution-cast on planar silver electrodes and the electrodes showed improved reproducibility and repeatability of response.[51]

1.3.2.3 Carbon Material

Carbon materials have stable electrical signals due to their excellent electronic and chemical properties: the fast ion-to-electron transduction leads to short response time and the hydrophobic behavior prevents the formation of water layers. The water layer is the major reason of redox reactions with O_2 and CO_2 that cause instabilities in the emf signal. Thus carbons solve some of the problems encountered in ISEs, where the transduction layer is a conducting polymer.

A K^+-selective electrode with single wall carbon nanotube (SWCNT) contact layer was fabricated by spraying a SWCNT suspension onto a substrate and applying a coating of plasticized PVC. The device exhibits a Nernstian slope (58.4 mV/decade), dynamic ranges of four logarithmic units, and selectivities and limits of detection comparable to other solid-contact electrodes. The short response time (less than 10 s for activities higher than $10^{-5.5}$ M) and the potential stability over several days make these new electrodes very promising candidates for miniaturization.[55] Further studies of the charge transfer mechanism of the SWCNT-based transducer showed that the impedance characteristics of the SWCNT layer were very similar to those of PEDOT. Both materials can be considered as an asymmetric capacitor with one side formed by electrons/holes in the carbon nanotube wall or along the conjugated polymer chain and the other side formed by cations/anions in the ion-selective membrane.[56] SWCNT transducer-based miniaturized Ca^{2+}-selective sensors were successfully applied to measure calcium in plant sap samples.[57]

Three dimensionally ordered macroporous carbon is another carbon material that was applied as transducer for K^+-selective ISEs with PVC membranes. This carbon based ion-selective electrode were characterized with typical analytical performances, high stability of potential (including water layer test) and insensitivity of the sensor to the influence of redox couples present in solution, oxygen, carbon dioxide or light.[58-59] Also fullerene, C_{60}, was drop-casted from toluene solution on substrates and applied as transducer for K^+-selective electrode with PVC membranes yielding a sensor of normal performance, increased stability of potentials and short testing time compared to coated wire arrangements tested as controls. The electrochemically active interfacial C_{60} layer

facilitates the ion-to-electron transduction, providing a stable and reversible solid-state ISE system.[60] Recently, graphene was applied as solid contact for K^+-selective plasticized PVC based membrane sensors. Graphenes are promising for applications as transducer layer based on their excellent performance on potentiometry, electron spray ionization (ESI), light effect, oxygen/carbon dioxide or redox couple influence on potentiometric responses.[61-62]

1.3.2.4 Nanoparticles

Nanoparticles were either doped into single piece ion-selective membranes or membranes were drop-casted onto nanoparticle layer acting as transducer. The introduction of Pt nanoparticles in the membrane resulted in significant lowering of the resistance of polyacrylate membranes. The analytical performance of the sensors with Pt nanoparticles and a POT solid contact layer was comparable with that of unmodified polyacrylate membranes tested as controls. It was found that the presence of a small amounts of Pt nanoparticles (1% w/w) in the polyacrylate membrane resulted in a significant increase of potential stability over 600 h.[63] A layer of gold nanoparticles modified with thiols of different length of hydrocarbon chains was applied as transducer for K^+-selective electrode, resulting in high stability of potentials with standard deviations lower than 1 mV. The sensors' performance was tested and found to be comparable with that of those based on POT as transducer. A water layer test indicated the absence of a water film beneath the ion-selective membrane.[64]

1.4 Reference Electrode

1.4.1 Theory

In an electrochemical sensor, the working electrode is responsible for the conversion of the quantity and type of analyte into a distinct electrical signal. Therefore, it is one of the most important components of the measurement. The conversion results in either a potential change at the interface or a current when the potential is maintained constant. A critical part in controlling and measuring potentials is the reference electrode, which must be insensitive to all changes in the sample solution and maintain a constant potential at all times. A reference electrode has a pronounced influence on the measurement accuracy and precision of all kinds of electrochemical measurements such as conventional electrochemical sensors, biological field effect transistors[65-66] and impedance biosensors.[67-68] It plays an equally important role as the sensing element in guaranteeing accurate and precise operations and reliable results.

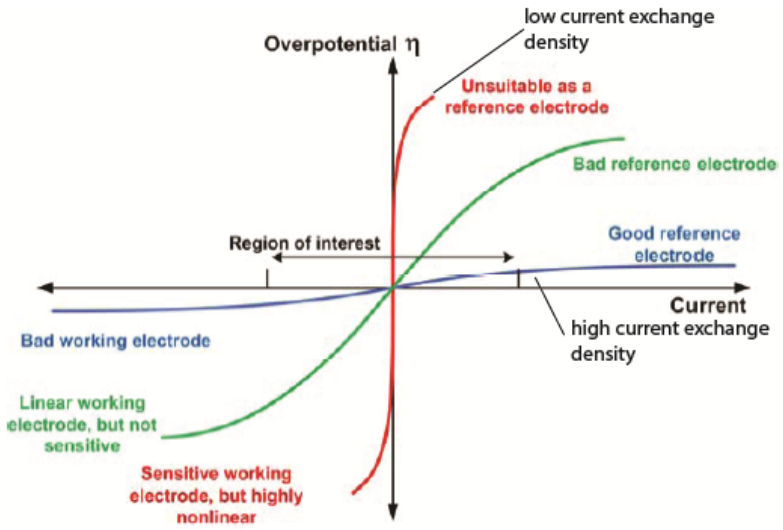

Figure 7. Symmetric I-V curves for electrodes of varying exchange current density[69]

Requirement for a conventional reference electrode are as follows:

1) The reference electrode must have a high current exchange density and a high reversibility and non-polarizability, which will allow for an exchange of charges at the electrode interface without affecting the potential significantly (Figure 7). Moreover, it is also required to be resistant to potential fluctuations due to random charge injection at the interface.[69]

2) There should be a saturated solution in contact with the reference electrode. There are many advantages to having a saturated solution to separate the sample solution from the reference electrode. First, the potential of the electrode will not be affected by the solvent since the evaporation of the solvent does not change the concentration of the saturated solution; second, the high concentration of the reactants at the interface generates stable exchange current density and resistance to the minute fluctuations, which allows the electrode to maintain a constant potential; third, the interfacial potential is mainly attributed to the net-dipoles of the metal/solution interface. If the reference electrode is in direct contact with the sample solution of different components, the surface potential could vary significantly but it is desirable to have a potential independent of the sample as much as possible. The liquid junction potential of the sample solution/saturated solution interface can be made very small and time independent and therefore will not change the reference electrode potential much.[69] The analysis of liquid junction has been investigated extensively in the literature.[70-71]

1.4.2 Types of Reference Electrode

Different reference electrodes might be used depending on the test environment. Generally, a single type of reference electrode cannot satisfy all the requirements for a good reference electrode but the negative effects may be minimized if proper reference electrodes are adopted for different measurement environments.

1.4.2.1 Standard Hydrogen Electrode

The absolute potential of an electrode cannot be measured. So the potential of an electrode is defined in this way: the standard hydrogen electrode (SHE) is the origin of the scale and its potential contribution is arbitrarily defined as zero. All other electrode potentials are measured with respect to it. The SHE involves a platinum surface coated with black platinum black catalyst which facilitates the reactions at the electrode surface and also increases the surface area, thereby enhancing exchange current density.[69] The coated platinum wire is immersed into an acidic solution and the associated reaction is:

$$2H^{+}(aq) + 2e^{-} \rightarrow H_2(g)$$

The Nernstian equation for this electrode is

$$E = E^{0} + \frac{RT}{2F}\ln\left\{(a_{H^{+}})^{2}/P_{H_2}\right\} \qquad (13)$$

The SHE has enjoyed a lot of research interest possibly due to its importance as a universal reference, and the significance of the hydrogen reaction especially in the research of acid, base, buffer and many biological systems. However, a SHE is difficult to handle and is so impractical for routine use that several other reference electrodes have been developed.[72]

1.4.2.2 Ag/AgCl Reference Electrode

The Ag/AgCl reference electrode is the most commonly used reference electrode by far due to its simple construction, low cost of fabrication, stable potentials and non-toxic components. It is comprised of a Ag/AgCl wire inserted into a AgCl-saturated chloride solution such as AgCl-saturated KCl, all of which are enclosed in a glass tube and separated from the sample solution by a salt bridge. The reaction below is used to characterize the Ag/AgCl reference electrode:

$$AgCl(s) + e^{-} \rightarrow Ag(s) + Cl^{-}(aq)$$

According to the reaction above, Cl^{-} is the reactive species in the electrode and its concentration is a determining factor of the potential.[73] The potential can be obtained from the Nernst equation:

$$E_{Ag,AgCl,Cl^{-}} = E^{0}_{Ag,Ag^{+}} + \frac{RT}{F}\ln Ks - \frac{RT}{F}\ln a_{Cl^{-}} \qquad (14)$$

where $K_s = a_{Ag^{+}} \times a_{Cl^{-}}$ is the solubility product of AgCl and is often incorporated into the standard potential of Ag/AgCl electrode to produce:

$$E_{Ag,AgCl,Cl^{-}} = E^{0}_{Ag,Ag^{+}Cl^{-}} - \frac{RT}{F}\ln a_{Cl^{-}} \qquad (15)$$

In a saturated Cl^{-} filling solution, the flow of current will not affect the Cl^{-} concentration significantly, which is the reason for the potential stability. The commonly used electrode potential for a Ag/AgCl electrode is 0.199V.

1.4.2.3 Calomel Electrode

The standard calomel electrode is comprised of Hg/ Hg_2Cl_2 (Hg_2Cl_2, calomel), which is contact with a saturated KCl solution. It has benefits of ease of construction and stable potential but has the drawback of containing hazardous mercury. The redox reaction is as follows:

$$Hg_2Cl_2(s) + 2e^- \rightarrow Hg(l) + 2Cl^-(aq)$$

The electrode potential can be expressed as

$$E_{Hg,Hg_2Cl_2,Cl^-} = E^0_{Hg_2Cl_2} - \frac{RT}{F}\ln a_{Cl^-} \quad (16)$$

The standard potential for a saturated calomel electrode is 0.245 V.[69]

1.4.2.4. Solid State Wire Reference Electrodes

A so-called pseudo reference electrode is sometimes employed in special situations. It is a simple metal wire such as Pt or Ag/AgCl of which the potential is constant at most in a well defined solution. For miniature current based electrochemical systems, such as disposable screen printed electrodes setups, where long time stability is not a must, usually a Ag/AgCl system is used.[74] However, it is not suitable for longer operation (as in routine potentiometric measurements), which requires stabilization of these systems.[75] A powder of tungsten-substituted lithium molybdenum oxide bronze, $Li_{0.4}Mo_{0.95}W_{0.05}O_3$, was proved to show inert responses to changes in pH value, dissolved oxygen and redox potential of the test solution. But it is sensitive to some alkali ions with increasing response in the sequence of K^+, Na^+ and Li^+. However, it can be still used as

reference electrodes for electrochemical measurements under restricted conditions.[76-77]

1.4.2.5 Membrane-based All-Solid-State Reference Electrode

The miniaturization of liquid-junction reference electrodes is limited by the internal electrolyte present in the liquid reservoir.[78-79,80-84] Moreover, the potential is affected by the internal solution. Thus, a solid-state reference electrode is attractive due to elimination of the liquid reservoir, improved robustness, ease of fabrication, and heat- and pressure- resistance.[85] Typically, the filling solution is substituted by a solid state ion exchange membrane that contains the ions that the electrode equilibrium requires.[86] One way to achieve this is to incorporate an agar gel saturated with KCl spin-coated[87] or screen-printed[88] on a micro fabricated Ag/AgCl film. This produces a reference electrode which is insensitive to pH of 4 – 10 [89] and Cl^- concentration of 10^{-6} to 0.3 M.[90]

Recently, the application of micro- and nano-structures to obtain stable and reliable all-solid-state reference electrodes has been explored. A reference electrode was successfully prepared using carbon nanotubes as ion-to-electron transducers.[91-92] The composition of reference membranes was poly(*n*-butyl acrylate) or a copolymer of n-butyl acrylate and methyl methacrylate prepared by photopolymerization (cross-linked), which was previously reported.[93] The carbon nanotube based electrode shows no difference to previously reported ones in terms of sensitivity to various salts, pH and light, as well as time of response and stability.[91] The same type of reference electrode was prepared in small, disposable, planar arrangement using carbon nanotubes modified by grafting with octadecylamine group and photopolymerization of poly(n-butyl acrylate), which resulted in a high stability of potentials readings.[92]

Microcapsules of polymers filled either with KCl or AgCl solutions can be applied to deliver those reagents directly to the inside of a plasticized PVC.[94-95] Then POT was drop-casted as transducer in between the electron conductor and the ISM. It was observed that incorporation of polypyrrole microvessels improved the stability of reference electrodes' potentials and lowered membrane resistances as well, which was clearly advantageous.[96]

1.4.2.6 Liquid junction free reference electrode

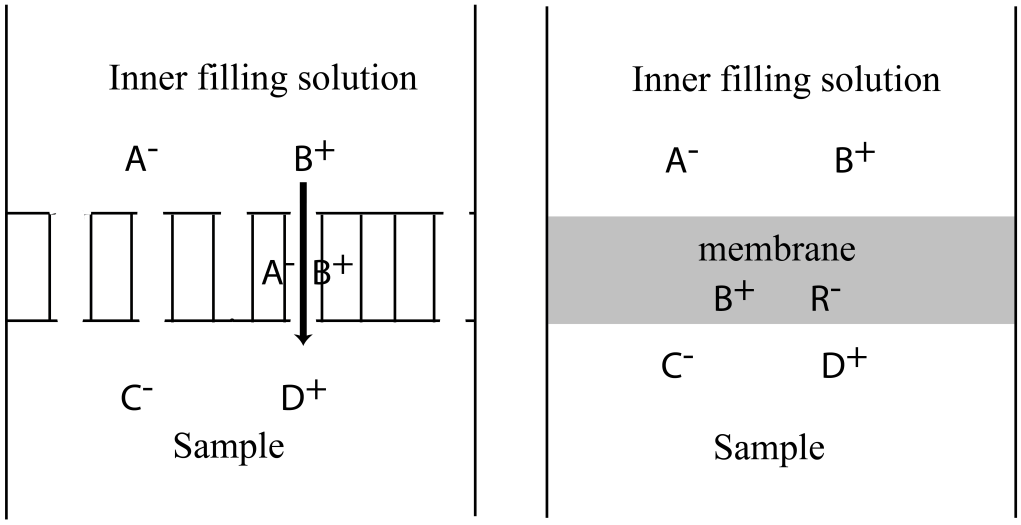

Figure 8. Reference electrode with a salt bridge (left) and a liquid junction free reference electrode (right).

The vast majority of electrochemical measurements are performed with a reference electrode with a salt bridge (Figure left) Unfortunately, salt bridges have several disadvantages. When used in real life samples, they clog with proteins and lipids, suffer from contamination by sample components, and because they rely on comparatively large ion fluxes into the samples, they can considerably contaminate small

volume samples.[97-100] In continuous measurements, salt bridges eventually run out of electrolyte, which is a problem particularly for miniaturized devices. A few approaches have been proposed to address this problem, such as the use of a pseudo reference electrode consisting of an ISE with a hydrophobic anion exchanger membrane loaded with the polyanionic heparin.[101-102] Alternatively, hydrophobic polymeric membranes doped with an ionic liquid[103-107] or different hydrophilic salts were suggested.[91, 93, 108-109] These approaches distinguish themselves from a reference electrode with a conventional salt bridge by the elimination of the sample/salt bridge interface, which is an interface of two *miscible* electrolyte solutions that exhibits a liquid junction potential.[110] Instead, the interface of the sample and the reference electrode is an interface between two immiscible phases, i.e., the aqueous sample and a hydrophobic ion-doped polymeric membrane. The salts or ionic liquids incorporated into these hydrophobic reference electrode membranes are slightly soluble in water. As they continuously leach at a small rate into the sample solution, a local equilibrium of salt or ionic liquid distribution between the reference membrane and aqueous phase is established.[111] This ideally results in an interfacial potential that does not depend on the composition of the sample.

1.5 Calibration Free Ion-Selective Electrodes

Potentiometry with ion-selective electrodes with polymeric membranes is a fully established technique in clinical chemistry; however, its main limitation has been the stability of calibration, which can be attributed to the standard potential of the measuring cell.[112-113] The stabilities of the standard potentials of both the working electrode and the reference electrode represent the major common source of measuring errors. Besides

measuring inaccuracy, calibration procedures take time and require standard solutions, which is already troublesome for a regular test and certainly inadequate for emergency rooms that demand fast and accurate measurements.

A symmetric ISE membrane has been developed by applying optimal membrane technologies and optimized reference electrodes in a perfectly symmetric measuring system. Thus, calibration-free cell assemblies with stable standard potentials were obtained for both K^+ and Na^+ in aqueous calibration solutions. Results were also presented both before and after serum contact and in undiluted human serum.[114]

An ionophore-based ion-selective membrane as a coulometric electrode was employed in various types of calibration-free titrations. An anodic current of constant magnitude and length may be applied across a membrane to release a defined quantity of ions with high selectivity and precision. Calibration-free coulometric titrations were applied to the release of calcium ions for complexometric titrations, including back titrations, and the release of barium ions to determine sulfate.[115]

More work has been focusing directly on ion-selective electrodes. Systems containing Ag^+ ionophore complexes on a silver epoxy substrate reduced the standard deviation of the cell constant[18-19] but the extension of the $Ag^{+/0}$ system to samples containing Ag^+ or to ISE membranes doped with a variety of ionophores has not been reported. Redox-active self-assembled monolayers (SAMs) with a redox potential controlled by an applied current[116] show a small redox buffering capacity, and mixtures of gold nanoclusters with two different charge states[117] are difficult to prepare. Applying a current pulse in the nA range provides a route to electrochemically adjust standard

potential (E^{o}) [118] but it still requires tuning for individual electrode and has not been applied to practical applications yet.

CHAPTER TWO

Current Pulse Based Reference Electrodes Without Liquid Junctions

In part from:

Xu U. Zou and Philippe Bühlmann. *Analytical Chemistry* **2013**, 85(8), 3817-3821.

Reproduced in part with permission from Analytical Chemistry, 85(8), 3817.

Copyright © 2005 American Chemical Society.

Abstract

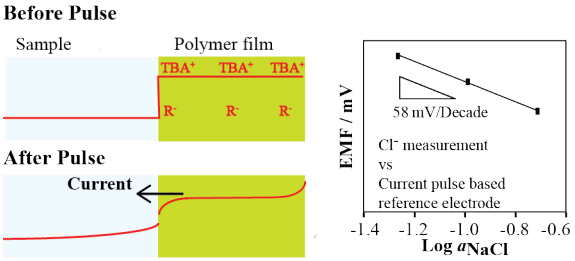

Reference electrodes with hydrophobic ion-doped polymeric membranes offer a promising alternative to reference electrodes with conventional salt bridges. This report introduces the current pulse operation of liquid junction free reference electrodes. A brief current pulse is applied to a cation exchanger membrane, releasing a well-controlled amount of cations from the membrane into to the sample and, thereby, determining the boundary potential of the sample/reference membrane interface. Measurements with ion-selective electrodes (ISEs) are performed relative to these reference electrodes immediately after the current pulse and exhibit the same Nernstian responses as typical for potentiometry, which is demonstrated with Cl^- ISE measurements. The use of current pulse based reference electrodes avoids the sample sensitivity and clogging of conventional salt bridges and the often poorly controlled loss of bridge electrolyte into samples. Current mode measurements in serum over 2 days showed a much higher stability of the reference potential than conventional potentiometric measurements with the same ion-doped polymeric membranes.

2.1 Introduction

The vast majority of electroanalytical measurements are performed with reference electrodes separated from samples by salt bridges. The latter were introduced more than 100 years ago[119] and, in the absence of alternatives, enable the analysis of billions of samples per year, in particular in clinical chemistry. This includes many measurements with ion-selective electrodes (ISEs),[1, 9, 120-122] which require reference electrode potentials with a high reproducibility. For example, an error of 5 mV for an ISE measurement of a monovalent ion results in an error of 18% in the determined ion activity.

Unfortunately, salt bridges have several disadvantages. When used in real life samples, they clog with proteins and lipids, suffer from contamination by sample components, and because they rely on comparatively large ion fluxes into the samples, they can considerably contaminate small volume samples.[97-98] In continuous measurements, salt bridges eventually run out of electrolyte, which is a problem particularly for miniaturized devices. In a routine laboratory setting, such problems can be counteracted by frequent flushing of reference electrodes with cleaning solutions, free flowing liquid junctions, and regular replenishing of salt bridge solutions.[123] These options are cumbersome enough in a laboratory setting, but they are difficult to implement in many real life scenarios, such as in intensive care units at hospitals or at remote environmental monitoring stations. Clearly, other options to the reference electrode problem are needed.

A few approaches have been proposed to address this problem, such as the use of a pseudo reference electrode consisting of an ISE with a hydrophobic anion exchanger

membrane loaded with the polyanionic heparin.[101-102] Alternatively, hydrophobic polymeric membranes doped with an ionic liquid[103-107] or different hydrophilic salts were suggested.[91, 93, 108-109] These approaches distinguish themselves from a reference electrode with a conventional salt bridge by the elimination of the sample/salt bridge interface, which is an interface of two *miscible* electrolyte solutions that exhibits a liquid junction potential.[110] Instead, the interface of the sample and the reference electrode is an interface between two immiscible phases, i.e., the aqueous sample and a hydrophobic ion-doped polymeric membrane. The salts or ionic liquids incorporated into these hydrophobic reference electrode membranes are slightly soluble in water. As they continuously leach at a small rate into the sample solution, a local equilibrium of salt or ionic liquid distribution between the reference membrane and aqueous phase is established.[111] This ideally results in an interfacial potential that does not depend on the composition of the sample. While several reports of reference electrodes with hydrophobic ion-doped polymeric membranes have been described in the literature, only few applications of such reference electrodes for measurements in real life samples have been reported. A study using a reference electrode membrane doped with the ionic liquid 1-methyl-3-octylimidazolium bis(trifluoromethylsulfonyl)imide and three-dimensionally ordered macroporous (3DOM) carbon as solid contact successfully measured pH in milk. However, it also demonstrated the difficulties that can arise due to the transfer of sample ions into the reference membrane and fluxes of ions across reference membranes.[105] Clearly, the composition of such reference membranes has to be carefully optimized for individual samples.

Here, we report a new method of operating reference electrodes with hydrophobic ion-doped polymeric membranes. It involves the application of a current pulse to a hydrophobic ion-doped membrane,[122] thereby controlling transmembrane ion fluxes to obtain a sample independent reference electrode potential. Current pulses were applied in the past to ion-selective membranes to control transmembrane ion fluxes and, thereby, lower detection limits of ISEs.[124-128] Moreover, current pulses were used in ion-transfer stripping voltammetry[129-130] to accumulate analyte ions at the working electrode prior to analysis and to release ionic reagents for the detection and quantification of biomolecules.[131] In contrast to efforts aimed at lowering the detection limits for analyte ions, we use current pulses to "worsen" (i.e., increase) detection limits, causing the reference electrodes to respond only to the ions released by the current pulse.

2.2 Experimental Section

2.2.1 Materials

Deionized water (0.18 MΩ m specific resistance) was purified with a Milli-Q PLUS reagent grade water system (Millipore, Bedford, MA) and used for the preparation of all sample solutions. High molecular weight poly(vinyl chloride) (PVC), 2-nitrophenyl octyl ether (o-NPOE), potassium tetrakis(4-chlorophenyl)borate (KTpClPB), and tetradodecylammonium tetrakis(4-chlorophenyl)borate (ETH500) were purchased from Fluka (Buchs, Switzerland). Lyophilized animal-based control serum (Autonorm REF 100005) was purchased from SERO (Billingstad, Norway) and dissolved in deionized water.

2.2.2 Electrode Membrane Preparation

Master membranes were prepared from 66 mg PVC, 132 mg *o*-NOPE, 10 mg KTpClPB, and 16 mg ETH500. Tetrahydrofuran (THF) was used to dissolve all the membrane components, and the resulting solution was poured into a glass dish (32 mm i.d.). The THF was then allowed to evaporate overnight at room temperature. Individual membranes were cut out of the master membrane and glued with THF onto the end of a Tygon tube (3/16 inch, i.d.; 5/16 inch, o.d.). An inner filling solution of 1.0 mM tetrabutylammonium chloride (TBA^+Cl^-) was filled into the Tygon tube, and a AgCl coated Ag wire was inserted into the solution as inner reference electrode. The thus mounted membrane was conditioned in 1.0 mM TBA^+Cl^-.

2.2.3 Electrochemical Measurements

A Solartron SI 1287 electrochemical interface (Boston, MA) was used to apply current pulses, measure open circuit potentials, and perform cyclic voltammetry. Current pulses were programmed with CorrWare software (Scribner Associates, Southern Pines, NC). A four-electrode system was used as follows: A Pt wire and a AgCl-coated Ag wire were inserted as counter and reference electrodes into the inner filling solution of the membrane-based reference electrode. A Pt counter electrode and a conventional double-junction reference electrode (DX200, Mettler Toledo, OH; 3.0 M KCl saturated with AgCl as inner filling solution and 1.0 M LiOAc as bridge electrolyte) were inserted into the sample. All EMF values of measurements involving this conventional reference electrode were corrected with the Henderson equation[132] for liquid-junction potentials at

the interface of its salt bridge and the sample except for serum samples. Activity coefficients were calculated as described in ref.[133]

2.3. Results and Discussions

2.3.1 Experimental Design

For an experimental proof of concept of the current-based operation of liquid junction free reference electrodes, poly(vinylchloride) membranes plasticized with nitrophenyl octyl ether were loaded with tetrabutylammonium tetrakis(4-chlorophenyl)-borate and, to lower the electrical membrane resistance, tetradodecylammonium tetrakis(4-chlorophenyl)borate (ETH500). The membranes were then mounted onto electrode bodies as they are used commonly for ISEs,[122] and the electrodes were preconditioned in the same tetrabutylammonium (TBA^+) chloride solution that was also used as the inner filling solution of the reference electrodes. A four-electrode system was used to ensure potential measurements were not affected by concentration polarization.

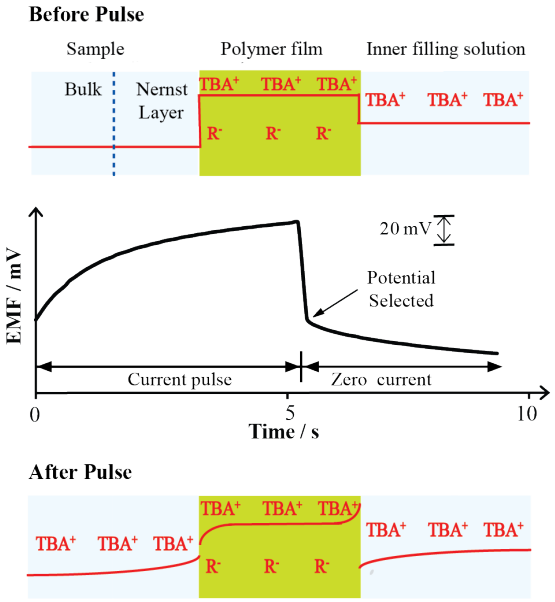

Figure 1. Schematic illustration of pulse mode operation of hydrophobic ion-doped polymeric reference electrodes. Top and bottom: TBA^+ concentration profiles through the sample, reference membrane, and inner filling solution of the reference electrode before and after the current pulse. A typical pulse of current in the direction from the inner filling solution to the sample releases TBA^+ into the sample. Center: The open circuit potential (highlighted by an arrow) is measured immediately after the current pulse; real life measurements with ISEs vs this reference electrode, such as the ones depicted for calibration curve C in Figure 3, are measured at this point in time. The experimental EMF profile shown here was measured with a pulse of 0.3 μA amplitude and 5.3 s length.

2.3.2 Operation in Different Current Parameters

The mode of operation of these reference electrodes is illustrated in Figure 1. A current pulse is applied to the membrane, resulting in the release of TBA^+ from the membrane into the (unstirred) Nernst layer of the real sample. This current pulse serves an analogous purpose as the controlled release of ions in coulometric titrations, in which a known amount of reagent is accurately released into the sample. In this regard, current pulses are preferable over potential pulses. Immediately after the current pulse, the potentiometric measurement is performed, and the membrane based electrode ideally behaves as the reference electrode whose potential does not depend on the sample composition, but only on the activity of the TBA^+ released by the current pulse into the Nernst layer. This TBA^+ will not have had enough time to diffuse away from the sensor surface into the bulk of the sample yet, and, because of the lipophilicity of TBA^+, the cation exchanger membrane with its Hofmeister selectivity[2] exhibits a high preference for

TBA^+ over ions originally present in the sample. After the potentiometric measurement, the polymer membrane is allowed to recover, restoring the original concentration profile.

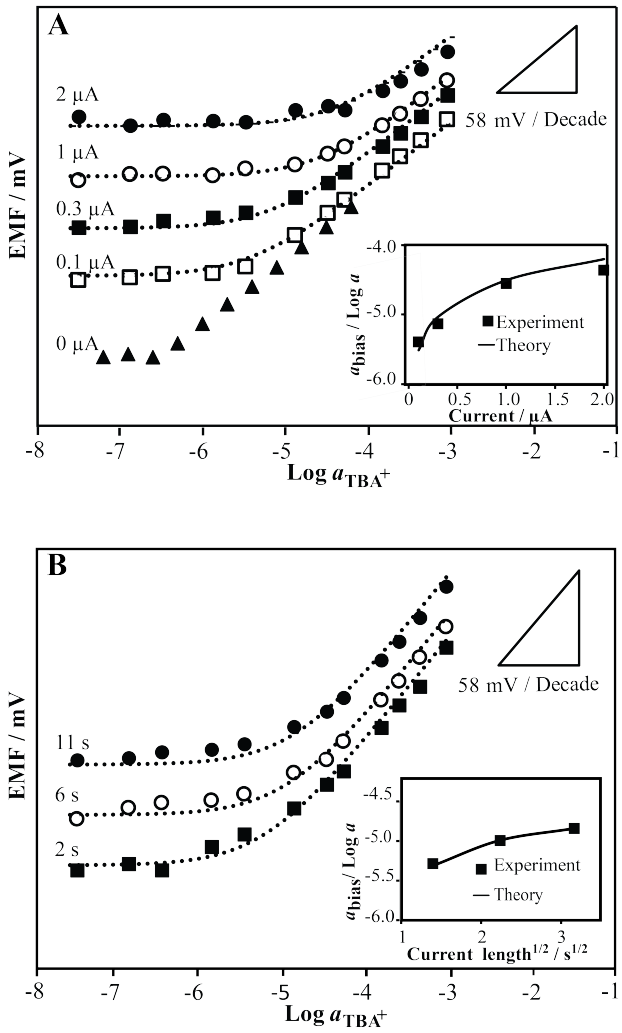

Figure 2. EMF responses to TBA^+Cl^- of a reference electrode with a hydrophobic membrane vs a conventional double junction reference electrode. (A) Without current pulse and for current pulses of 6 s length and different current amplitudes. Response curves are shifted vertically for enhanced clarity. (B) For 0.3 µA pulses of different lengths. Dotted lines are predictions based on the Nernst equation. Insets: Experimental and theoretical a_{bias} values as a function of (A) current amplitude and (B) length of the current pulse.

Figure 2 A illustrates how current pulses with different amplitudes release different amounts of TBA^+ into sample solutions containing a varying activity of TBA^+. As the figure shows, larger current amplitudes extend the range of the sample-independent electromotive force (EMF) to higher TBA^+ activities in the sample. Without a current, the electrode has a Nernstian response to TBA^+ down to the detection limit of $10^{-6.7}$ M, below which the potential becomes constant and is determined by the flux of TBA^+ from the membrane to the sample. [1, 134] The use of current pulses shifts this detection limit by several orders of magnitude. The higher the current is, the more ions can be released into the sample, and the higher the TBA^+ activities in the sample have to be to affect the measured EMF. In analogy to the detection limit seen in the calibration curve for the currentless measurements, we refer to the TBA^+ activity below which the electrode potential becomes constant as a_{bias}. This value corresponds directly to the activity of TBA^+ that is released by ion fluxes into the sample and, thereby, biases the potentiometric measurement. While the membrane without any current has a a_{bias} of $10^{-6.7}$ M (as determined from the intersection of the two linear sections of the calibration curve), current pulses of 0.1 and 2.0 μA shift a_{bias} to $10^{-5.6}$ and $10^{-4.3}$ M, respectively.

As the insets in Figures 2A and 2B show, the effect of the current pulse on a_{bias} can be quantitatively understood using diffusion theory, with a good match between theory and experiment. The mass transfer model predicting the theoretical relationship is based on the following assumptions: (1) Only the concentration profile on the sample side matters for the potentiometric measurements because identical current pulses always generate the same concentration profiles on the membrane side of the sample/membrane

interface and at the membrane/inner filling solution interface; (2) the only ion transferred across the two surfaces of the reference membrane is TBA^+; (3) the total concentration of TBA^+ on the aqueous side of the sample/membrane interface, $c_{sample}(x=0, t)$, as a function of the time t is the sum of $c_{bias}(0,t)$, which is the result of the current pulse, and the TBA^+ concentration in the bulk of the sample, $c_{sample}(x\rightarrow\infty,t)$:

$$c_{sample}(0,t) = c_{sample}(\infty,t) + c_{bias}(0,t) \tag{1}$$

As discussed in the Supporting Information, it can be readily shown by use of the above assumptions, Fick's second law, and appropriate boundary conditions that c_{bias} is given by:

$$c_{bias} = \frac{2 i t^{1/2}}{\mathrm{F} A D_{sample}^{1/2} \pi^{1/2}} \tag{2}$$

where i is the amplitude of the current pulse, t is the length of the current pulse, A is the surface area of the membrane, D is the diffusion coefficient of the ion released into the sample, and F is the Faraday constant. To determine the predicted EMF from the amplitude and duration of the current pulse, it is further assumed that the amount of ions removed by the pulse from the inner filling solution is negligible and does not affect concentrations in the inner filling solution. This is readily ensured by use of an inner filling solution of high concentration. It follows that upon conversion of $c_{sample}(0, t)$ to activity, the predicted EMF is obtained from the Nernst equation:

$$\mathrm{EMF} = E^0 + \frac{2.303\,\mathrm{R}\,T}{z\,F} \mathrm{Log}\, a_{sample}(0,t) \tag{3}$$

If $a_{sample}(0, t)$ is dominated by the current pulse, inclusion of the activity coefficient into $E^{o\prime}$ gives

$$\mathrm{EMF} \approx E^{0'} + \frac{2.303\,\mathrm{R}\,T}{z\,F}\,\mathrm{Log}\,\frac{2it^{1/2}}{\mathrm{F}A D_{\mathrm{sample}}^{1/2}?^{1/2}} \qquad (4)$$

As the dotted lines in Figures 2A and 2B show, this equation predicts the EMF responses very well. Moreover, the predicted dependences of c_{bias} on the current amplitude and the square root of the pulse length are in good agreement with experimental findings, as shown in the insets of Figures 2A and 2B.

Note that c_{bias} only shows a very small dependence on the temperature, T. For example, due to the proportionality of D and the absolute temperature, an increase of T from 37 to 39 ºC lowers c_{bias} by only 0.32%. Moreover, the effect of this decrease in c_{bias} is diminished by the slight increase in the Nernstian slope (from 61.5 to 61.9 mV/decade in this example, resulting in a reference potential change of only 0.5 mV for a ratio of the concentration of TBA^+ in the inner filling solution and c_{bias}).

2.3.3 Charge Carriers at the Interface

As the above expression for c_{bias} shows, large current amplitudes can shorten the experiment. However, it is important to note that the current amplitude should not be too large since too large applied currents result in phase boundary potentials at which sample anions start to transfer from the sample into the reference membrane. This was demonstrated by cyclic voltammetry, which showed a peak at a potential of +125 mV vs AgCl/Ag for a sample of 1 mM TBA^+Cl^-. This peak was associated with TBA^+ transferring from the membrane to the sample, coupled with TBA^+ transferring from the inner filling solution to the membrane (see Figure S1 of the Supporting Information). At potentials beyond +400 mV, Cl^- transferred from the sample into the membrane, coupled with TBA^+ transferring from the inner filling solution to the membrane. Similar coupled

ion transfer across the two interfaces of a supported nitrophenyl octyl ether membrane separating two aqueous solutions has been reported in the past.[135-136] Clearly, the operation of these reference electrodes at applied currents as large as to result in such high voltages must be avoided.

2.3.4 Application with Chloride-Selective Electrode

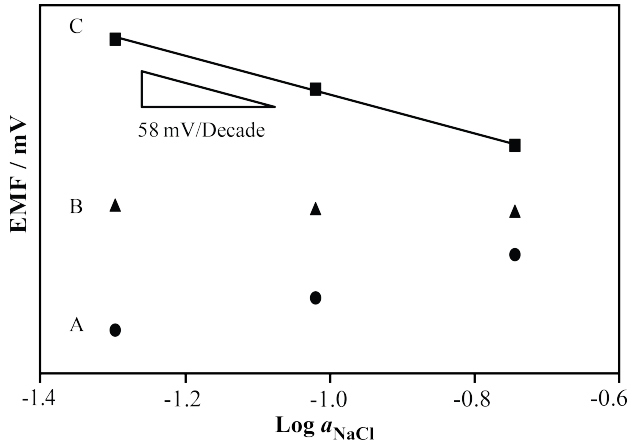

Figure 3. Use of reference electrodes with hydrophobic cation exchanger membranes in NaCl solutions. (A) Conventional EMF measurement with a hydrophobic membrane based electrode vs a double junction reference electrode with LiOAc as bridge electrolyte. (B) Pulse operated reference electrode (0.3 μA pulse of 6 s) vs a conventional double junction reference electrode (standard deviation 0.9 mV). (C) Cl^--selective electrode based on a AgCl-coated Ag wire vs a pulse operated reference electrode (0.3 μA pulse of 6 s).

The new reference electrode was tested in NaCl solutions with Na^+ and Cl^- concentrations close to those typical for blood. When no current was applied to the reference membrane and the potential of this electrode was measured relative to a conventional double junction reference electrode, a sub-Nernstian Na^+ response was

observed as the NaCl activity was increased (response A in Figure 3). This result is not surprising because the ion exchange selectivity of the reference membrane strongly favors TBA^+ over Na^+. The TBA^+ released into the sample as a result of interfacial ion exchange with Na^+ does not diffuse away from the ISE membrane fast enough and competes with the Na^+ from the sample, resulting in a mixed response of the reference electrode membrane to Na^+ and TBA^+. Also, tetrabutylammonium tetrakis(4-chlorophenyl)borate is not hydrophilic enough to establish a sample-independent phase boundary potential as a result of leaching of this salt into the sample. Evidently, without the current pulse, this electrode is not suitable as reference electrode.

To the contrary, the potential of the reference electrode membrane became sample independent when a current was applied to release TBA^+ into the sample prior to the potentiometric measurement (Figure 3, response B; again measured relative to a conventional double junction reference electrode). As an example for the proposed use of this reference electrode in electroanalytical measurements, the reference electrode was used for measurements with a AgCl-coated Ag wire as Cl^- ISE (Figure 3, response C). The Nernstian response to Cl^- confirms the usefulness of this current pulse operated reference electrode.

2.3.5 Application in Serum

The new reference electrode was further tested in undiluted serum (Figure 4). Without a current pulse, the potential of the electrode in serum kept drifting over a two-day period. This can probably be explained by the interference from hydrophobic components of serum.[137] However, when operated with current pulses, the reference

electrode showed a constant potential over the same time period, with a standard deviation of only 0.5 mV.

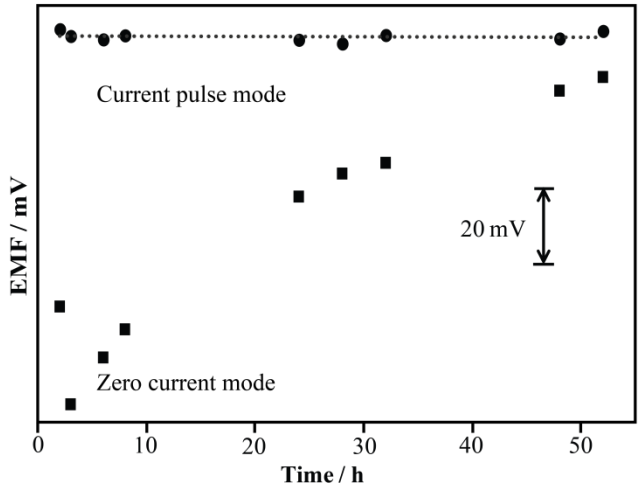

Figure 4. Potential response of reference electrodes exposed to serum over a two-day period, operated in current pulse (0.3 μA, 6 s) or zero current mode.

2.4 Conclusions

In summary, this work has shown how an electrode with a simple ion exchanger membrane can be used as a reference electrode when operated in a current pulse mode. The concentration of the ions released into the sample depends on the amplitude and length of the current pulse and can be explained quantitatively by the diffusion theory. This operating mechanism is not limited to ion exchanger membranes and may also be applied to ionophore doped membranes.[120, 122] This suggests a high level of flexibility in the design of reference electrodes optimized for specific applications. As for conventional salt bridges too, the exact composition of the reference electrode membrane may have to be optimized for samples that pose unusual challenges, such as a very high ionic strength or high concentrations of lipophilic ions. In such cases, ion exchanger membranes loaded

with ions of particularly high hydrophobicity may be used, or reference membranes may be doped with ionophores that exhibit a low selectivity for the sample ions. The good stability of the EMF exhibited by pulse operated reference electrodes exposed to serum is particularly promising in view of biological and medical applications that require long term monitoring.

2.5 Supporting Information

2.5.1 Cyclic Voltammetry of Ion Transfer

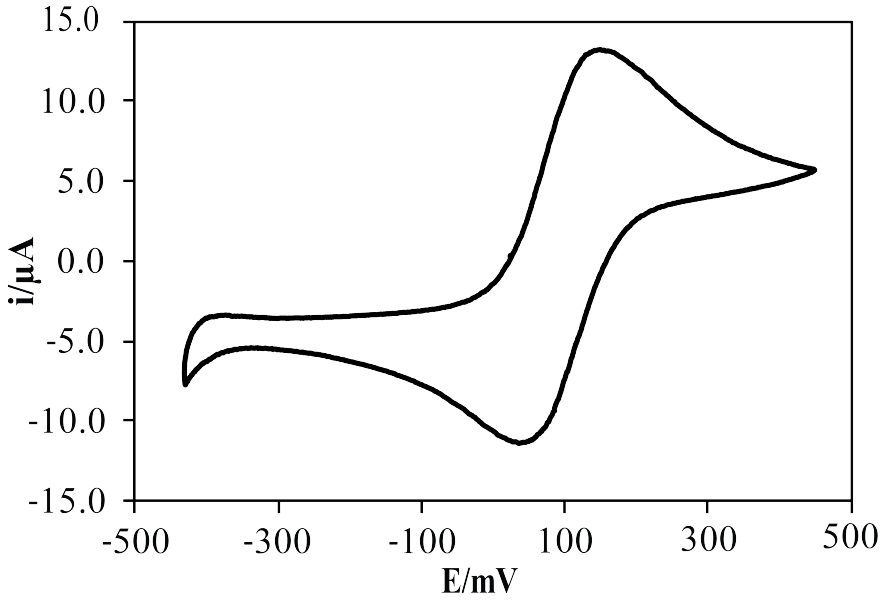

Figure S1. Resistance corrected cyclic voltammogram of a hydrophobic reference membrane based electrode with 0.1 M LiCl and 1 mM TBA^+Cl^- as both inner filling and sample solutions. Potential sweep rate: 0.01 V/s. E vs Ag/AgCl; bridge electrolyte: 1 M LiOAc.

Two charge carriers may cross the two interfaces of the hydrophobic reference membrane and the adjacent two aqueous phases (i.e., the sample and the inner filling

solution). For example, a current flowing from the inner filling solution towards the sample may cause at large applied potentials TBA^+ transfer from the membrane into the aqueous sample and chloride transfer from the sample into the membrane. For the purpose of the current pulse-operated reference electrodes introduced here, the potential resulting from the current application should not become large enough to cause interfacial *chloride* transfer. The cyclic voltammogram shown in Figure 3 shows at which potentials the phase transfer of specific ions occurs. The peak at 125 mV (positive current) is associated with TBA^+ transfer from the membrane into the sample, coupled with TBA^+ transfer from the inner filling solution into the membrane.[135-136] The peak on the return scan (negative current) is caused by TBA^+ transfer at both interfaces of the reference membrane to aqueous solutions, but in a direction opposite from that of the forward scan. Potentials over +400 mV or below –400 mV result in the interfacial transfer of anions, i.e., chloride.

2.5.2 Modeling of Mass Transport and Prediction of c_{bias}

Concentration profiles in the sample can be described by Fick's second law. Ion transfer from the membrane into the sample depletes these same ions on the membrane side of this interface. The concentration profiles that result in the sample are similar to those observed for electron transfer reactions at the surface of electron conducting electrodes.[72] Consequently, diffusion equations and boundaries conditions well known from electron transfer reactions can be applied similarly for these pulse operated reference membranes.

The assumptions here are that the working electrode is planar, that the sample solution is unstirred, that the only ion that transfers across the two interfaces of the reference membrane is TBA^+, and that prior to the pulse application TBA^+ is found (with the concentration c^*_{membrane}) only on the membrane side of the sample/membrane interface. The TBA^+ concentration on the sample side as a function of the time, t, is given by $c_{\text{bias}}(x,t)$, and the distance from the membrane surface is x. It follows that the diffusion equations can be written with Fick's second law:

$$\frac{\partial c_{\text{bias}}(x,t)}{\partial t} = D_{\text{sample}}\left(\frac{\partial^2 c_{\text{bias}}(x,t)}{\partial x^2}\right) \tag{S1}$$

$$\frac{\partial c_{\text{membrane}}(x,t)}{\partial t} = D_{\text{membrane}}\left(\frac{\partial^2 c_{\text{membrane}}(x,t)}{\partial x^2}\right) \tag{S2}$$

where c_{membrane} is the concentration of TBA^+ on the membrane side of the sample/membrane interface, D_{sample} is the diffusion coefficient of TBA^+ in the aqueous solution, and D_{membrane} is the diffusion coefficient of TBA^+ in the membrane.

The boundary conditions are as follows:

$$c_{\text{membrane}}(x, t=0) = c^*_{\text{membrane}} \tag{S3}$$

$$c_{\text{membrane}}(x \to \infty, t) = c^*_{\text{membrane}} \tag{S4}$$

$$c_{\text{bias}}(x \to \infty, t) = 0 \tag{S5}$$

$$c_{\text{bias}}(x, t = 0) = 0 \tag{S6}$$

Because the flux of TBA^+ transferring out of the membrane must equal the flux of this species into the aqueous sample, it follows that:

$$D_{\text{membrane}}\left[\frac{\partial c_{\text{membrane}}(x,t)}{\partial t}\right]_{x=0} + D_{\text{sample}}\left[\frac{\partial c_{\text{bias}}(x,t)}{\partial t}\right]_{x=0} = 0 \tag{S7}$$

Since current is applied, $i(t)$ is known. As long as TBA^+ is the only species carrying current across the sample/membrane interface, $i(t)$ is proportional to the flux of TBA^+ across this interface:

$$-J_{\text{bias}}(0,t) = \frac{i(t)}{z\text{F}A} = D_{\text{sample}}\left[\frac{\partial c_{\text{bias}}(x,t)}{\partial x}\right]_{x=0} \tag{S8}$$

The set of Equations S1 to S8 can be solved for $c_{\text{bias}}(0,t)$, giving

$$c_{\text{bias}}(0,t) = \frac{2it^{1/2}}{z\text{F}AD_{\text{sample}}^{1/2}\pi^{1/2}} \tag{S9}$$

where $c_{\text{bias}}(0,t)$ is the concentration of TBA^+ on the sample side of the sample/membrane interface, z is the charge of TBA^+, F is the Faraday constant, and A is the surface area of the membrane.

The concentration of TBA^+ released by the current into the sample, ☒, can be predicted using Equation S9. For numerical calculations, the value of 0.82×10^{-5} cm^2/s was

used for D_{sample}. Experimentally, $\times$ can be determined by extrapolation of the linear section of the Nernstian TBA^+ response to the concentration-independent EMF observed at very low TBA^+ concentrations. All fits and calculations were performed with Mathematica 8.0 (Wolfram Research, Champaign IL).

2.5.3 Reference Electrode Potential

Because of the assumption used above that prior to the pulse application TBA^+ ions are found only on the membrane side of the sample/membrane interface, $c_{bias}(0,t)$ represents only the concentration of the TBA^+ released by the current into the sample. However, if the bulk of a sample contains TBA^+ of the concentration $c_{sample}(x \to \infty, t)$, the total TBA^+ concentration on the aqueous side of the sample/membrane interface, $c_{sample}(0,t)$, is given by

$$c_{sample}(0,t) = c_{sample}(x \to \infty, t) + c_{bias}(0,t) \tag{S10}$$

Upon conversion of the concentration term $c_{sample}(0,t)$ to activity, the response of the current pulse based reference electrode to solutions that contain TBA^+ (e.g., Figure 2 of the main manuscript) can be described using the Nernst equation:

$$\text{EMF} = E^0 + \frac{2.303\,\text{R}\,T}{z\,F}\,\text{Log}\,a_{sample}(0,t) \tag{S11}$$

where R is the gas constant and T is the temperature. It follows from Equations S10 and S11 that the EMF is dominated by the current pulse when $c_{sample}(x \to \infty, t) << c_{bias}(0,t)$.

CHAPTER THREE

The Application of Pulse To Convert Ionophore Based Ion-Selective Electrode To Reference Electrodes

Abstract

Current pulses and potential pulses have been adopted by a few researchers as new methods to improve ion-selective electrode performances and study ion transfer mechanisms. This report introduces the current and potential pulse operation of liquid junction free reference electrodes. A brief current or potential pulse is applied to a K^+-selective membrane, releasing a certain amount of K^+ from the membrane into the sample and uptaking Cl^- from the sample to the membrane, thereby, generating a constant boundary potential of the sample/reference membrane interface. Measurements with traditional reference electrode are performed relative to these reference electrodes immediately after the pulse and exhibit the constant potential responses as typical for potentiometry. The use of pulse based reference electrodes avoids the sample sensitivity and clogging of conventional salt bridges and the often poorly controlled loss of bridge electrolyte into samples.

3.1 Introduction

Ionophore based ion-selective electrodes have been widely used as a potentiometric sensors for decades. In recent years, researchers have been searching for new techniques to improve ion-selective electrodes performance as well as expand their application. The application of current pulses to ion-selective membranes was introduced as a method of controlling transmembrane ion fluxes, which leads to a variety of novel applications.[138-140] Galvanostatic current control was applied to improve the detection limit of ISEs. The undesirable primary ion leaching from the sensing membrane into the sample, contaminating the sample, was eliminated through controlled ion transport by driving the primary ion flux backwards, i.e., through the membrane into the inner filling solution.[124-128] A voltammetric ISE was developed for the stripping analysis of nanomolar perchlorate in drinking water samples. A constant anodic potential is externally applied to an electrode such that perchlorate is preconcentrated into the thin PVC membrane. After this preconcentration step, the potential is swept to the cathodic direction such that the preconcentrated perchlorate in the membrane phase was stripped into the aqueous sample to obtain the enhanced ionic current response ion-transfer stripping voltammetry with a thin-layer liquid membrane offers the advantages of a lowered detection limit, a response time, and selectivity.[129-130]. Polymeric membrane ion-selective electrode (ISE) for potentiometric sensing were further explored for the detection of biomolecules using enzymes and their inhibitors. The substrate ions released by an external current at the membrane-sample interface are consumed by reaction with the enzyme in solution or immobilized on the surface of the membrane, which can be sensed potentiometrically. This approach is applied to the detection of both free and labeled enzymes in biosensors

and enzyme immunoassays.[131]

The vast majority of electroanalytical measurements are performed with reference electrodes separated from samples by salt bridges. Unfortunately, salt bridges have several disadvantages. When used in real life samples, they clog with proteins and lipids, suffer from contamination by sample components, and because they rely on comparatively large ion fluxes into the samples, they can considerably contaminate small volume samples.[97-98] In continuous measurements, salt bridges eventually run out of electrolyte, which is a problem particularly for miniaturized devices. In a routine laboratory setting, such problems can be counteracted by frequent flushing of reference electrodes with cleaning solutions, free flowing liquid junctions, and regular replenishing of salt bridge solutions.[123] These options are cumbersome enough in a laboratory setting, but they are difficult to implement in many real life scenarios, such as in intensive care units at hospitals or at remote environmental monitoring stations. Clearly, other options to the reference electrode problem are needed.

Hydrophobic polymeric membranes doped with an ionic liquid[103-107] or different hydrophilic salts were suggested[91, 93, 108-109] to fabricate liquid junction free reference electrode. The electrodes distinguish themselves from a reference electrode with a conventional salt bridge by the elimination of the sample/salt bridge interface, which is an interface of two *miscible* electrolyte solutions that exhibits a liquid junction potential.[110] Instead, the interface of the sample and the reference electrode is an interface between two immiscible phases, i.e., the aqueous sample and a hydrophobic ion-doped polymeric membrane. The salts or ionic liquids incorporated into these hydrophobic reference electrode membranes are slightly soluble in water. As they continuously leach

at a small rate into the sample solution, a local equilibrium of salt or ionic liquid distribution between the reference membrane and aqueous phase is established.[111] This ideally results in an interfacial potential that does not depend on the composition of the sample. While several reports of reference electrodes with hydrophobic ion-doped polymeric membranes have been described in the literature, only few applications of such reference electrodes for measurements in real life samples have been reported. A study using a reference electrode membrane doped with the ionic liquid 1-methyl-3-octylimidazolium bis(trifluoromethylsulfonyl)imide and three-dimensionally ordered macroporous (3DOM) carbon as solid contact successfully measured pH in milk.[105]

Previously, we successfully applied the current pulse to an ion exchanging membrane to transform it to a reference electrode used in serum.[141] In contrast to efforts aimed at lowering the detection limits for analyte ions, we use current pulses to "worsen" (i.e., increase) detection limits, causing the reference electrodes to respond only to the ions released by the pulse. The composition of such reference membranes has to be carefully optimized for individual samples. Here, we report the current pulse method of operating reference electrodes with an ionophore (valinomycin) based hydrophobic ion-doped polymeric membranes. It involves the application of a current pulse or potential pulse to facilitate ion transfer between an aqueous phase and the membrane phase,[122, 142-147] thereby controlling transmembrane ion fluxes to obtain a sample independent reference electrode potential.

3.2 Experimental Section

3.2.1 Materials

Deionized water (0.18 MΩ m specific resistance) was purified with a Milli-Q PLUS reagent grade water system (Millipore, Bedford, MA) and used for the preparation of all sample solutions. Valinomycin was purchased from Sigma Aldrich (St. Louis, MO). High molecular weight poly(vinyl chloride (PVC), 2-nitrophenyl octyl ether (o-NPOE), potassium tetrakis(4-chlorophenyl)borate (KTpClPB), and tetradodecylammonium tetrakis(4-chlorophenyl)borate (ETH500) were purchased from Fluka (Buchs, Switzerland).

3.2.2 Electrode Membrane Preparation

Master membranes were prepared from 66 mg PVC, 132 mg *o*-NOPE, 2.8mg valinomycin, 0.6 mg KTpClPB, and 20 mg ETH500. Tetrahydrofuran (THF) was used to dissolve all the membrane components, and the resulting solution was poured into a glass dish (32 mm i.d.). The THF was then allowed to evaporate overnight at room temperature. Individual membranes were cut out of the master membrane and glued with THF onto the end of a Tygon tube (3/16 inch, i.d.; 5/16 inch, o.d.). An inner filling solution of 1.0 mM KCl was filled into the Tygon tube, and a AgCl coated Ag wire was inserted into the solution as inner reference electrode. The thus mounted membrane was conditioned in 1.0 mM KCl.

3.2.3 Electrochemical Measurements

A Solartron SI 1287 electrochemical interface (Boston, MA) was used to apply current pulses, measure open circuit potentials, and perform cyclic voltammetry. Current pulses were programmed with CorrWare software (Scribner Associates, Southern Pines, NC). A four-electrode system was used as follows: A Pt wire and a AgCl-coated Ag wire were inserted as counter and reference electrodes, respectively, into the inner filling solution of the membrane-based reference electrode. A Pt counter electrode and a conventional double-junction reference electrode (DX200, Mettler Toledo, OH; 3.0 M KCl saturated with AgCl as inner filling solution and 1.0 M LiOAc as bridge electrolyte) were inserted into the sample. All EMF values of measurements involving this conventional reference electrode were corrected with the Henderson equation[132] for liquid-junction potentials at the interface of its salt bridge and the sample except for serum samples. Activity coefficients were calculated as described in ref.[133]

3.3 Results and Discussions

3.3.1 Current Parameters

For an experimental proof of concept, poly(vinylchloride) membranes plasticized with nitrophenyl octyl ether were loaded with valinomycin, a K^+ ionophore, and, to lower the electrical membrane resistance, tetradodecylammonium tetrakis(4-chlorophenyl)-borate (ETH500). The membranes were then mounted onto electrode bodies as they are used commonly for ISEs,[122] and the electrodes were preconditioned in the same KCl solution that was also used as the inner filling solution of the reference electrodes. A

four-electrode system was used to ensure that potential measurements were not affected by concentration polarization.

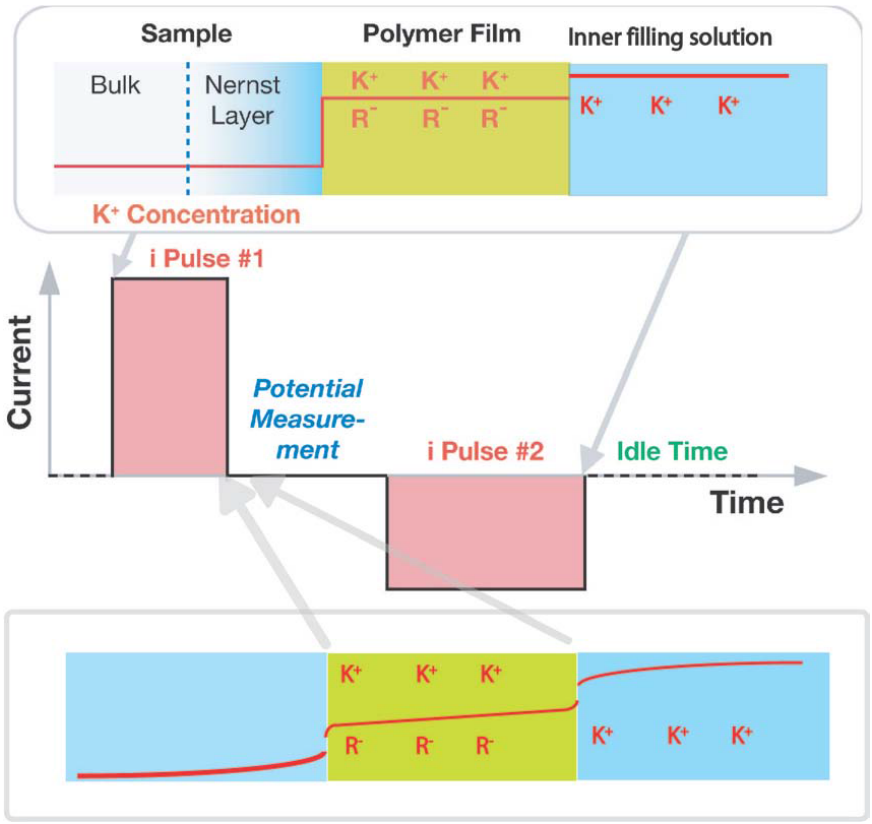

Figure 1. Schematic illustration of pulse mode operation. Top and bottom: K^+ concentration profiles through the sample, reference membrane, and inner filling solution before and after the current pulse. A typical pulse of current in the direction from the inner filling solution to the sample releases K^+ into the sample.

The mode of operation of these reference electrodes is illustrated in Figure 1. A current pulse is applied to the membrane, resulting in the release of K^+ from the membrane into the (unstirred) Nernst layer of the real sample. This current pulse serves an analogous purpose as the controlled release of ions in coulometric titrations, in which a known amount of reagent is accurately released into the sample. In this regard, current

pulses are preferable over potential pulses. Immediately after the current pulse, the potentiometric measurement is performed, and the membrane based electrode ideally behaves as the reference electrode whose potential does not depend on the sample composition, but only on the activity of the K^+ released by the current pulse into the Nernst layer. This K^+ will not have had enough time to diffuse away from the sensor surface into the bulk of the sample yet, and, because of the membrane's selectivity for K^+, the electrode ideally only exhibits a response for the released K^+ rather than for ions originally present in the sample. After the potentiometric measurement, the polymer membrane is allowed to recover, restoring the original concentration profile.

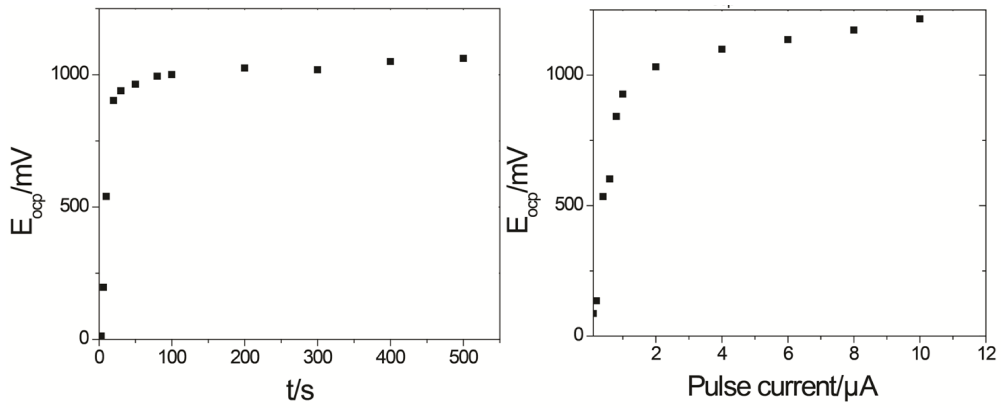

Figure 2. Open circuit potential response in 0.1 mM KCl. Right: versus pulsed current magnitude after 30 s pulse time. Left: versus duration of pulsed length of 10^{-6} A. All the data are selected immediately after the current pulse.

The solution of Fick's second law gives the concentration of the potassium ions in the sample on the solution side of the sample/membrane interface after *t* period pulse of *i* current is applied. (Details of solutions and boundary conditions can be found in Supporting Information)

$$C_{K^+samplesolution}(0,t) = C^*_{K^+samplesolution} + \frac{2it^{1/2}}{nFAD^{1/2}_{K^+solution}\pi^{1/2}} \quad (1)$$

where n is the charge of K^+, F and π have their regular values, and A is the area of the membrane. $C_{K^+samplesolution}(0,t)$ refers to the K^+ concentration on the sample solution side at the distance zero from the sample solution/membrane interface at time t. $D_{K^+,solution}$ is the diffusion coefficient of K^+ in water. The concentration of the ionophore-K^+ complex on the membrane side at the interface is,

$$C_{complex1}(0,t) = C^*_{complex1} - \frac{2it^{1/2}}{nFAD^{1/2}_{complex}\pi^{1/2}} \quad (2)$$

$$C_{valinomycin}(0,t) = C^*_{valinomycin1} + \frac{2it^{1/2}}{nFAD^{1/2}_{complex}\pi^{1/2}} \quad (3)$$

where $D_{complex}$ is the diffusion coefficient of the ionophore-K^+ complex in the membrane.

When the K^+ is complexed with valinomycin, the K^+ concentration on the membrane side can be determined,

$$K^+ + Valinomycin \rightarrow Complex$$

$$\frac{C_{Complex1}}{C_{K^+membrane1} \times C_{valinomycin}} = K_A \Rightarrow C_{K^+membrane1} = \frac{C_{Complex1}}{K_A \times C_{valinomycin}} \quad (4)$$

$$C_{K^+membrane1}(0,t) = \frac{\left(C^*_{complex} - \frac{2it^{1/2}}{nFAD^{1/2}_{complex}\pi^{1/2}}\right)}{K_A \times \left(C^*_{valinomycin} + \frac{2it^{1/2}}{nFAD^{1/2}_{complex}\pi^{1/2}}\right)} \quad (5)$$

So the phase boundary potential at the sample solution/membrane interface can be determined:

$$E_1 = E^0 + 2.303\frac{RT}{zF}\log\frac{C_{K^+samplesolution}(0,t)}{C_{K^+membrane1}(0,t)} \quad (6)$$

Similarly, the potential at the membrane/inner filling solution interface can be calculated as

$$C_{K^+innerfillingsolution}(0,t) = C^*_{innnerfillingsolution} - \frac{2it^{1/2}}{nFAD^{1/2}_{K^+}\pi^{1/2}} \quad (7)$$

$$C_{K^+membrane2}(0,t) = \frac{C^*_{Complex1} + \frac{2it^{1/2}}{nFAD^{1/2}_{complex}\pi^{1/2}}}{K_A \times \left(C^*_{valinomycin} - \frac{2it^{1/2}}{nFAD^{1/2}_{complex}\pi^{1/2}}\right)} \quad (8)$$

$$E_2 = E^0 + 2.303\frac{RT}{zF}\log\frac{C_{K^+membrane2}(0,t)}{C_{K^+innerfillingsolution}(0,t)} \quad (9)$$

The total potential at the sample solution/membrane interface and at the membrane/inner filling solution interface can be obtained

$$E_{ocp} = E_1 + E_2 \rightarrow E_{ocp} \propto 2.303\frac{RT}{zF}\left(\log\frac{C_{K^+samplesolution}(0,t)}{C_{K^+membrane1}(0,t)} + \log\frac{C_{K^+membrane2}(0,t)}{C_{K^+outerfillingsolution}(0,t)}\right) \quad (10)$$

All fits and calculations were performed with Mathematica 8.0 (Wolfram Research, Champaign IL).

E_{ocp} has a greater dependence on both i and t for 30 s pulses in a low range of 0.1-2 μA current and of 3-100s of 1 μA amplitude; this dependence decreased in a higher range of current or pulse length, respectively (Figure 2). Understandably, E_{ocp} increases with i and t based on equation 10 because the accumulation of K^+ ions on one side at the interface leads to the increase of $C_{K^+ samplesolution}(0,t)$ and $C_{K^+ membrane2}(0,t)$ and the depletion on the other side lead to the decrease of $C_{K^+ membrane1}(0,t)$ and $C_{K^+ outerfillingsolution}(0,t)$. This causes the increase of E_{ocp}. The leveling off of E_{ocp} at higher current magnitude and longer pulse length could originate from two sources. One is the depletion of the ionophore as K^+ enters into the membrane on the membrane side of membrane/inner filling solution interface, which is illustrated in Figure 3. Free ionophores are depleted on the membrane side at the second interface (left side in Figure 3). The open circuit potential begins to plateau at a current of 2 μA or at the pulse length of 40 s, which corresponds to the depletion point of free ionophore at the second interface in the model.

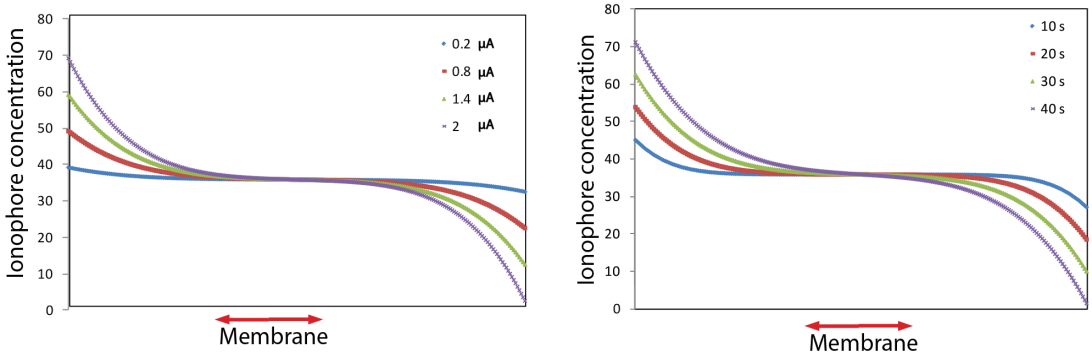

Figure 3. Numerical analysis of concentration profile of free ionophore within the membrane (the numerical analysis was performed in Comsol 4.2).

3.3.2 Ion Transfer

Two charge carriers may cross the two interfaces of the hydrophobic reference membrane and the adjacent two aqueous phases (i.e., the sample and the inner filling solution). For example, a current flowing from the inner filling solution towards the sample may cause at large applied potentials K^+ transfer from the membrane into the aqueous sample and chloride transfer from the sample into the membrane. The cyclic voltammogram shown in Figure 4 shows at which potentials the phase transfer of specific ions occurs. The peak at 210 mV (positive current) is associated with K^+ transfer from the membrane into the sample, coupled with K^+ transfer from the inner filling solution into the membrane.[135-136] The peak on the return scan (negative current) is caused by K^+ transfer at both interfaces of the reference membrane to aqueous solutions, but in a direction opposite from that of the forward scan. Potentials over +520 mV result in the interfacial transfer of anions, i.e., chloride.

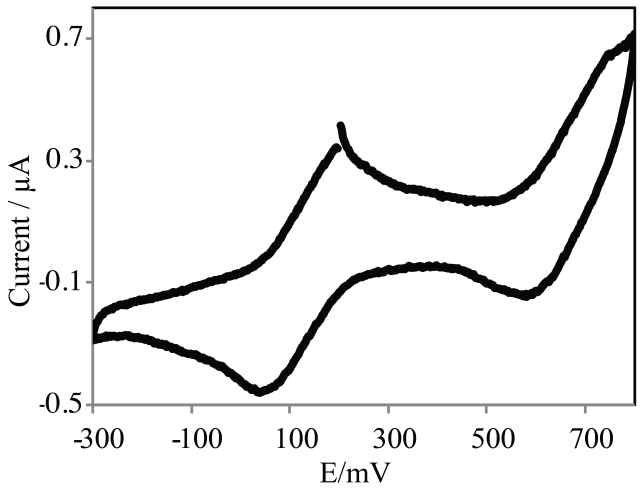

Figure 4. CV Resistance corrected cyclic voltammogram of a valinomycin based membrane with 1 mM KCl as both inner filling solution and 10 mM KCl as sample solutions. Potential sweep rate: 0.01 V/s. E vs Ag/AgCl; bridge electrolyte: 1 M LiOAc.

Interestingly, the Cl^- transfer into the membrane could transform the K^+-selective electrode into a Cl^--selective electrode. (Figure 5) When applied a current of 1 μA and 30 s was applied, the electrodes started to show an anion response with a slope of -56.4 mV / decade. By keeping a constant Cl^- concentration, the response potential did not change, indicating a Cl^- response. It was possibly because local cationic sites were created at the interface, which changed the permselectivity of the membrane.

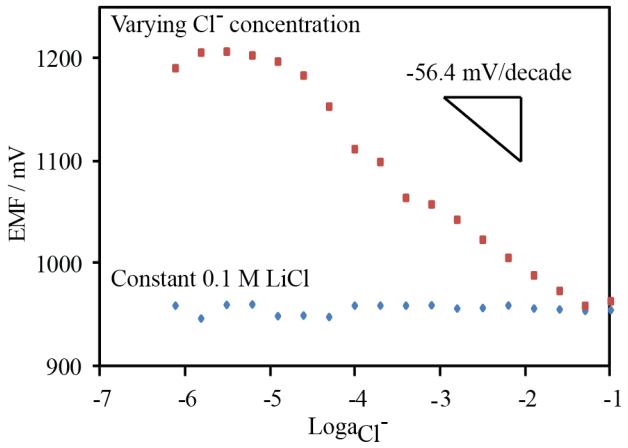

Figure 5. Emf response immediately after a current pulse of 0.1 μA and 30 s when varying the Cl^- concentration and keeping a constant Cl^- concentration.

In order to obtain a constant potential as the mechanism indicates, the ion transfer at the interface has to be carefully tuned. By preventing the potential from exceeding into Cl^- transfer range, the current pulse length and magnitude should be limited. Figure 6 shows the constant potential concentration range is shifted to a higher value as the current

length and magnitude increase due to an increasing amount of released K^+. However, we could not obtain a higher range because Cl^- transfer might happen if the applied potential exceeds a threshold limit. Potential pulse at a certain level can limit the species of charge carriers across the interface. Thus, a potential pulse was selected so that K^+ is the only carrier of charge across the sample/membrane interface. With 20 s potential pulses of 0.45 V, a stable potential is obtained in the range of 0.1 M and 0.1 mM KCl. (Figure 7)

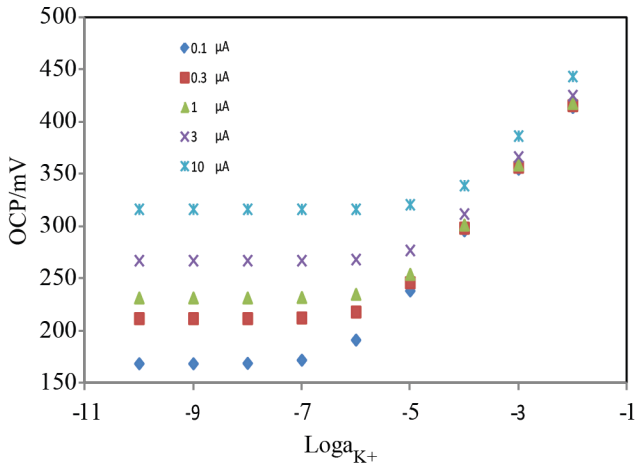

Figure 6. Open circuit potential (OCP) immediately after current pulse of 5 s and 0.1 µA, 0.3 µA, 1 µA, 3 µA and 10 µA amplitude as a function of the in K^+ concentration in the sample.

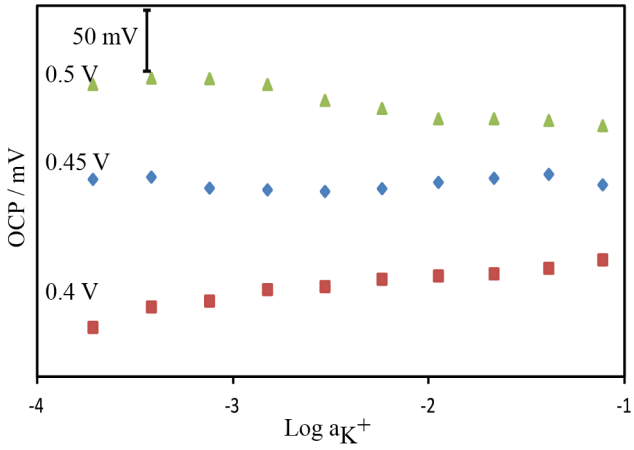

Figure 7. Open circuit potential (OCP) immediately after potential pulses of 20 s length and 0.5 V, 0.45 V or 0.4 V amplitude as a function of the K^+ concentration in the sample.

3.3.3 Water Uptakes of PVC Membranes

The long term stability of this type of reference electrode was evaluated by monitoring the OCP in 10 mM KCl within a month. (Figure 8) The OCP increased during the first 12 days but leveled off from day 12 to 1 month. Experiments also showed that the OCP of the membrane was not affected when it was stored dry for several months so the OCP change was solely from the water exposure. The increase is probably due to the water uptake by PVC membrane, which directly affects the diffusion of ions in the membrane. This change was also verified by cyclic voltammetry (Figure 9) and impedance (Figure 10) of the membrane. The peak current for the new membranes is almost 10 times smaller than for membranes that had been kept in solution for 3 weeks, indicating an increasing resistance over time. Water uptake also leads to an increase in the membrane impedance (Figure 10). Interestingly, the impedance increase of the PVC membranes was found to be permanent because the impedance stayed the same when

membranes were completely dried and reconditioned in 1 mM KCl for one day. This indicates that the membrane structure has been changed and water molecules probably reorganize around hydrophilic clusters.

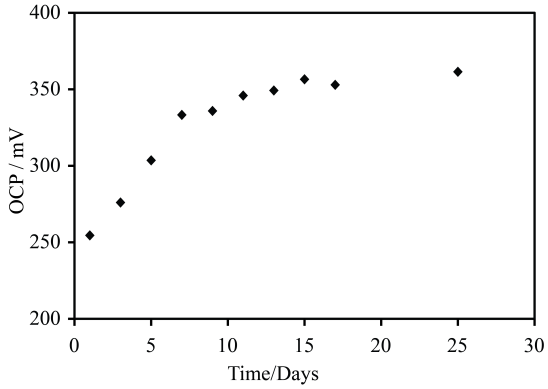

Figure 8. The open circuit potential immediately after the pulse (20s and 0.4 V) in 10 mM KCl within 1 month

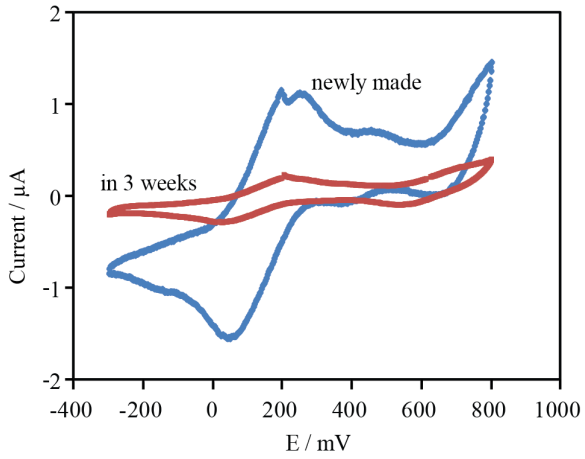

Figure 9. Cyclic voltammogram (resistance is not corrected) of a valinomycin based membrane with 1 mM KCl as both inner filling solution and 10 mM KCl as sample solutions. Potential sweep rate: 0.01 V/s. E vs Ag/AgCl; bridge electrolyte: 1 M LiOAc. Blue: newly made membrane, Red: membrane kept in 1 mM KCl for 3 weeks.

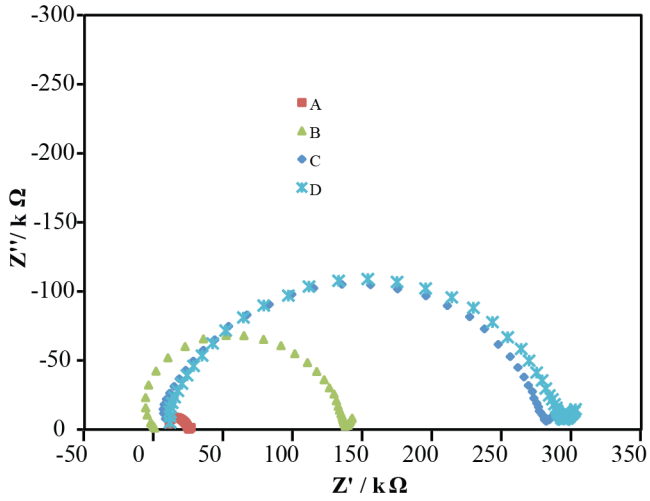

Figure 10. Impedance spectrum of a valinomycin based membrane with 0.1 M KCl as both inner filling solution and sample solution over time. (A) Newly made electrode conditioned in 10mM KCl for 1 day; (B) electrode conditioned in 10mM KCl solution for 2.5 weeks; (C) electrode conditioned in 10mM KCl for 1.5 months; (D) membrane dried on both sides in air for 2 days, electrode refilled with 10 mM KCl and reconditioned in 10 mM KCl for 3 days.

3.4 Conclusions

In summary, this work has shown how a current or potential pulse converted a K^+-selective membrane into an anion-selective electrode and a reference electrode. This suggests a high level of flexibility in the design of reference electrodes with ionophore-doped membranes. The ion transfer has to be finely controlled for each application. The PVC water uptake into plasticized PVC membrane was also investigated, showing a permanent structure change in membranes during water exposure.

3.5 Supporting Information

3.5.1 Diffusion at the Electrode Surface

The diffusion-process of ion transfer between an aqueous phase and a membrane phase is analogous to that of a diffusion-limited redox reaction at an electrode surface, A simple example of Fe^{3+}/Fe^{2+} here is used to demonstrate how a current pulse works in oxidation and reduction processes at the electrode surface. Assume a steady current, *i*, is applied to the working electrode to reduce Fe^{3+} to Fe^{2+} at a constant rate. The potential of the electrode shifts to the typical value of the redox couple and changes with the ratio of the concentration of Fe^{3+} and Fe^{2+}. After the concentration of Fe^{3+} at the electrode surface decreases to zero, there is no sufficient flux of Fe^{3+} ions to accept all the electrons from the electrode to the solution. Then, the potential of the electrode will rapidly shift toward more negative values until a new second reduction process begins.

For the electrochemical process described above, we can consider a simple electron transfer reaction  . The assumptions here are a planar working electrode, an unstirred solution and only species *O* at a concentration C_O^* in the beginning. The linear diffusion equation can be written as Fick's second law[72]:

$$\frac{\partial C_O(x,t)}{\partial t} = D_O\left[\frac{\partial^2 C_O(x,t)}{\partial x^2}\right] \tag{S1}$$

$$\frac{\partial C_R(x,t)}{\partial t} = D_R\left[\frac{\partial^2 C_R(x,t)}{\partial x^2}\right] \tag{S2}$$

where $C_o(x,t)$ and $C_R(x,t)$ are the concentration of species *O* and *R* at the distance x from the electrode surface at time *t* respectively; D_O and D_R are the diffusion coefficient for species *O* and *R* respectively.

With the boundary condition:

$$\begin{aligned} &C_O(x,0) = C_O^* && C_R(x,0) = 0 \\ &\lim_{x\to\infty} C_O(x,t) = C_O^* && \lim_{x\to\infty} C_R(x,t) = 0 \\ &C_O(0,t) = 0 && C_R(0,t) = C_R^* \end{aligned} \tag{S3}$$

where C_O^* is the initial concentration of species O and C_R^* is the final concentration of species R.

The flux balance is

$$D_O\left[\frac{\partial C_O(x,t)}{\partial t}\right]_{x=0} + D_R\left[\frac{\partial C_R(x,t)}{\partial t}\right]_{x=0} = 0 \tag{S4}$$

Since the applied current $i(t)$ is already known, the flux at the electrode surface is also know at any time

$$-J_O(0,t) = \frac{i(t)}{nFA} = D_O\left[\frac{\partial C_O(x,t)}{\partial x}\right]_{x=0} \tag{S5}$$

First, derivatives with respect to the transformation variables need to be converted into algebraic expressions in *s*. For species O, Laplace transformation of equation (S1) under the condition of (S3) yields

$$\overline{C_O}(x,s) = \frac{C_O^*}{s} + A(s)\exp\left[-\left(\frac{s}{D_O}\right)^{1/2} x\right] \tag{S6}$$

where s is a function of *t* and regarded as constant for purposes of conversion.

The transform of equation (S5) is

$$D_O\left[\frac{\partial\overline{C_O}(x,s)}{\partial x}\right]_{x=0} = \frac{\bar{i}(s)}{nFA} \tag{S7}$$

Taking the derivative of (S6) and substituting in (S7) we can obtain

$$\overline{C}_O(x,s) = \frac{C_O^*}{s} - \left[\frac{\bar{i}(s)}{nFAD_O^{1/2}s^{1/2}}\right]\exp\left[-\left(\frac{s}{D_O}\right)^{1/2}x\right] \tag{S8}$$

If $i(t)$is constant, then $i(s) = i/s$and (S8) becomes

$$\overline{C}_O(x,s) = \frac{C_O^*}{s} - \left[\frac{i}{nFAD_O^{1/2}s^{3/2}}\right]\exp\left[-\left(\frac{s}{D_O}\right)^{1/2}x\right] \tag{S9}$$

The inverse transform of this equation yields

$$C_O(x,t) = C_O^* - \frac{i}{nFAD_O}\left\{2\left(\frac{D_Ot}{\pi}\right)^{1/2}\exp\left(-\frac{x^2}{4D_Ot}\right) - xerfc\left[\frac{x}{2\left(D_Ot\right)^{1/2}}\right]\right\} \tag{S10}$$

$C_O(0,t)$ can be obtained by setting x=0 in equation (26)

$$C_O(0,t) = C_O^* - \frac{2it^{1/2}}{nFAD_O^{1/2}\pi^{1/2}} \tag{S11}$$

At the transition time, τ , $C_O(0,t)$ drops to zero and it yields the Sand equation

$$\frac{i\tau^{1/2}}{C_O^*} = \frac{nFAD_O^{1/2}\pi^{1/2}}{2} \tag{S12}$$

If the flux of *O* is large enough to satisfy the applied current within the transition time,

equation (S10) can be written in dimensionless forms of $\frac{C_O(x,t)}{C_O^*}$, t/τ and $\chi_O = \frac{x}{2\left(D_Ot\right)^{1/2}}$

$$\frac{C_O(x,t)}{C_O^*} = 1 - \left(\frac{t}{\tau}\right)^{1/2}\left[\exp\left(-\chi_O^2\right) - \pi^{1/2}\chi_O erfc\left(\chi_O\right)\right] \tag{S13}$$

$$\frac{C_O(0,t)}{C_O^*} = 1 - \left(\frac{t}{\tau}\right)^{1/2} \tag{S14}$$

Similarly, for R

$$\frac{C_R(x,t)}{C_O^*} = \xi\left(\frac{t}{\tau}\right)^{1/2}\left[\exp\left(\chi_R^2\right) - \pi^{1/2}\chi_R erfc\left(\chi_R\right)\right] \tag{S15}$$

where $\chi_R = \frac{x}{2\left(D_R t\right)^{1/2}}$ and $\xi = \left(\frac{D_O}{D_R}\right)^{1/2}$

Combination with equation (S14) yields

$$C_R(0,t) = \frac{2it^{1/2}}{nFAD_R^{1/2}\pi^{1/2}} = \xi\left(\frac{t}{\tau}\right)^{1/2} C_O^* \tag{S16}$$

CHAPTER FOUR

Solid Contact Ion-Selective Electrodes With a Well- Controlled Co(II)/Co(III) Redox Buffer Layer

In part from:

Xu U. Zou, Jia H. Cheong, Brandon J. Taitt, and Philippe Bühlmann. *Analytical Chemistry* **2013**, 127(25), 8958-8959.

Reproduced in part with permission from Analytical Chemistry, 127(25), 8958.

Copyright © 2005 American Chemical Society.

Abstract

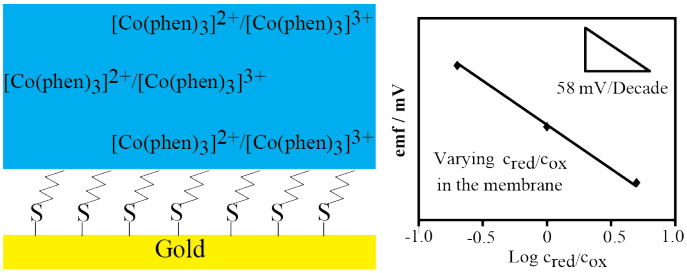

Solid contact ion-selective electrodes (ISEs) typically have an intermediate layer between the ion-selective membrane and the underlying solid electron conductor that is designed to reduce the irreproducibility and instability of the measured electromotive force (emf). Nevertheless, the electrode-to-electrode reproducibility of the emf of current solid contact ISEs is widely considered to be unsatisfactory. To address this problem, we report here a new method of constructing this intermediate layer based on the lipophilic redox buffer consisting of the Co(III) and Co(II) complexes of 1,10-phenanthroline ($[Co(phen)_3]^{3+/2+}$) paired with tetrakis(pentafluorophenyl)borate as counterion. The resulting electrodes exhibit emf values with an electrode-to-electrode standard deviation as low as 1.7 mV after conditioning of freshly prepared electrodes for 1 hour. While many prior examples of solid contact ISEs also used intermediate layers that contained redox active species, the selection of a balanced ratio of the reduced and oxidized species has typically been difficult and was often ignored, contributing to the emf irreproducibility. The ease of the control of the $[Co(phen)_3]^{3+}$ / $[Co(phen)_3]^{2+}$ ratio explains the high emf reproducibility, as confirmed by the emf decrease of 58 mV per tenfold increase in the ratio of the reduced and oxidized redox buffer species. Use of a gold electrode modified with a self-assembled 1-hexanethiol monolayer as underlying electron conductor suppresses the

formation of a water layer and results in an electrode-to-electrode standard deviation of E^o of 0.7 mV after at least 1 week of exposure to KCl solution.

4.1 Introduction

Ion-selective electrodes (ISEs) are widely used in clinical diagnostics, process control, and environmental monitoring.[1, 9, 120, 122, 148] In view of implantable devices, measurements in small volumes, and mass production, the miniaturization of these devices has drawn a lot of attention. However, difficulties in minimizing and stabilizing the volume of the internal electrolyte solution impede the successful miniaturization of conventional ISEs.[4-5] Consequently, the development of solid contact electrodes with an ion-selective membrane directly attached onto a solid substrate has attracted considerable interest.[5-9] The design of solid contacts poses its own challenges, though, as it must avoid the formation of a water layer at the interface between the ion-selective membrane and the solid substrate.[16, 45, 149-151] Moreover, the phase boundary potential at the interface of the ISE membrane and the solid substrate must be stable for measurements over extended time periods, and its value must be reproducible from electrode to electrode, or else each electrode needs to be calibrated individually.

Efforts from various research groups have addressed these problems. In particular, conducting polymers such as polypyrrole,[21-23, 25, 27, 32] polythiophene,[20, 35, 39, 43-45] and polyaniline[44, 47, 49] derivatives are widely used as an intermediate ion-to-electron transducer layer between the ion-selective membrane and the underlying electron conductor.[4] More recently, the use of carbon materials with large surface areas, such as three-dimensionally ordered macroporous (3DOM) carbon,[58-59] carbon nanotubes,[55-56, 92]

fullerene,[60] and graphene,[61-62] was proposed. In these latter cases, the high capacitances of the ISE membrane/carbon interfaces minimize drifts in the measured potential.

Although several of the conducting polymer and carbon intermediate layers effectively prevent the formation of a water layer, significantly improving the life time of solid contact sensors,[5] the electrode-to-electrode reproducibility of the interface between the ISE membrane and the underlying electron conductor continues to be a challenge. The ill-defined interfacial potential at this interface often depends on oxygen and other redox-active components of the sample.[152] To address this issue, it has been suggested that the ion-to-electron transducer layer exhibit redox buffer capacity. In analogy to the well-known pH buffers, which resist changes in pH upon addition of moderate amounts of acid or bases, redox buffers maintain a stable and reproducible potential in the presence of oxidizing or reducing impurities or when small electrical currents pass through an electrochemical cell.[153] Solid contacts specifically designed to contain both the oxidized and reduced form of a redox couple include systems containing Ag^+ ionophore complexes on a silver epoxy substrate,[18-19] redox-active self-assembled monolayers (SAMs) with a redox potential controlled by an applied current,[116] and mixtures of gold nanoclusters with two different charge states.[117] None of these systems is without its weakness, though. The extension of the $Ag^{+/0}$ system to samples containing no Ag^+ or to ISE membranes doped with different ionophores has not been reported. The redox buffer capacity of redox active SAMs is small. Also, the charging of the gold nanoclusters is technically not trivial, and it has not been confirmed experimentally that the interfacial potential between the nanocluster layer and the underlying substrate follows the Nernst equation. Finally, while ferrocene tagged polymers have interesting

applications, for example, in ion transfer voltammetry,[154-155] the use of ferrocene/ferrocenium redox buffers to improve the emf stability for potentiometric purposes is limited by the instability of ferrocenium in the presence of molecular oxygen.[156]

Here we report a well-controlled redox couple prepared from the tetrakis(pentafluorophenyl)borate ($TPFPB^-$) salts of cobalt(II)tris(1,10-phenanthroline) ($[Co(phen)_3]^{2+}$) and cobalt(III)tris(1,10-phenanthroline) ($[Co(phen)_3]^{3+}$) and their use to dope a plasticized poly(vinyl chloride) (PVC) layer drop-casted onto gold or glassy carbon electrodes. This redox couple shows electrode potentials with a standard deviation as low as 0.7 mV. Moreover, the electrode potential depends on the ratio of the $[Co(phen)_3]^{2+}$ and $[Co(phen)_3]^{3+}$, as predicted by the Nernst equation, i.e., with a slope of –58 mV per tenfold increase in the ratio of these two species. In order to prevent the formation of a water layer, self-assembled monolayers of 1-hexanethiol were formed on the gold contacts prior to coating with the plasticized PVC layer doped with the redox couple. This hybrid system combines the hydrophobicity of the alkanethiol with the buffer capacity of the redox couple, successfully suppressing the water layer formation and generating reproducible potentials.

4.2 Experimental Section

4.2.1 Materials

All reagents were of the highest commercially available purity and were used as received. Deionized water (0.18 MΩ m specific resistance) was purified with a Milli-Q PLUS reagent grade water system (Millipore, Bedford, MA) and was used for preparing

all sample solutions. 1-Hexanethiol was purchased from Acros Organics (Geel, Belgium). High molecular weight poly(vinyl chloride) (PVC) and 2-nitrophenyl octyl ether (*o*-NPOE) were purchased from Fluka (Buchs, Switzerland), lithium tetrakis(pentafluorophenyl)borate ethyl etherate from Boulder Scientific (Boulder, CO), ammonium hexachloroosmate(IV) from Alfa Aesar (Ward Hill, MA), and ammonium tetrakis(3-chlorophenyl)borate, bis(pentamethylcyclopentadienyl)iron(II), 2,2'-bipyridyl, and 1,10-phenanthroline from Sigma Aldrich (St. Louis, MO). Elemental analyses were performed by MHW Laboratories (Phoenix, AZ). ^{1}H NMR spectroscopy was performed with a VAC-300 Varian Mercury spectrometer (Varian, Palo Alto, CA).

4.2.2 Electrode Fabrication

The 1 mm diameter gold electrodes were polished over polishing cloths with aqueous dispersions of alumina (0.3 and 0.05 μm, Buehler, Lake Bluff, IL) and then cleaned in piranha solution (concentrated sulfuric acid and 30% hydrogen peroxide solution in a 3:1 ratio). *Caution: piranha solution is a strong oxidizing reagent, is highly corrosive, and should be handled with care.* The 3 mm diameter glassy carbon electrodes were polished over polishing cloths with aqueous dispersions of alumina (0.3 μm). The electrodes were then cleaned by ultrasonication in water and ethanol, and dried with a flow of nitrogen. For the formation of a 1-hexanethiol self-assembled monolayer (SAM), the gold electrodes were immersed into 1 mM 1-hexanethiol solutions in ethanol for 24 hours.

Solvent polymeric membranes doped with a redox couple were prepared by dissolving the membrane components (66 mg PVC as polymer matrix, 132 mg *o*-NPOE

as plasticizer, 0.6 mg LiTPFPB ethyl etherate to provide anionic sites, and various amount of $[Co(II)(phen)_3](TPFPB)_2$ and $[Co(III)(phen)_3](TPFPB)_3$) in 500 μL freshly distilled tetrahydrofuran (THF). 40 μL of the above cocktail was drop-casted onto bare or SAM-modified gold or glassy carbon electrodes and left to dry overnight. The electrodes prepared in this way were conditioned in 1.0 mM KCl solution for 1 hour prior to measurements. The short conditioning time ensures that there is no water layer effect that might interfere with the observation of the redox capacity.

4.2.3 Potentiometric Measurements

Potentials were measured with an EMF 16 potentiometer (input impedance 10 TΩ) controlled with EMF Suite 1.03 software (Lawson Labs, Malvern, PA). A double-junction type external reference electrode (DX200, Mettler Toledo, Switzerland; 3.0 M KCl saturated with AgCl as inner filling solution and 1.0 M LiOAc as bridge electrolyte) was used. All ISE response times were fast and seemed to be determined only by the speed with which samples could be changed. Activity coefficients were calculated according to a two-parameter Debye-Hückel approximation,[133] and all emf values were corrected for liquid-junction potentials with the Henderson equation.[2]

4.3 Results and Discussions

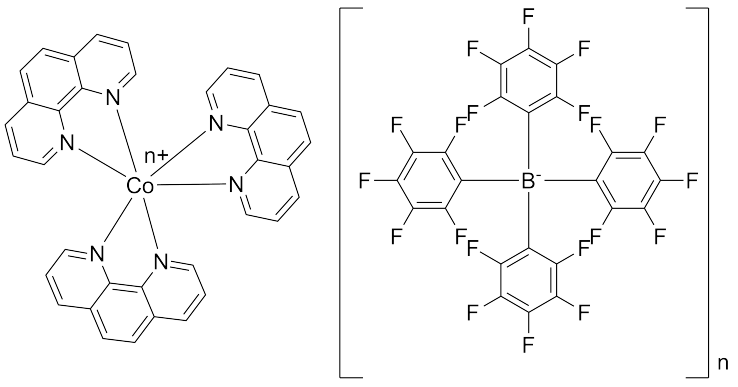

Figure 1. Structure formulas of cobalt(II/III)tris(1,10-phenanthroline) and tetrakis(pentafluorophenyl)borate.

4.3.1 Selection of the Redox Couple

$TPFPB^-$ salts of $[Co(phen)_3]^{3+}$ and $[Co(phen)_3]^{2+}$ (Figure 1) were selected because of their electrochemical stabilities and their high solubility in the plasticized polymeric membrane. Cyclic voltammograms (CVs) of $[Co(phen)_3]^{2+}$ in acetonitrile taken with a scan rate of 100 mV/s show a fully reversible one-electron transfer for the reaction $\left[Co(phen)_3\right]^{3+} + e^- \Leftrightarrow \left[Co(phen)_3\right]^{2+}$, with an oxidation potential of +56 mV vs AgCl/Ag (for a CV, see Figure S2). This confirms a fast rate of the heterogeneous electron transfer. $TPFPB^-$ is oxidized only at potentials larger than +1.0 V, i.e., well above the reduction potential of $[Co(phen)_3]^{3+}$. It follows that $TPFPB^-$ and $[Co(phen)_3]^{3+}$ are stable in the presence of each other.

4.3.2 Reproducibility of Electrode Potentials

To demonstrate the suitability of the $[Co(phen)_3]^{3+/2+}$ redox couple, all solvent polymeric membranes used for this work contained an excess of $TPFPB^-$ (5.40 mmol/kg), making the membranes cation selective. To test the potentiometric response, the emf responses of these solid contact electrodes to K^+ were measured. E^o values of electrochemical cells with these solid contact electrodes versus a conventional reference electrode were obtained by extrapolation of the linear section of the emf response to the K^+ activity of 1.0 M. Control membranes with this ion exchanger but no $[Co(phen)_3]^{3+/2+}$

redox couple exhibited the same poor reproducibility of E^o as it is often observed when no redox couple controls the phase boundary potential at the interface between the polymeric membrane and the underlying electron conductor. Without added redox couple, even the E^o values of electrodes fabricated in one batch under apparently the exact same conditions differed from one another substantially. As shown in Table 1, without a redox couple, the standard deviations of E^o values for electrodes with glassy carbon and gold contact were 23.0 mV and 63.5 mV, respectively. The large variability indicates significant and uncontrolled variations in the concentration of redox impurities at the surface of these solid contacts.

Addition of 0.07 mmol/kg of both $[Co(phen)_3]^{3+}$ and $[Co(phen)_3]^{2+}$ into the plasticized polymer membrane did not reduce the standard deviation substantially, as shown by the standard deviations of E^o of 33.8 mV for glassy carbon and 18.7 mV for gold contacts. Apparently, the redox buffer capacity is not high enough at this concentration level to stabilize the phase boundary potential at the interface of the polymeric cation exchanger membrane and the underlying electron conductor. However, when the total concentration of the redox couple was increased to 1.4 mmol/kg, the standard deviations improved significantly, reaching values of 3.5 mV for the glassy carbon and 1.7 mV for the gold contacts. No further improvements were found when the concentration of the redox couple was increased by another factor of ten (see Table 1).

Table 1. E^o values of different types of electrodes after conditioning for 1 hour in 1.0 mM KCl solution.

	Concentration of redox couple	Glassy carbon n=6		Gold (no SAM) n=3	
Electrode type	Co(II) / Co(III) (each in mmol/kg)	Slope (mV / decade)	E^o (mV)	Slope (mV / decade)	E^o (mV)
1	0	64.1 ± 5.8	121.3 ± 23.0	62.8 ± 3.6	261.5 ± 63.5
2	0.07 / 0.07	61.2 ± 1.5	162.7 ± 33.8	62.5 ± 0.2	252.6 ± 18.7
3	0.70 / 0.70	61.4 ± 0.4	303.5 ± 3.5	61.1 ± 0.2	305.4 ± 1.7
4	7.10 / 7.10	60.9 ± 0.2	323.5 ± 2.3	61.8 ± 0.1	324.4 ± 2.2

All membranes contained besides the redox couple the same components: PVC : o-NPOE (1:2 wt/wt), LiTPFPB: 0.6 wt%. E^o values refer to the potential of the ISE cell as obtained by extrapolation of the linear section of the emf response to the K^+ activity of 1.0 M.

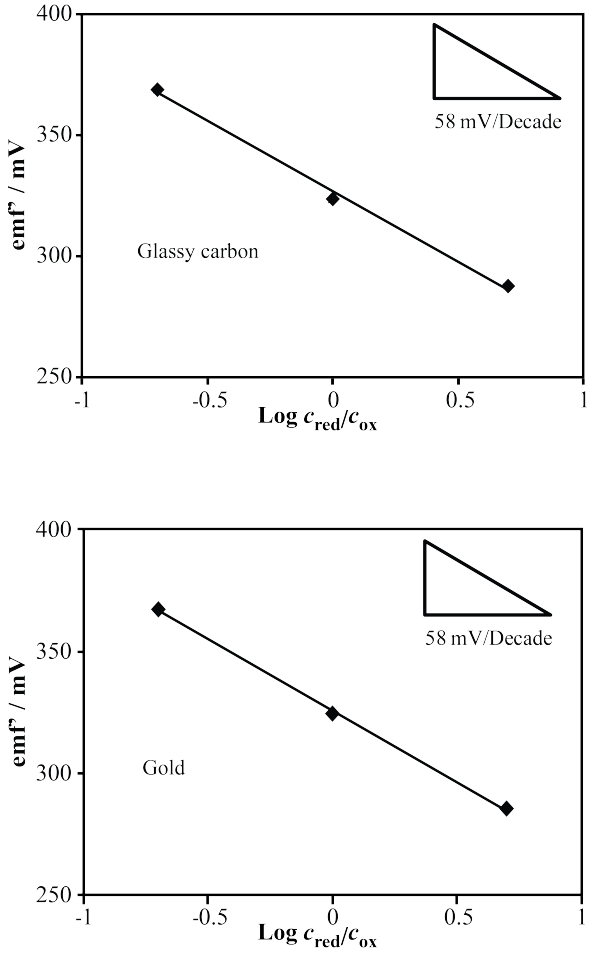

Figure 2. Potential emf' of the ISE cell with electrode type 4 with a glassy carbon or gold substrate, as obtained by extrapolation of the linear section of the emf response to the K^+ activity of 1.0 M. The two graphs illustrate the dependence of emf' on the ratio of the reduced and oxidized components of the redox buffer.

If the phase boundary potential at the interface of the polymeric membrane and the underlying electron conductor is determined by a redox couple, the phase boundary potential at the interface of the ion-selective membrane and the underlying electron

conductor is determined by the ratio of the concentrations of the reduced and oxidized species, as predicted by the Nernst equation and the standard redox potential of the redox couple in the ion-selective membrane. Consequently, the experimentally observed emf' of the electrochemical cell with the ISE at a potassium activity of 1.0 M should depend on the concentrations of the reduced and oxidized species (C_{ox} and C_{red}) of the redox buffer as follows:

$$\text{emf}' = E^{\circ\prime} - \frac{2.303\,\text{R}\,T}{n\,F}\,\text{Log}\,\frac{C_{red}}{C_{ox}}$$

where R is the gas constant, T is the temperature, F is the Faraday constant, n is the number of electrons transferred, and $E^{\circ\prime}$ is the emf of the electrochemical cell with the ISE at a potassium activity of 1.0 M. To confirm this relationship experimentally, polymeric membranes with C_{red}/C_{ox} ratios of 5:1, 1:1, and 1:5 were prepared. The emf' values of these electrodes were found to depend on log (C_{red}/C_{ox}) with a slope of –58.1 mV/decade for glassy carbon contacts (n = 6) and –58.5 mV/decade for gold contacts (n = 3), which is in excellent agreement with the Nernst equation (Figure 2).

Table 1 also shows that, for a sufficiently high redox buffer concentration, the experimentally observed values of $E^{\circ\prime}$ for the SAM modified gold contact electrodes do not differ from those of the glassy carbon electrodes. Since standard redox potentials do not depend on the type of electrode use, this is further evidence that the phase boundary potential between the ion-selective membrane and the solid contact is determined by the redox buffer.

Polymer membranes doped with only one reduced or oxidized form of a redox buffer were also prepared to assess their effectiveness in stabilizing the electrode potential. When polymer membranes were doped with the reduced compound

bis(pentamethylcyclopentadienyl)iron(II) at the same concentration as for membranes of Type 4 in Table 1, the standard deviation of E^o was found to be 35.2 mV for glassy carbon and 11.8 mV for gold contacts. For membranes doped with the alternative reduced compound $[Os(II)(bpy)_2](TmClPB)_2$, the standard deviation of E^o was 8.5 mV for glassy carbon and 13.8 mV for gold contacts. As expected for a system that contains either only a reduced species or only an oxidized species but not both (i.e., no redox buffer), these standard deviations are much larger than for the sufficiently concentrated $[Co(phen)_3]^{3+/2+}$ buffer. Interestingly, the standard deviations of E^o of polymer membranes doped only with $[Co(II)(phen)_3](TPFPB)_2$ was surprisingly small, i.e., 2.6 mV for glassy carbon and 0.5 mV for gold contacts. Since the standard redox potential of the $[Co(phen)_3]^{3+/2+}$ couple is 458 mV lower than for the $[Os(bpy)_3]^{3+/2+}$ couple (see Figures S2 and S3), it may be that some impurities in the membranes doped with $[Co(II)(phen)_3](TPFPB)_2$ are reduced by $[Co(II)(phen)_3]^{2+}$, resulting in the formation of $[Co(II)(phen)_3]^{3+}$ and, thereby, the in situ formation of a redox buffer.

4.3.3 Effects of Oxygen and Light

The possible interference from oxygen needs to be considered since this gas easily permeates plasticized PVC membranes. For example, it has been reported that oxygen can form a half cell at the surface of platinum[14, 157] which affects the boundary potential. To investigate the possibility of oxygen interference, solid contact electrodes with polymer membranes doped with redox buffer were immersed into 100 mM KCl solutions, and O_2 and Ar were bubbled alternatingly into the sample solution while recording the emf. As shown in Figure 3, no significant potential changes were observed. In

comparison, a drift of 25 mV/h upon O_2 exposure was reported in the literature for polypyrrole-coated glassy carbon electrodes coated with a valinomycin-doped solvent polymeric membrane.[37]

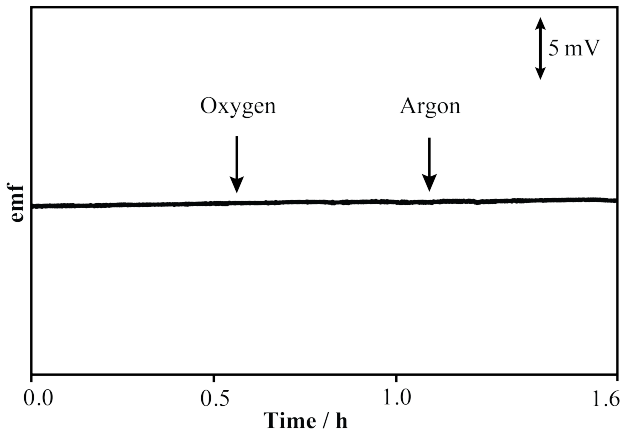

Figure 3. Effect of oxygen on the potential stability of a solid contact ISE of Type 4 (glassy carbon) immersed into a 100 mM KCl solution.

Solid contact ISEs with polymeric membranes doped with a redox couple can be expected to be photoresponsive if the redox couple and the underlying metal electrode exhibit a suitable band gap permitting the excitation of an electron either from the reduced species of the redox buffer to the electrode, or from the metal electrode to the oxidized species of the redox buffer. To investigate the possibility of light sensitivity, electrodes with polymer membranes doped with $[Co(phen)_3]^{3+/2+}$ were inserted in a 100 mM KCl solution in the dark, and the emf was continuously recorded as ambient room light was turned on for 20 min (see Figure 4). No significant effect of the room light was observed, indicating that the redox couple based layer is insensitive to light.

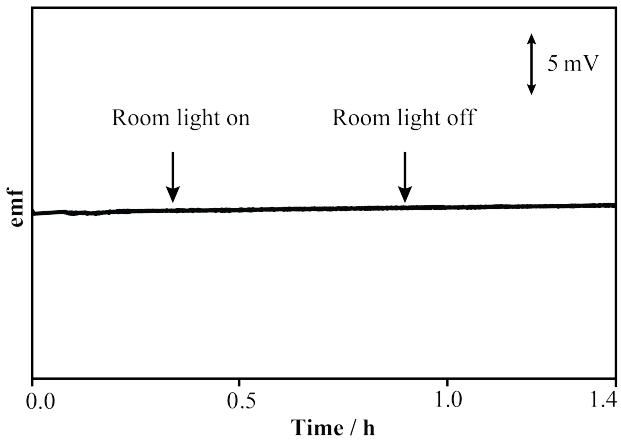

Figure 4. Effect of light on the potential stability of a solid contact ISE of Type 4 (glassy carbon) immersed into a 100 mM KCl solution

4.3.4 Polymeric Membranes Doped with a Redox Couple in Contact with Gold Contacts Modified with a Self-Assembled Alkanethiol Monolayer

The formation of an aqueous layer between the polymeric membrane and an underlying solid contact such as gold or glassy carbon not only causes mechanical failure but also results in chemical hysteresis caused by the distribution of ions or carbon dioxide into this aqueous layer. To overcome this problem, gold contacts were chemically modified with a hydrophobic self-assembled monolayer of 1-hexanthiol. A polymeric membrane doped with the $[Co(phen)_3]^{3+/2+}$ couple was then deposited onto the SAM-modified gold, generating a hybrid system with hydrophobicity and redox capacity.

Table 2. Response of an ISE with a solvent polymeric membrane doped with a redox buffer in contact with a SAM modified gold contact after storage in 1.0 mM KCl for up to 2 weeks (n=3).

Conditioning time	Slope (mV / decade)	E^o values (mV)
1 hour	60.6 ± 0.2	319.0 ± 1.1
1 day	61.6 ± 0.1	324.2 ± 1.0
2 days	61.8 ± 0.1	325.2 ± 0.7
3 days	62.0 ± 0.1	324.5 ± 0.7
7 days	61.7 ± 0.1	325.8 ± 0.7
2 weeks	61.6 ± 0.1	327.0 ± 1.0

Table 2 shows E^o values and standard deviations of this hybrid system when the electrodes were kept in 1.0 mM KCl solution for up to 2 weeks. Because of the redox buffer capacity, the standard deviation of E^o was only 1.1 mV after one hour of solution exposure. It has been known that an aqueous layer may form between a PVC membrane and solid substrate, which can cause drastic changes of the standard deviation of the potential. However, after 24 hours of solution exposure, the electrodes still showed excellent performance with a E^o values of 324.2 mV and a standard deviation of 1.0 mV. The standard deviation remained at 1.0 mV even after 2 weeks of conditioning, indicating effective prevention of the formation of an aqueous layer and strong redox buffering ability. The decrease in E^o values during the initial 24 hours is probably caused by water

absorption of the solvent polymeric membrane, affecting the K^+ ion activity in the polymeric membrane.

A water layer test[16] was conducted by immersing the electrodes sequentially into 100 mM KCl, 100 mM NaCl, and 100 mM KCl solutions. As soon as the solution was switched from the 100 mM KCl to the 100 mM NaCl solution, an immediate emf change of 106 mV occurred, which can be explained by a change in the phase boundary potential at the PVC/ sample solution interface and reflects the membrane selectivity. No positive potential drift was observed after the sample was changed to the 100 mM NaCl solution, as was no negative potential drift observed when the electrodes were returned into the 100 mM KCl solution, indicating that no water layer was formed at the surface of the gold electrode. Figure S4 shows there is no water layer formed after storing the electrodes in 1.0 mM KCl for 1 hour and 72 hours while Figure 5 indicates no water layer formation after at least 2 weeks.

The self-assembled monolayer on the gold contacts and the use of a redox couple are both necessary for a high reproducibility of E^o, as shown in two control experiments. In the case of ISEs with membranes doped with the $[Co(phen)_3]^{3+/2+}$ redox couple and bare gold contacts, the extent of emf differed strongly from electrode to electrode (Figure S5). The same result was found for electrodes with glassy carbon contacts (Figure S6). Moreover, ISEs with a hexanethiol-modified gold contact and an ion-selective membrane that contained no redox active metal complexes exhibited E^o values with a standard deviation of 77.5 mV (n=3), which is consistent with the fact that the phase boundary potential at the interface of SAM-modified gold contacts and ion-selective membrane is poorly defined if the latter contains no redox buffer.

4.4 Conclusions

The results reported in this contribution demonstrate an easy approach to accurately control the phase boundary potential at the interface between an ion-selective membrane and the underlying electron conductor. The redox buffer approach based on well-controlled concentrations of both the oxidized and reduced species of a redox couple ensures a high redox buffer capacity and stability. The thus prepared solid contact ISEs show a standard deviation of the E^o values as low as 1.0 mV. This is the first experimental demonstration of the quantitative control of the interfacial potential between the ISE membrane and the solid substrate as predicted with the Nernst equation. A hybrid system combining this redox buffer approach with advantages of monolayer-modified gold conductors shows E^o values with a standard deviation of 1.0 mV over 2 weeks and resistance to water layer formation.

Ongoing efforts in our laboratory are applying this approach to ionophore-doped solid contact ISEs. Moreover, with a view to clinical chemistry applications, we are developing redox buffer species with a hydrophobicity much larger than that of $[Co(phen)_3]^{3+}$ and $[Co(phen)_3]^{2+}$.

4.5 Supporting Information

4.5.1 Synthesis of Metal Complexes

$[Co(phen)_3]$ $(TPFPB)_2$: First, the cobalt(II) salt $[Co(phen)_3](ClO_4)_2$ was synthesized as reported.[1] Briefly, an ethanolic solution of $CoC1_2 \cdot 6H_2O$ and phenanthroline monohydrate was heated to boiling, and addition of $NaClO_4$ solution after the solution was cooled down resulted in the precipitation of a yellow-brown product.

The purity of the latter was confirmed by elemental analysis (C, 54.07 (54.15); H, 3.02 (3.03); N, 10.41 (10.53), where the values in parentheses are the calculated values). Then, $[Co(II)(phen)_3](ClO_4)_2$ and LiTPFPB ethyl etherate were dissolved in a 1:2 mole ratio in a minimum of acetonitrile, followed by addition of 25 mL water and 25 mL diethyl ether. Upon equilibration of the two resulting layers, the diethyl ether layer was washed 3 times with water and dried with magnesium sulfate. The solvent was evaporated with a rotary evaporator and the resulting solid further dried in a high vacuum, giving the product as a yellow-brown salt. Elemental analysis (calculated): C, 51.36 (51.54); H, 1.50 (1.24); N, 4.13 (4.29).

$[Co(phen)_3](TPFPB)_3$: The cobalt(III) salt $[Co(phen)_3](TPFPB)_3$ was synthesized by modification of a reported procedure for the synthesis of $[Co(phen)_3](ClO_4)_3 \cdot 3H_2O$.[2] Briefly, to $CoC1_2 \cdot 6H_2O$ (0.101 g) in water (2 mL) was added a solution of 1,l0-phenanthroline (0.255 g) in methanol (0.5 mL). The mixture was brought to reflux for 1 h with an excess of Br_2 and left to cool overnight. The above solution was then added dropwise into a stirred solution of LiTPFPB ethyl etherate (1.120 g) in 2 mL methanol. The orange precipitate that formed was filtered off, washed with water, and dissolved in diethyl ether. Upon drying of the resulting solution with magnesium sulfate and filtering off of the solid phase, the solvent was evaporated on a rotary evaporator, and the resulting solid was further dried on a high vacuum, giving the product as an orange salt. Elemental analysis (calculated): C, 49.25 (49.20); H, 1.18 (0.92); N, 2.85 (3.19).

$[Os(II)(bpy)_3]$ $(TmClPB)_2$: Osmium(II) tris(bipyridyl) tetrakis(3-chlorophenyl)borate ($[Os(II)(bpy)_3]$ $(TmClPB)_2$) was synthesized by metathesis according to a modified literature procedure.[3] In a 50 mL round-bottom flask, 0.308 g of bipyridyl

was added to $(NH_4)_2[OsCl_6]$ (0.248 g, 0.556 mmol) dissolved in ethylene glycol (25 mL). The rapidly stirred solution was brought to reflux for 1 hour under argon. After cooling to room temperature, 2 equivalents of ammonium tetrakis(3-chlorophenyl)borate in ethylene glycol were added. Then, 20 mL water and 20 mL dichloromethane were added, and upon thorough equilibration of the two resulting phases, the dichloromethane layer was collected and washed 3 times with water. Upon evaporation of the majority of the dichloromethane, the remaining solution was added dropwise into diethyl ether. A dark green precipitate of the desired compound formed and was filtered off, washed with water, and dissolved in dichloromethane. Evaporation of the solvent with a rotary evaporator and further drying in a high vacuum yielded $[Os(II)(bpy)_3](TmClPB)_2$ as a green salt. The identity of this compound was confirmed by ^1H NMR (300 MHz, CD_2Cl_2, δ): 8.06 (d, 6 H, J = 8.2 Hz, bpy), 7.66 (t, 6 H, J = 7.9 Hz, bpy), 7.46 (d, 6 H, J = 5.6 Hz, bpy), 7.15-7.1 (broad, 22H), 7.00 (t, 4 H, J = 7.6 Hz, TmClPB), 6.88 (d, 4 H, J = 8.1 Hz, TmClPB); for a spectrum, see Figure S1.

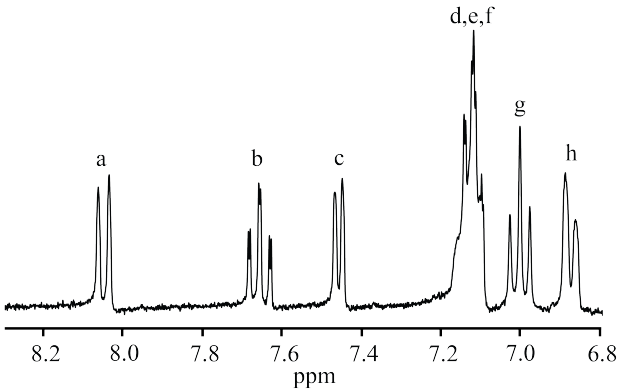

Figure S1. ^{1}H NMR spectrum of $[Os(II)(bpy)_3](TmClPB)_2$ in CD_2Cl_2. Signals a, b, c, and d belong to protons of bpy, and e, f, g, and h belong to protons of $TmClPB^{-}$. The relative integrals of a, b, and c are 6.00, 6.18, and 5.94, respectively (expected 6:6:6). The integrals of g and h are 8.16 and 7.98, respectively (expected: 8:8). The sum of the integrals of d, e, and f is 23.16 (expected: 22).

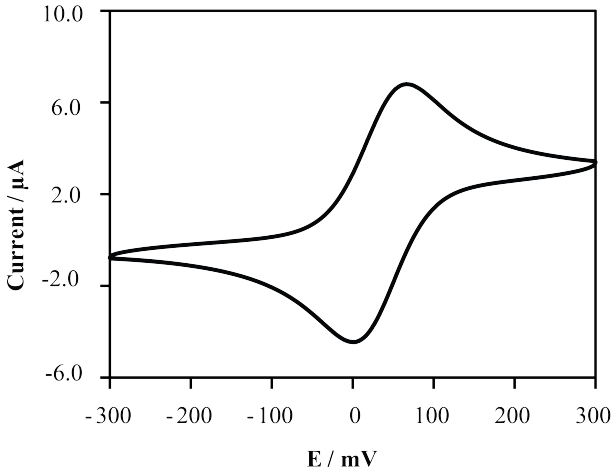

Figure S2. Cyclic voltammogram of 1.0 mM $[Co(II)(phen)_3](ClO_4)_2$ and 100 mM tetrabutylammonium perchlorate in acetonitrile. Potential sweep rate: 0.10 V/s. *E* vs AgCl/Ag.

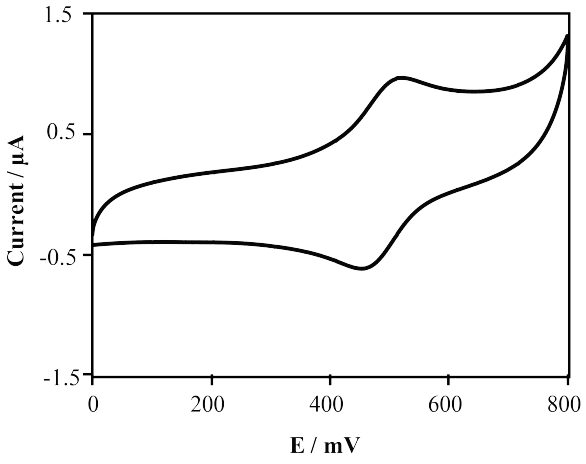

Figure S3. Cyclic voltammogram of 0.10 mM $[Os(II)(bpy)_3](TmClPB)_2$ and 100 mM tetrabutylammonium perchlorate in acetonitrile. Potential sweep rate: 0.1 V/s. *E* vs AgCl/Ag.

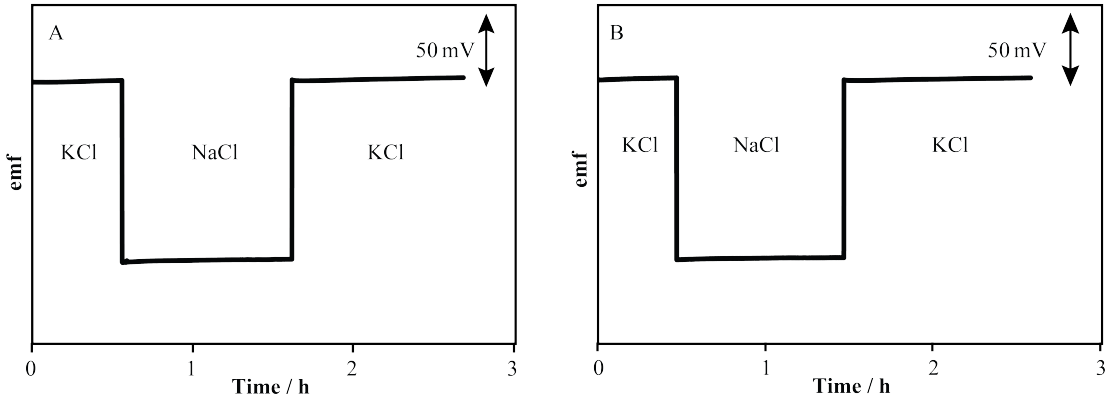

Figure S4. Water layer test of an ISE with a solvent polymeric membrane doped with a $[Co(phen)_3]^{3+/2+}$ redox buffer in contact with a SAM modified gold contact: the electrodes were first immersed in 100 mM KCl, then the sample was exchanged for 100 mM NaCl and then back to 100 mM KCl. The electrodes were stored in 1.0 mM KCl after 1 hour (A) and 72 hours (B).

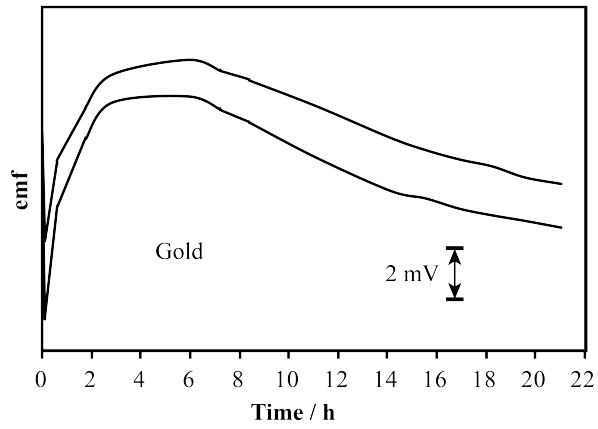

Figure S5. Time dependence of the potentiometric response of two representative ISEs with a solvent polymeric membrane doped with $[Co(phen)_3]^{3+/2+}$ redox buffer and a bare gold contact. The newly prepared electrodes, which had not been in contact with aqueous solutions before, were immersed at t = 0 h into a 100 mM KCl solution.

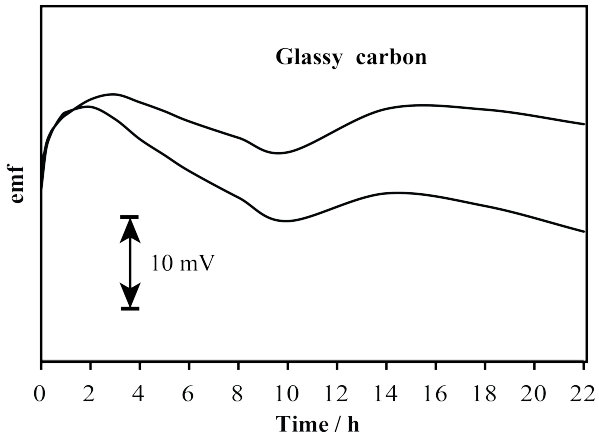

Figure S6. Time dependence of the potentiometric response of two representative ISEs with a solvent polymeric membrane doped with $[Co(phen)_3]^{3+/2+}$ redox buffer and a glassy carbon contact. The newly prepared electrodes, which had not been in contact with aqueous solutions before, were immersed at t = 0 h into a 100 mM KCl solution.

CHAPTER FIVE

Calibration-Free Ionophore-Based Solid-Contact Ion-Selective Electrodes With a Co(II)/Co(III) Redox Couple

In part from:

Xu U. Zou, Xue Zhen, Jia H. Cheong and Philippe Bühlmann Manuscript in preparation

Abstract

In order to reduce irreproducibility and instability of the measured electromotive force (emf), solid contact ion-selective electrodes (ISEs) typically have an intermediate layer between the ion-selective membrane and the underlying solid substrate. However, the electrode-to-electrode reproducibility of the emf of current solid contact ISEs is widely considered to be unsatisfactory, rendering them not suitable for a calibration free system. Many prior examples of ionophore-based solid contact ISEs also used an intermediate layers that contained a redox active species. Nevertheless, they have not achieved highly reproducible standard potentials, presumably because they made no attempt to use both the oxidized and reduced species of a redox couple in a well defined ratio. We report here a new method of preparing ionophore based solid contact ISEs with a redox buffer platform based on the lipophilic redox buffer consisting of the Co(III) and Co(II) complexes of 4,4'-dinonyl-2,2'-bipyridyl ($[Co(C_9,C_9\text{-bipy})_3]^{3+/2+}$) paired with tetrakis(pentafluorophenyl)borate as counterion. The resulting K^+-selective electrodes exhibit emf values with an electrode-to-electrode standard deviation as low as 0.7 mV after conditioning of freshly prepared electrodes for 1 h. The high redox buffer capacity resulting from doping amount with equivalent amounts of $[Co(C_9,C_9\text{-bipy})_3]^{3+}$ and $[Co(C_9,C_9\text{-bipy})_3]^{2+}$ explains the high emf reproducibility. Monitoring the emf change of a gold electrode modified with a self-assembled 1-hexanethiol monolayer as underlying electron conductor reveals the reproducibility loss during long term measurement is not due to the water layer formation between the membrane and the substrate but is instead caused by the leaching of redox species from the ion-selective membrane into the sample solution, which has been experimentally verified.

5.1 Introduction

Ion-selective electrodes (ISEs), which are the most important electroanalytical sensors, are widely used in clinical analysis, process control and environmental monitoring.[1, 9, 12, 120, 122, 148] As the need for mass production, affordable manufacturing cost and portability of devices increases, traditional ISEs with internal electrolyte have been overshadowed by the next generation solid contact ISEs, in the ion-selective membrane is directly attached to a solid substrate.[5-8] Solid contact ISEs usually have an intermediate layer to prevent water layer formation and stabilize the interfacial potential to the underlying electron conductor. This layer is often a conducting polymer[4, 21-23, 25, 27, 32, 39, 42-47, 49] or a carbon material with a high surface area.[55-56, 59-62, 92] The electromotive force (emf) of an ISE is the sum of the sample-dependent potential at the sample/membrane interface and the sample-independent interfacial potentials at all other interfaces between differing materials.[1, 120] Due to poorly defined sample-independent interfaces, especially in the case of solid contact ISEs that do not possess membrane/substrate interfaces with well-defined phase boundary potentials, calibration is an essential processes to guarantee accurate measurement results.[120] However, calibration is cumbersome for routine analysis due to the need for standard solutions and the need for equipment to perform the calibration. Also, time spent in performing calibrations before every measurement is often not available, such as in an emergency room, where fast and accurate medical checks are necessary.

Effort to find well-defined interfaces, subsequently leading to a calibration free system, has been made in various groups. Ion-selective membranes doped with Ag^+ ionophore complexes on a silver epoxy substrate reduced the standard deviation of cell

constant[18-19] but the extension of the $Ag^{+/0}$ system to ISE membranes doped with a variety of ionophores has not been reported. Redox-active self-assembled monolayers (SAMs) with a redox potential controlled by an applied current[116] shows a small redox buffer capacity, and mixtures of gold nanoclusters with two different charge states[117] are technically not trivial to prepare. Applying a current pulse in the nA range to poly(3,4-ethylene dioxythiophene) doped with poly(sodium 4-styrenesulfonate) based electrode provides a route to electrochemically adjusting standard potential (E^o)[118] but still requires tuning of individual electrodes and has not been applied to practical applications yet. Synchrotron radiation-X-ray photoelectron spectroscopy (SR-XPS) and near edge X-ray absorption fine structure (NEXAFS) were applied to poly(3-octylthiophone) based solid contact ISEs to reveal that a mixed oxidation state exists, which offers a plausible explanation for the stable potential readings for this type of electrodes.[158] The same techniques also found iron chalcogenide glass ISE comprises a mixture of iron(II) and iron(III) redox states in a confined interface.[155, 159] These findings emphasize the importance of redox characteristics for solid contact ISEs.

We previously reported that an ion exchanger membrane with the redox couple cobalt(II/III)tris(1,10-phenanthroline) tetrakis(pentafluorophenyl)borate significantly reduced the standard deviation of E^o.[160] However, preliminary results showed that that this redox couple was not suitable for use with ionophore-based ISEs because binding of the target ions to the ionophore is energetically so favorable that it causes primary ion transfer from the sample into the ISE membrane coupled with loss of redox-active cations from the ISE membrane into the aqueous solution. Here, we describe a new, more lipophilic redox couple buffer system consisting of the tetrakis(pentafluorophenyl)borate

(TPFPB$^-$) salts of cobalt(II)tris(4,4'-dinonyl-2,2'-bipyridyl) ($Co(C_9,C_9\text{-bipy})_3]^{2+}$) and cobalt(III) tris(4,4'-dinonyl-2,2'-bipyridyl) ($Co(C_9,C_9\text{-bipy})_3]^{3+}$) and their use to dope ionophore-based plasticized poly(vinyl chloride) (PVC) membranes. To prepare solid contact ISEs, tetrahydrofuran (THF) solution of the membrane components were drop-casted onto glassy carbon electrodes or gold electrodes modified with a self-assembled monolayer of 1-hexanethiol. This new redox couple gives Nernstian responses to target ions and electrode potentials with a standard deviation as low as 0.7 mV for K^+. This redox platform has also been successfully applied to sodium, potassium, calcium, hydrogen and carbonate ion-selective electrodes, which all exhibit the high selectivity over interfering ions as expected for ionophore-doped ISE membranes.

5.2 Experimental Section

5.2.1 Materials

All reagents were of the highest commercially available purity and were used as received. Deionized water (0.18 MΩ m specific resistance) was purified with a Milli-Q PLUS reagent grade water system (Millipore, Bedford, MA). 1-Hexanethiol was purchased from Acros Organics (Geel, Belgium). High molecular weight poly(vinyl chloride) (PVC) and 2-nitrophenyl octyl ether (*o*-NPOE) were purchased from Fluka (Buchs, Switzerland), dioctyl sebacate (DOS) from Wako Pure Chemical Industries (Osaka. Japan), bis[(12-crown-4)methyl] dodecylmethylmalonate (sodium ionophore) and *N,N*-dicyclohexyl-*N',N'*-dioctadecyl-3-oxapentanediamide (calcium ionophore) from Fluka (St. Louis, MO), lithium tetrakis(pentafluorophenyl)borate ethyl etherate from Boulder Scientific (Boulder, CO), and valinomycin (potassium ionophore), heptyl 4-

trifluoroacetylbenzoate (carbonate ionophore), octadecyl isonicotinate (hydrogen ionophore) and 4,4'-dinonyl-2,2'-bipyridyl from Sigma Aldrich (St. Louis, MO). Elemental analyses were performed by MHW Laboratories (Phoenix, AZ). Glassy carbon and gold electrodes were purchased from CH Instruments (Austin, TX). ^{1}H NMR spectroscopy was performed with a VAC-300 Varian Mercury or Varian Inova 500 spectrometer (Varian, Palo Alto, CA). UV-Vis spectroscopy was performed with JASCO V-630 spectrophotometer (Easton, MD).

The synthesis details of all redox active metal complexes are included in the supporting information. The cobalt(II) salt $[Co(C_9,C_9\text{-bipy})_3]$ $(TPFPB)_2$ was obtained by metathesis from LiTPFPB ethyl etherate and $[Co(II)$ $(C_9,C_9\text{-bipy})_3]]Cl/Br$, which was synthesized as reported.[161] The cobalt(III) salt $[Co(C_9,C_9\text{-bipy})_3](TPFPB)_3$ was synthesized using a modified reported procedure.[161-162]

5.2.2 Electrode Fabrication

The 3 mm diameter glassy carbon electrodes were polished over polishing cloths with aqueous dispersions of alumina (0.3 μm). The 2 mm diameter gold electrodes were polished over polishing cloths with aqueous dispersions of alumina (0.3 and 0.05 μm, Buehler, Lake Bluff, IL) and then cleaned in piranha solution (concentrated sulfuric acid and 30% hydrogen peroxide solution in a 3:1 ratio). All electrodes were then cleaned by ultrasonication in water and ethanol, and dried with a flow of nitrogen. *Caution: piranha solution is a strong oxidizing reagent, is highly corrosive, and should be handled with care.* For the formation of a 1-hexanethiol self-assembled monolayer (SAM), the gold electrodes were immersed into 1 mM 1-hexanethiol solutions in ethanol for 24 h.

Solvent polymeric membranes doped with a redox couple were prepared by dissolving the membrane components (33 mg PVC as polymer matrix, 66 mg DOS as plasticizer, 0.8 mmol/kg $[Co(C_9,C_9\text{-bipy})_3](TPFPB)_2$ and 0.8 mmol/kg $[Co(C_9,C_9\text{-bipy})_3](TPFPB)_3$, Na^+-selective membrane: 1.0 % (wt/wt) sodium ionophore and 51 mol % LiTPFPB; K^+-selective membrane: 1.2 % (wt/wt) valinomycin and 59 mol % LiTPFPB; Ca^{2+}-selective membrane: 1.3 % (wt/wt) calcium ionophore and 43 mol % LiTPFPB; H^+-selective membrane: 1 % (wt/wt) hydrogen ionophore and 71 mol % LiTPFPB; CO_3^{2-}-selective membrane: 41 mg PVC, 55 mg DOS, 2.6 % (wt/wt) carbonate ionophore and 43 mol % TDDMACl, 8 mmol/kg $[Co(C_9,C_9\text{-bipy})_3](TPFPB)_2$ and 8 mmol/kg $[Co(C_9,C_9\text{-bipy})_3](TPFPB)_3$) in 500 µL freshly distilled tetrahydrofuran (THF). 40 µL of the above cocktail was dropcast onto SAM-modified gold or glassy carbon electrodes and left to dry overnight. The electrodes prepared in this way were conditioned in 1.0 mM KCl solution for 1 h prior to measurements. The short conditioning time ensures that there is no water layer effect that might interfere with the observation of the redox capacity.

5.2.3 Potentiometric Measurements

Potentials were measured with an EMF 16 potentiometer (input impedance 10 TΩ) controlled with EMF Suite 1.03 software (Lawson Labs, Malvern, PA). A double-junction type external reference electrode (DX200, Mettler Toledo, Switzerland; 3.0 M KCl saturated with AgCl as inner filling solution and 1.0 M LiOAc as bridge electrolyte) was used. The solution's pH was measured with a pH glass electrode. CO_3^{2-} concentrations were calculated as suggested by Herman and Rechnitz.[163] Activity

coefficients were calculated according to a two-parameter Debye-Hückel approximation,[133] and all emf values were corrected for liquid-junction potentials with the Henderson equation.[2]

5.3 Results and Discussions

5.3.1 Selection of the Redox Couple

It was previously reported that an ion exchanger membrane doped with cobalt(II/III)tris(1,10-phenanthroline) tetrakis(pentafluorophenyl)borate ensured a high redox buffer capacity and stability[160] in analogy to traditional pH buffers.[153] However, when this redox buffer was added to an ISE membrane doped with valinomycin as potassium ionophore, the standard deviation of E^o became very big and the selectivity over interfering ions was immediately lost, apparently because valinomycin was so good at facilitating the transfer of K^+ from the aqueous samples into the membrane that this process was driving the loss of the redox active cations from the sensing membrane into the aqueous phase. Therefore, a more hydrophobic redox couple was synthesized using the commercially readily available bipyridyl substituted with two nonyl groups. $TPFPB^-$ salts of $[Co(C_9,C_9\text{-bipy})_3]^{3+}$ and $[Co(C_9,C_9\text{-bipy})_3]^{2+}$ (Figure 1) were prepared. They are electrochemically stable, soluble in the plasticized polymeric membrane and hydrophobic enough to stay in the membrane. Cyclic voltammograms (CVs) of $[Co(C_9,C_9\text{-bipy})_3]^{3+}$ in acetonitrile taken with a scan rate of 100 mV/s show the same peak separation of 73 mV for both bare gold electrode and 1-hexanethiol-modified gold electrodes (for a CV, see Figure S2), which is consistent with $\left[Co(C_9,C_9\text{-bipy})_3\right]^{3+} + e^- \Leftrightarrow \left[Co(C_9,C_9\text{-bipy})_3\right]^{2+}$ and indicates that the self-assembled layer has no substantial effect on the heterogeneous

electron transfer at the underlying substrate. The 73 mV peak separation rather than the expected 59 mV is probably a double layer effect rather than an indication of slow electron transfer.

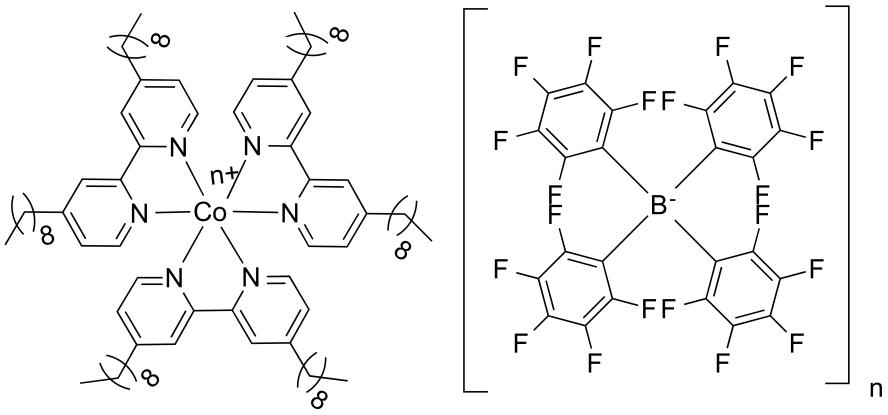

Figure 1. Structure formulas of cobalt(II/III) (4,4'-dinonyl-2,2'-bipyridyl) and tetrakis(pentafluorophenyl)borate.

5.3.2 Reproducibility of Electrode Potentials

The redox platform was applied to ionophore based ion-selective electrodes, whose performances are summarized in Table 1. For cation-selective electrodes, the slopes of the emf response were 60.0 ± 0.8, 62.1 ± 0.5, 32.1 ± 0.7 and 56.4 ± 0.4 mV/decade for K^+, Na^+, Ca^{2+}, and H^+ respectively while the standard deviations of E^o were 2.6 mV, 1.4 mV, 2.8 mV, and 1.4 mV. Importantly, the selectivity of these electrodes is maintained over interfering ions ($\log K^{pot}_{K^+, Na^+} = -4.22 \pm 0.03$, $\log K^{pot}_{Na^+, K^+} = -1.65 \pm 0.03$, $\log K^{pot}_{Ca^+, K^+} = -5.57 \pm 0.21$, $\log K^{pot}_{Ca^+, Na^+} = -4.10 \pm 0.09$, $\log K^{pot}_{H^+, Na^+} = -5.60 \pm 0.05$), which is consistent or comparable with the values reported without a redox couple ($\log K^{pot}_{K^+,Na^+} = -4.50$,[61] $\log K^{pot}_{Na^+, K^+} = -1.52$,[164] $\log K^{pot}_{Ca^+, K^+} = -5.6$, $\log K^{pot}_{Ca^+, Na^+} = -6.4$[165] (*o*-

NOPE as plasticizer), $\log K^{pot}_{H^+, Na^+} = -5.6$[166] (*o*-NOPE as plasticizer). As an example for an anion-selective electrode, a CO_3^{2-}-selective electrode was prepared. It shows a slope of 29.9 ± 1.5 mV/decade, a standard deviation of the E^o of 1.7 mV, and a selectivity over Cl^- with $\log K^{pot}_{CO_3^{2-}, Cl^-} = -5.34 \pm 0.12$ (without redox couple $\log K^{pot}_{CO_3^{2-}, Cl^-} = -4.8$).[167] The minor discrepancy between the experimental values for ISE membranes with the redox couple and the reported values for conventional ISE membranes without the redox couple is likely due to the use of a different plasticizers in this work and due to differences in the method used for the determination of the selectivity coefficients.[122] The phase boundary potential at the interface of the polymeric membrane and the underlying electron conductor is determined by a redox couple and the reduced and the oxidized species form a redox buffer system with 1:1 mole ratio, leading to highly reproducible E^o values. The hydrophobicity of the cobalt complexes prevents the loss of the redox active species into the aqueous phase, which is crucial to maintain the selectivity for the primary over interfering ions.

Table 1. E^{o} values of electrodes based on different ionophores after conditioning for 1 hour in 1.0 mM corresponding solution.

Electrode type	K^+	Na^+	H^+	Ca^{2+}	CO_3^{2-}
Slope (mV / decade)	60.0 ± 0.8	62.1 ± 0.5	56.4 ± 0.4	32.1 ± 0.7	29.9 ± 1.5
E^{o} (mV)	731.3 ± 2.6	571.7 ± 1.4	328.2 ± 1.4	586.0 ± 2.8	273.3 ± 1.7
$\log K_{i,j}^{pot}$	j = Na^+ -4.22 ± 0.03	j = K^+ -1.65 ± 0.03	j = Na^+ -5.60 ± 0.05	j = Na^+ -5.57 ± 0.21 j = K^+ -4.10 ± 0.09	j = Cl^- 5.34 ± 0.12

All membranes contained, besides the ionophore and ion exchanger, PVC and DOS in a 1:2 weight ratio. E^{o} values refer to the potential of the ISE cell as obtained by extrapolation of the linear section of the emf response to the primary ion activity of 1.0 M.

5.3.3 Polymeric Membranes Doped with a Redox Couple in Contact with Gold Contacts Modified with a Self-Assembled Alkanethiol Monolayer.

Modified gold electrodes with ion exchanger membranes showed a good long term stability in 1.0 mM KCl solution over 2 weeks due to the successful suppression of water layer formation between the membrane and the underlying substrate.[160] Na^+- and K^+-selective membranes on modified gold electrodes were fabricated in the same way, and show an excellent standard deviation of the E^o of 0.9 mV and 0.7 mV, respectively, and selectivities of $\log K^{pot}_{Na^+, K^+} = -1.65 \pm 0.01$ and $\log K^{pot}_{K^+, Na^+} = -4.08 \pm 0.01$, respectively, in the first 3 h of measurement. However, the reproducibility of E^o for both Na^+ and K^+-selective electrode is deteriorating as exposure to primary ion solutions extends beyond 3 h. For the Na^+-selective electrodes, the standard deviation increased from 0.9 mV to 2 mV after 24 h, 4.5 mV after 72 h and 8.2 mV after 8 d in 1.0 mM NaCl. The same deterioration also happens for K^+-selective electrodes, with the standard deviation of 0.7 mV after 1 h and 16.3 mV after 24 h in 1.0 mM KCl. The loss of reproducibility can be attributed to the exchange of cobalt(III)tris(1,10-phenanthroline) and cation, Na^+ or K^+ in this case, between the membrane and aqueous phase due to strong binding of the primary cation to the ionophore, as shown by the phase transfer equilibrium $K^+(aq) + \left[\mathrm{Co(C_9, C_9 - bipy)_3}\right]^{2/3+}(mem) \Leftrightarrow K^+ \bullet Valinomcin(mem) + \left[\mathrm{Co(C_9, C_9 - bipy)_3}\right]^{2/3+}(aq)$. Interestingly, the properties of the K^+-selective electrode are affected faster than those of the Na^+-selective counterpart, probably due to the stronger binding of K^+ to valinomycin in DOS. This is consistent with the binding constants of K^+ and valinomycin and Na^+ and sodium

ionophore VI in DOS, which have been reported as $10^{10.1}$ and $10^{6.6}$, respectively.[168] Although some cobalt complexes can reversibly add molecular oxygen to give binuclear dioxygen compounds[169] and oxygen might form a half cell at the solid substrate,[14, 157] solid contact electrodes with polymer membranes doped with redox buffers show no interference from oxygen. They were immersed into 1 mM KCl solutions, and O_2 and Ar were bubbled alternatingly into the sample solution while recording the emf. As shown in Figure S3, no significant potential changes were observed.

5.3.4 Leaching of Redox Complex From Polymeric Membranes to Aqueous Solution

Leaching of redox active species was suggested by potentiometric measurements when monitoring the emf of K^+-selective membranes in 0.1 mM KCl and 1 M KCl. The emf of membranes exposed to 0.1 mM KCl and 1 M KCl solutions increased within the first one hour by 44 mV and 35 mV, respectively, due to water uptake of the polymeric membranes. The electrode potential difference between the two solutions is 204 mV, which is consistent with the theoretically expected difference for 1 M and 0.1 mM of K^+ solutions, indicating that leaching of the cobalt complexes initially does not impede the normal response mechanism of the electrodes. However, discrepancies were found later. The 158 mV decrease of an electrode in 1 M KCl was much larger than the 9 mV decrease in emf for an electrode stored in 0.1 mM KCl after 48 hours (Figure 2). Figure 3 also shows that the electrodes' standard deviations of E^o increased from 3 mV after 1 h to 49 mV after 48 h in 1 M KCl while the range is 2.3 mV to 4.8 mV in 0.1 mM KCl. This data is consistent with K^+ transfer into the ionophore-doped membrane resulting in the loss of redox active species into the aqueous sample. Indeed, the transfer of the cobalt

complex into the aqueous phase could also be confirmed by UV-Vis spectroscopy (Figure S3). Compared to the spectrum of $[Co(C_9,C_9\text{-bipy})_3]^{3+}$ or $[Co(C_9,C_9\text{-bipy})_3]^{2+}$ in THF, the leached compound from K^+-selective membrane to the 1 M KCl solution shows the same absorption wavelength at 305 nm, indicating the leached compound is $[Co(C_9,C_9\text{-bipy})_3]^{3+}$ or $[Co(C_9,C_9\text{-bipy})_3]^{2+}$. (Details of extraction procedure can be found in Supporting Information) As indicated by $K_{equilibrium} = \frac{K^+ \bullet Valinomcin(mem) \bullet \left[Co(C_9, C_9\text{ - bipy})_3\right]^{2/3+}(aq)}{K^+(aq) \bullet \left[Co(C_9, C_9\text{ - bipy})_3\right]^{2/3+}(mem)}$ it is apparent that higher concentration of K^+ in aqueous phase decreases the cobalt complex concentration in membrane phase while increases the cobalt complex concentration in the aqueous phase, which deteriorate the performances of the electrodes to more extent by changing the optimized redox capacity.

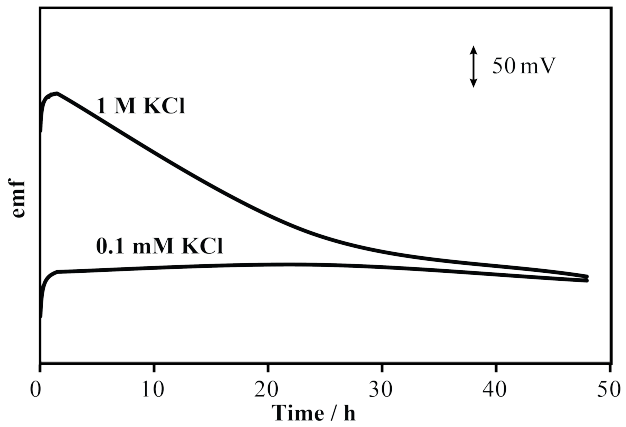

Figure 2. Emf response of K^+-selective electrodes on a 1-hexanethiol modified gold substrate in 1 M KCl and 0.1 mM KCl

Table 2. Response of an ISE with a solvent polymeric membrane doped with a redox buffer in contact with a SAM modified gold contact after storage in 1.0 mM KCl and 1.0 mM NaCl respectively.

Type	K^+ (N=5)			Na^+ (N=6)		
Time length	Slope (mV / decade)	E^o values (mV)	Selectivity over Na^+	Slope (mV / decade)	E^o values (mV)	Selectivity over K^+
1 hour	60.1 ± 0.3	731.4 ± 0.7	-4.08 ± 0.01	62.5 ± 0.6	561.1 ± 0.9	-1.65 ± 0.01
24 hour	60.9 ± 0.5	716.8± 16.3	-4.29 ± 0.12	63.4 ± 0.3	557.0 ± 2.0	-1.65 ± 0.03
48 hour	N/A	N/A	N/A	62.5 ± 0.2	549.6 ± 4.5	-1.61 ± 0.03
72 hour	N/A	N/A	N/A	62.2 ± 0.3	537.9 ± 8.2	-1.59 ± 0.03

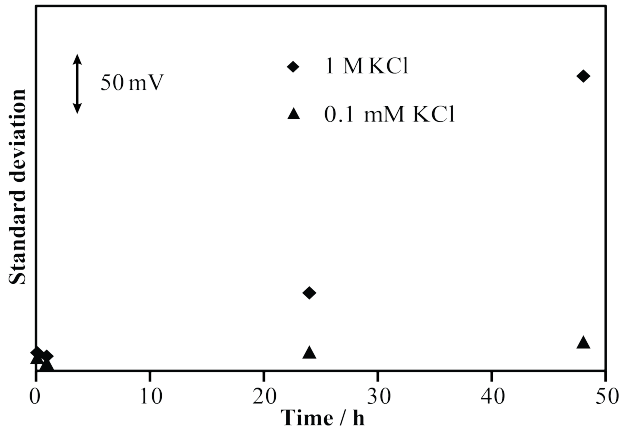

Figure 3. Standard deviation of E^o of K^+-selective electrodes on a 1-hexanethiol modified gold substrate when two groups of electrodes were continuously kept in 1.0 M KCl and 0.1 mM KCl.

5.4 Conclusion

The results reported in this contribution demonstrate a platform with high redox buffer capacity and stability to accurately generate a highly reproducible phase boundary potential at the interface between an ion-selective membrane and the underlying electron conductor. The thus prepared solid contact ISEs show a standard deviation of the E^o values as low as 0.7 mV. This platform was applied to K^+, Na^+, Ca^{2+}, H^+ and CO_3^{2-}-selective electrodes, all of which show highly reproducible E^o values while maintaining selectivity over interfering ions. An integrated system based on this redox buffer platform with advantages of monolayer-modified gold conductors reveals leaching of redox couples as the cause for loss of reproducibility of E^o values. Ongoing efforts in our

laboratory are developing redox couples with charged ligands and modified polymers with covalently attached redox couples.[170]

5.5 Supporting Information

5.5.1 Synthesis of Metal Complexes

$[Co(C_9,C_9\text{-bipy})_3]$ $(TPFPB)_2$: First, the cobalt(II) salt $[Co(C_9,C_9\text{-bipy})_3](Cl)_2$ was synthesized as reported.[161] Briefly, 4,4'-dinonyl-2,2'-bipyridyl was dissolved in methnol was heated to boiling followed by adding a water solution of $CoC1_2{\cdot}6H_2O$ and refluxed for 3 hours. After the solution was cooled down, 2 equivalent of LiTPFPB ethyl etherate in methanol were added, resulting in precipitate which stayed over night. The precipitate was collected and dissolved in diethylether, subsequently precipitating out in hexane. The precipitate was dissolved in 25 mL diethyl ether, followed by addition of 25 mL water. Upon equilibration of the two resulting layers, the diethyl ether layer was washed 3 times with water The precipitate was then dried in high vacuum over night. Elemental analysis (C, 60.26 (59.99); H, 5.23 (5.03); N, 2.94 (3.18), where the values in parentheses are the calculated values).

$[Co(C_9,C_9\text{-bipy})_3](TPFPB)_3$: The cobalt(III) salt $[Co(C_9,C_9\text{-bipy})_3](TPFPB)_3$ was synthesized by modification of a reported procedure for the synthesis of $[Co(C_9,C_9\text{-bipy})_3](Cl)_3$.[161-162] Briefly, to heated 4,4'-dinonyl-2,2'-bipyridyl in methanol was added a water solution of $CoC1_2{\cdot}6H_2O$. The mixture was brought to reflux for 3 h with an excess of Br_2 and left to cool overnight. NMR spectrum verified that the oxidation of $[Co(C_9,C_9\text{-bipy})_3]^{2+}$ was complete. The above solution was then added dropwise into a stirred solution of LiTPFPB ethyl etherate in methanol. The orange precipitate that formed was

filtered off, dissolved in methanol and washed with hexane three times. The methanol phase was collected and evaporated on a rotary evaporator, and the resulting solid was further dried on a high vacuum, giving the product as an orange salt. Elemental analysis (calculated): C, 56.76 (56.4); H, 4.36 (4.01); N, 2.76 (2.53).

Extraction of Co complex from the membrane: a K^+-selective membrane of the same composition used in the experiment was soaked in 1 M KCl for 24 h. Concentrated sodium tetraphenylborate was added dropwise into the same KCl, which produced precipitate. This precipitate was then dissolved in diethylether and washed with water.

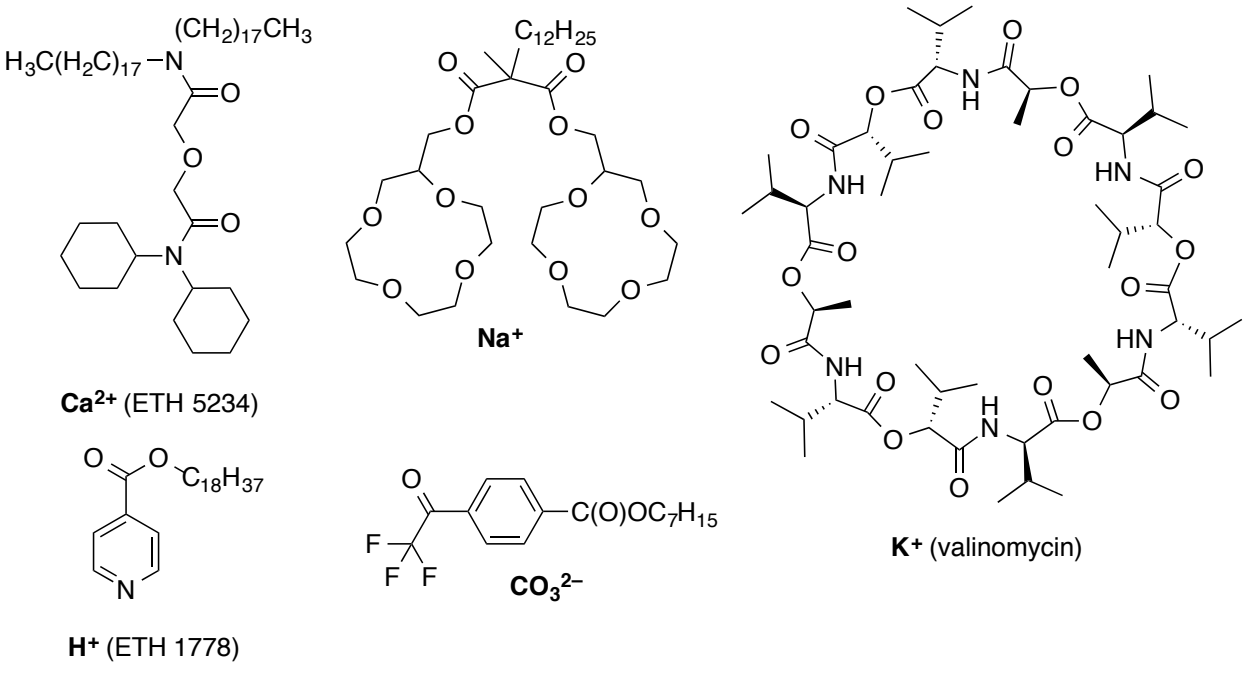

Figure S1. Molecular structures of ionophores

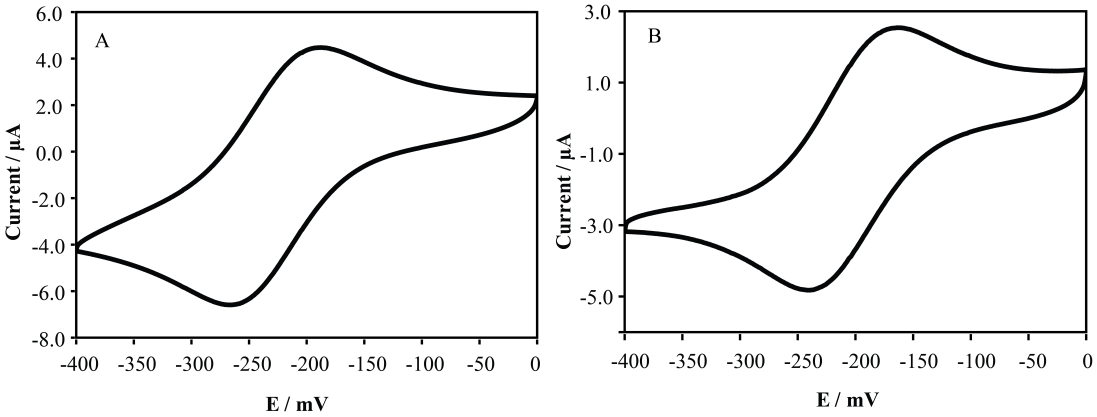

Figure S2. Cyclic voltammogram of 1 mM $[Co(II)(dibpy)_3](TPFPB)_3$ and 100 mM tetrabutylammonium perchlorate in acetonitrile on bare gold electrode (A) and modified gold electrode (B). Potential sweep rate: 0.10 V/s. *E* vs AgCl/Ag.

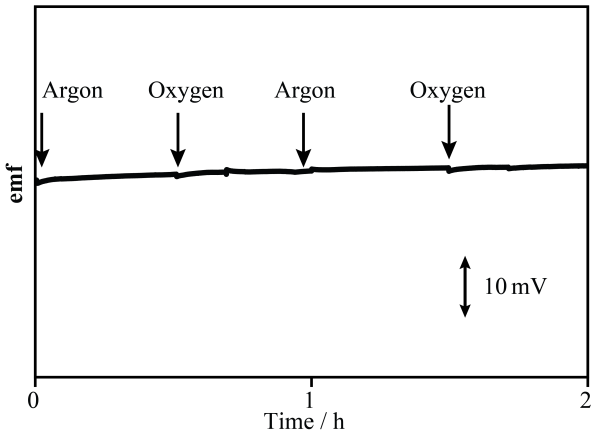

Figure S3. Effect of oxygen on the potential stability of a solid contact K^+-selective electrode (modified gold) immersed into a 1 mM KCl solution.

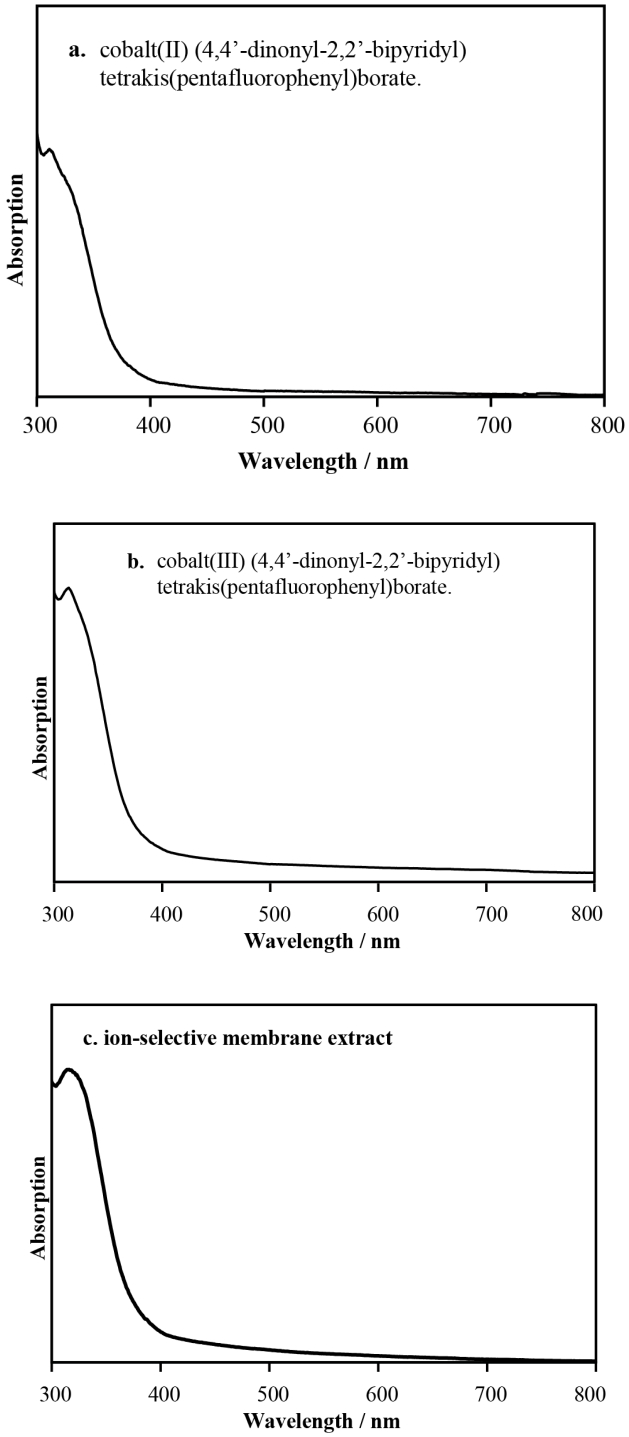

Figure S4. UV-Vis spectra in tetrahydrofuran of (a) 10 μM ($[Co(C_9,C_9\text{-bipy})_3]^{2+}$)$(TPFPB^-)_2$, (b) 10 μM ($[Co(C_9,C_9\text{-bipy})_3]^{3+}$)$(TPFPB^-)_3$, (c) ion-selective membrane extract.

Figure S5. List of NMR spectrum

(a)^{1}H spectrum of ([Co(C_9,C_9-bipy)$_3$]$^{3+}$)(TPFPB^{-})$_3$

(b)^{9}Fspectrum of ([Co(C_9,C_9-bipy)$_3$]$^{3+}$)(TPFPB^{-})$_3$

(c)^{1}H spectrum of ([Co(C_9,C_9-bipy)$_3$]$^{2+}$)(TPFPB^{-})$_2$

(d)^{19}F spectrum of ([Co(C_9,C_9-bipy)$_3$]$^{2+}$)(TPFPB^{-})$_2$

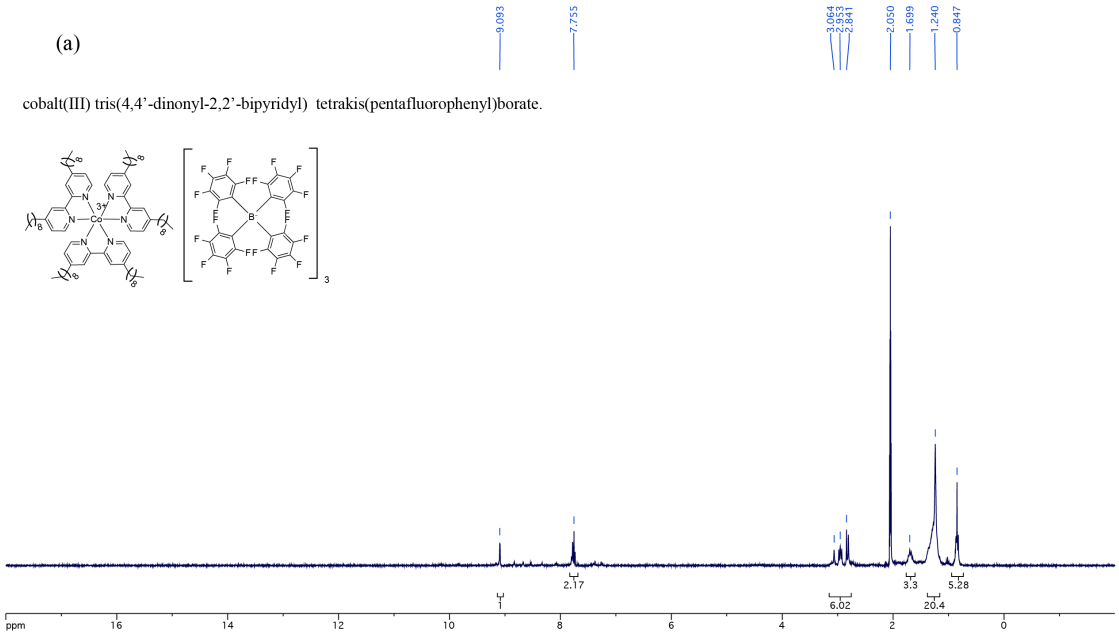

(b)

cobalt(III) tris(4,4'-dinonyl-2,2'-bipyridyl) tetrakis(pentafluorophenyl)borate.

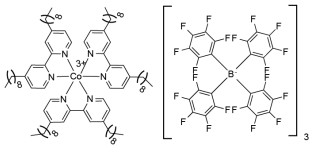

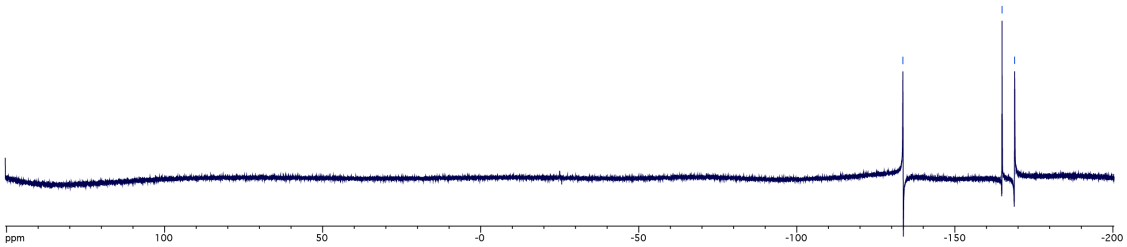

(c)

cobalt(II) tris(4,4'-dinonyl-2,2'-bipyridyl) tetrakis(pentafluorophenyl)borate.

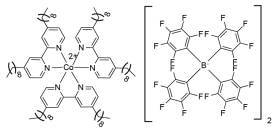

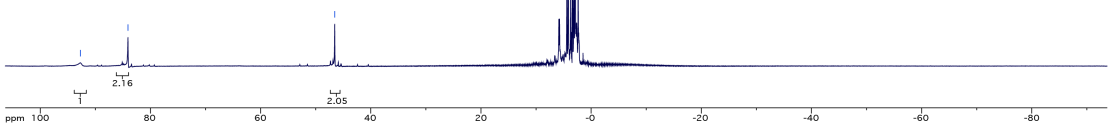

(d)

cobalt(II) tris(4,4'-dinonyl-2,2'-bipyridyl) tetrakis(pentafluorophenyl)borate.

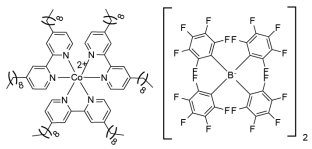

CHAPTER SIX

Ionic Liquid Reference Electrodes With a Well-Controlled Co(II)/Co(III) Redox Buffer as Solid Contacts

In part from:

Xu U. Zou, [§] Li D. Chen[§] Chun-Ze Lai, [§] and Philippe Bühlmann Manuscript in preparation [§]These authors contributed equally to this work.

Abstract

Solid contact reference electrodes with ionic liquid doped polymeric membranes are desired for potentiometric measurements as they eliminate the salt bridges that are vulnerable to interference from complex samples in the conventional reference electrodes. To enhance the electrode-to-electrode reproducibility, a lipophilic redox buffer consisting of the Co(III) and Co(II) complexes of 1,10-phenanthroline ($[Co(phen)_3]^{3+/2+}$) paired with tetrakis(pentafluorophenyl)borate as counterion, were added to the reference membranes to provide redox buffer capacity at the interface of the reference membrane and the underlying solid electron conductor. The potentials of the proposed reference electrodes are not sample dependent. As predicted by the Nernst equation, they depend on the ratio of $[Co(phen)_3]^{2+}$ and $[Co(phen)_3]^{3+}$ and decrease about 59 mV per tenfold increase in the ratio of the reduced and oxidized redox buffer species. The reference electrodes exhibit good electrode-to-electrode reproducibility, with a standard deviation of E^o as low as 2.1 mV. The reference electrodes with a gold lead surface-modified with a self-assembled 1-hexanethiol monolayer have good water-layer formation resistance. The E^o potential remains constant within error for up to 48 h of exposure to KCl solution.

6.1 Introduction

Ion-selective electrodes (ISEs) are well-established analytical devices and are widely used in clinical diagnosis, environmental analysis, process control and the food industry.[1, 9, 120, 122, 171] To make an ISE measurement, an external reference electrode that can exhibit a stable and reproducible potential upon exposure to samples is required. A conventional reference electrode such as a silver/silver chloride electrode is typically brought in contact with the sample through a salt bridge filled with an aqueous electrolyte solution.[119, 123] Ideally, the high concentration of ions (e.g., 3 M KCl) in the salt bridge, dominates the liquid junction potential at the interface of the salt bridge and the sample and, therefore, provides a sample-independent potential. However, the salt bridge can be contaminated by sample ions and get clogged by proteins, lipids, and precipitates from the sample matrix, resulting in slow responses and erratic liquid junction potentials.[97-98] Besides, the electrolyte ions in the salt bridge may contaminate the sample and interfere with the detection of target ions at very low concentrations. Eventual evaporation of the electrolyte solutions and loss of the electrolyte ions into the sample limit the lifetime and hinder miniaturization of reference electrodes. Therefore, liquid-junction free reference electrodes are highly desired.

Several approaches have been proposed to eliminate the liquid junction, including the use of hydrophobic anion-exchanger membranes loaded with polyanions such as heparin,[101-102] or hydrophobic polymeric membranes doped with lipophilic salts[91, 93, 108-109] or ionic liquids.[104, 107,103] All these methods took advantage of a water-immiscible phase in place of an aqueous salt bridge to separate the reference electrode from the sample. These phases are loaded with ions that slowly but continuously leach into the samples. In these

cases, distribution of ions between the hydrophobic reference membranes and the sample reaches local equilibrium quickly, providing a well-defined and sample-independent phase boundary potential at the sample/membrane interface.

To make ISE miniaturizable for portable and implantable devices, solid contact electrodes were introduced. Since 1990s, electronically conducting polymers, such as polypyrrole,[21-23, 25, 27, 32] polythiophene,[35, 39, 43-45, 172] and polyaniline,[44, 47, 49] along with their derivatives, have been reported and are widely used as solid contacts for ISEs.[4] More recently reported materials for solid contacts include carbon materials with large surface area, such as three-dimensionally ordered macroporous (3DOM) carbon,[173-174] carbon nanotubes,[55-56, 92] fullerene,[60] and graphene.[61-62] Their main limitation has been the reproducibility of calibration, i.e., the standard potential of the measuring cell.[112, 175] The stabilities of standard potential of both the working electrode and the reference electrode represent the major common source of measuring errors. Efforts have been spent developing solid contact systems that are calibration free, including systems containing Ag^+ ionophore complexes on a silver epoxy substrate,[18-19] redox-active self-assembled monolayers (SAMs) with a redox potential controlled by an applied current,[116] mixtures of gold nanoclusters with two different charge states,[117] and well controlled cobalt redox couples.[160]

However, there are only a few reports of liquid junction free solid contact reference electrodes,[91, 108] which play an equally important role in a calibration free system. Combining a hydrophobic reference membrane doped with an ionic liquid, 1-methyl-3-octylimidazolium bis(trifluoromethylsulfonyl)imide ($[C_8mim^+][C_1C_1N^-]$), and 3DOM carbon solid contact, a liquid junction free reference electrode was developed.[105]

Owing to the high capacitance of the reference membrane/carbon interfaces, this reference electrode exhibited outstanding long-term stability, with potential drifts as low as 42 μV/h over 26 days. However, the electrode-to-electrode reproducibility of this type of reference electrode is poor, with a standard deviation of E^{o} on the order of ten millivolts. The unsatisfactory reproducibility from electrode to electrode is a result of the ill-defined phase boundary potential at the interface of the sensing membrane and the underlying electron conductor, which may depend on oxygen and other redox-active components on the carbon or from the sample, and requires individual calibration for each electrode.

To address this issue, an ion-to-electron transducer layer, which contains the redox couple cobalt(II)tris(1,10-phenanthroline) ($[Co(phen)_3]^{2+}$) and cobalt(III)tris(1,10-phenanthroline) ($[Co(phen)_3]^{3+}$) and exhibits redox buffer capacity, was developed recently.[176] This redox couple was used to dope cation exchanger membranes. Solid contact electrodes with such membranes show potentials with a standard deviation as low as 0.7 mV. In this work, we doped ionic liquid based reference membrane with the Co(II)/Co(III) redox buffer, using glassy carbon or gold as underlying electron conductors. The reference electrodes exhibited sample independent potentials that solely depend on the ratio of the $[Co(phen)_3]^{2+}$ and $[Co(phen)_3]^{3+}$, as predicted by the Nernst equation. Both carbon and gold-based electrodes exhibit good electrode-to-electrode reproducibility. The reference electrodes with the modified gold substrate as underlying electron conductor exhibited the best long term stabilities.

6.2 Experimental Section

6.2.1 Materials

All reagents were of the highest commercially available purity and were used as received, unless noted otherwise. The ionic liquid 1-methyl-3-octylimidazolium bis(trifluoromethylsulfonyl)imide ($[C_8mim^+][C_1C_1N^-]$), poly(3-octylthiophene) (POT), and 1-hexanethiol were obtained from Io-Li-Tec (Tuscaloosa, AL), Sigma Aldrich (St. Louis, MO), and Acros Organics (Geel, Belgium), respectively. High molecular weight poly(vinyl chloride) (PVC) and 2-nitrophenyl octyl ether (*o*-NPOE) were purchased from Fluka (Buchs, Switzerland). The cobalt(II) salt $[Co(phen)_3](TPFPB)_2$ and the cobalt(III) salt $[Co(phen)_3](TPFPB)_3$ were prepared according to previously reported procedures.[176] Carbon rods were purchased from Graphtek LLC (Buffalo Grove, IL). Gold electrodes were purchased from CH Instruments (Austin, TX). Deionized and charcoal-treated water (18.2 MΩ cm specific resistance) was purified with a Milli-Q PLUS reagent-grade water system (Millipore, Bedford, MA) and was used for all sample solutions.

6.2.2 Membranes

The reference electrode membranes were composed by 40 mg ionic liquid ($[C_8mim^+][C_1C_1N^-]$), 80 mg PVC as polymeric matrix, 80 mg *o*-NPOE as plasticizer, and varying amounts of $[Co(phen)_3](TPFPB)_2$ and $[Co(phen)_3](TPFPB)_3$ (see below). All the membrane components were first dissolved in 2 mL tetrahydrofuran, and the resulting mixture was stirred for at least 2 h to ensure complete dissolution.

6.2.3 Electrodes

The 1.6 mm diameter carbon rods were cut to a length of 15 mm. One end of the carbon rods was polished successively over 100, 300, and 3000 grit sandpaper. A hole was drilled into the other end of the carbon rod. The end of an electrical wire, with the insulation layer removed, was inserted into the hole and glued to the carbon rod with conductive silver epoxy (Chemtronics, Kennesaw, GA). A 40 mm long heat shrink tube was used to shield the side of the carbon rod and the electrical wire (Figure 1), leaving the polished end of the carbon rod accessible for further modification. 10 μL of the solution containing all membrane components was dropcasted onto the polished end of the carbon rod and left to dry overnight.

For comparison, reference electrodes with POT as solid contact were prepared. A POT layer was formed by placing 10 μL POT solution in chloroform onto the polished end of a carbon rod. After waiting for 30 min until the chloroform had evaporated, reference electrode membrane without $[Co(phen)_3](TPFPB)_2$ or $[Co(phen)_3](TPFPB)_3$, was dropcasted onto the POT layer and left to dry overnight.

For reference electrodes with an underlying gold conductor, the 2 mm diameter gold electrodes were polished over polishing cloths with aqueous dispersions of alumina (0.3 and 0.05 μm, Buehler, Lake Bluff, IL) and then cleaned in piranha solution (concentrated sulfuric acid and 30% hydrogen peroxide solution in a 3:1 ratio). *Caution: piranha solution is a strong oxidizing reagent, is highly corrosive, and should be handled with care*. The gold electrodes were then immersed into 1 mM 1-hexanethiol solutions in ethanol for 24 h to form a 1-hexanethiol self-assembled monolayer (SAM). 40 μL of the

above solution of the membrane components was dropcasted onto the gold electrodes and left to dry overnight.

6.2.4 Potentiometric Measurements

Potentials were measured with an EMF 16 potentiometer (input impedance 10 TΩ) controlled with EMF Suite 1.03 software (Lawson Labs, Malvern, PA). A silver/silver chloride wire was used as the ion-selective measuring electrode. A double-junction type reference electrode (DX200, Mettler Toledo, Switzerland; 3.0 M KCl saturated with AgCl as inner-filling solution and 1.0 M LiOAc as bridge electrolyte) was used to monitor the long term stability of the emf. Activity coefficients were calculated according to a two-parameter Debye-Hückel approximation.[133]

6.3 Results and Discussions

As reported previously, plasticized PVC membranes doped with the ionic liquid $[C_8mim^+][C_1C_1N^-]$ have been successfully used to develop liquid-junction-free reference electrodes, using 3DOM carbon substrates. The best long term stability was achieved using membranes with the optimized ionic liquid/PVC/o-NPOE ratios of 1:2:2 (w/w), with potential drifts as low as 42 μV/h over 26 days.[105] Therefore, all experiments in this work were performed with PVC-based membranes with this composition. However, these reference electrodes exhibited electrode potentials with electrode-to-electrode variabilities on the order of tens of millivolts. To improve the potential reproducibility, a $[Co(phen)_3]$ $(TPFPB)_2$/$[Co(phen)_3](TPFPB)_3$ redox buffer, as recently developed in our

group to control the phase boundary potential of ion-selective measuring electrodes, was incorporated into the PVC-based ionic liquid reference membranes.

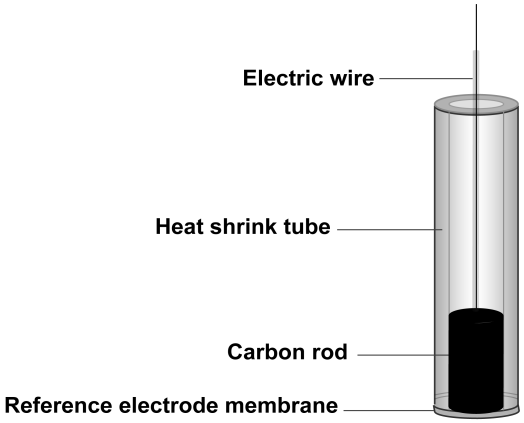

Figure 1. Schematics of reference electrodes based on carbon rods.

6.3.1 Use of Carbon-based Reference Electrodes with Co(II)/Co(III) Redox Buffer/ Ionic Liquid To Measure the Responses of a AgCl/Ag ISE to KCl

For the initial characterization of potentiometric responses, 0.70 mmol/kg of both $[Co(phen)_3]$ $(TPFPB)_3$ and $[Co(phen)_3]$ $(TPFPB)_2$ were added into the plasticized polymer membrane doped with 20% (wt/wt) of the ionic liquid $[C_8mim^+][C_1C_1N^-]$. Reference electrodes based on thus prepared membranes and carbon rods were made (see Figure 1). To assess the suitability of the ionic liquid reference electrodes with the Co(II)/Co(III) redox buffer solid contacts, they were used as reference electrodes in chloride measurements with AgCl-coated Ag wires as Cl^--selective electrodes. The calibration was performed by successive dilution of 50 mL KCl solution from 0.01 M

with stirring. As shown in Figure 2, the Ag/AgCl electrode exhibited theoretical Nernstian response to Cl^- (59.2 ± 0.7 mV increase per tenfold decrease of Cl^- activity). The response time was 5–10 s and all the responses were stable over the 5 min measuring time at different concentrations of KCl solutions, ranging from 10 to 0.1 mM. Calibration curve intercepts, E^o, of electrochemical cells with these solid contact reference electrodes versus a Ag/AgCl electrode were obtained by extrapolation of the linear section of the emf response to the Cl^- activity of 1.0 M. With an electrode-to-electrode standard deviation of 3.5 mV, the ionic liquid reference electrodes based on the Co(II)/Co(III) redox buffer exhibited a better E^o reproducibility than the electrodes without redox buffer. For comparison, the same type of experiment was carried out with ionic liquid reference electrodes based on the widely used conducting polymer poly(3-octylthiophene) (POT) as solid contact. With no added redox buffer, the standard deviation of E^o for electrodes with a POT contact was 14.6 mV, even though these electrodes were fabricated in one batch under apparently identical conditions. The significant improvement in E^o reproducibility by addition of the Co(II)/Co(III) redox couple demonstrates the success of the redox buffer to control the phase boundary potential at the interface of the polymeric membrane and the carbon rod.

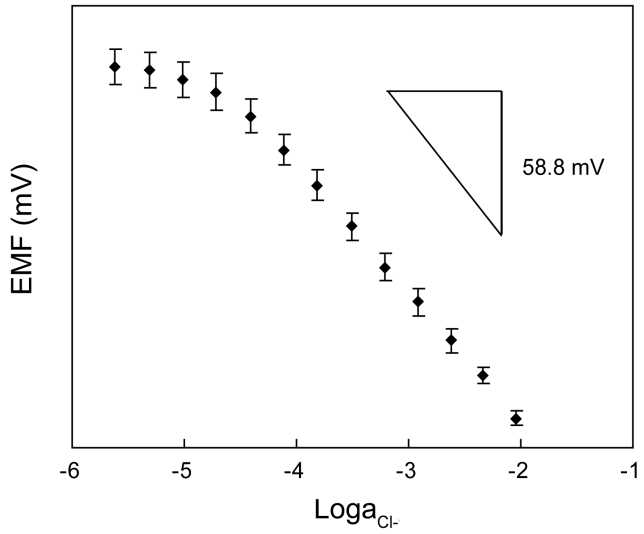

Figure 2. Potentiometric response to Cl^- of a AgCl/Ag electrode versus an ionic liquid reference electrode with $[Co(phen)_3](TPFPB)_2$/$[Co(phen)_3](TPFPB)_3$ (0.70 mmol/kg/0.70 mmol/kg) redox buffer as solid contact.

The total concentration of the Co(II)/Co(III) redox buffer in the ionic liquid reference membranes was optimized. Electrodes based on membranes with varying amounts of $[Co(phen)_3](TPFPB)_2$ and $[Co(phen)_3](TPFPB)_3$ were prepared and their performance was tested after conditioning overnight in 50 mL 0.01 M KCl with stirring. As shown in Table 1, the smallest standard deviation was achieved for a concentration of 0.70 mmol/kg of both $[Co(phen)_3]^{3+}$ and $[Co(phen)_3]^{2+}$, giving a value of 2.1 mV. When the concentrations of the $[Co(phen)_3]^{3+}$ and $[Co(phen)_3]^{2+}$ were as low as 0.07 mmol/kg, the resulting redox buffer capacity was apparently not high enough to stabilize the phase boundary potential at the interface of the polymeric reference membrane and the underlying electron conductor. As a result, the standard deviation of E^o increased to 5.3 mV. When the concentration of the redox couple was raised to 7.10 mmol/kg (see Table 1), no further improvement was found.

Table 1. Performance of different types of reference electrode with carbon rods.

	Concentration of redox couple	Conditioned in 0.01 M KCl for 1 h (n=4)		Conditioned in 0.01 M KCl overnight (n=4)	
Electrode type	Co(II) / Co(III) (each in mmol/kg)	Slope (mV / decade)	E^o (mV)	Slope (mV / decade)	E^o (mV)
1	0.07 / 0.07	59.1 ± 0.3	227.2 ± 9.7	58.3 ± 1.3	163.3 ± 5.3
2	0.70 / 0.70	59.2 ± 0.7	229.4 ± 3.5	59.1 ± 0.5	181.9 ± 2.1
3	7.10 / 7.10	59.0 ± 0.7	324.2 ± 6.8	54.2 ± 0.7	273.7 ± 6.4

All membranes contained besides the redox couple the same components: PVC : o-NPOE : ionic liquid = 2:2:1 (wt/wt). E^o values refer to the potential of the ISE cell of the AgCl/Ag electrode versus the reference electrode as obtained by extrapolation of the linear section of the response to the Cl^- activity of 1.0 M.

6.3.2 Dependence of emf on the Ratio of the Reduced/Oxidized Components of the Co(II)/Co(III) Redox Buffer

If the phase boundary potential at the interface of the polymeric reference membrane and the underlying electron conductor is determined by a redox couple, the phase boundary potential at this interface is expected to follow the Nernst equation. Therefore, the experimentally observed E^{o} values of an electrochemical cell consisting of a reference electrode and a Ag/AgCl electrode inserted into a solution with a chloride activity of 1.0 M should depend on the concentrations of the reduced and oxidized species (C_{red} and C_{ox}) of the redox buffer as follows:

$$emf = E^{0'} - \frac{2.303RT}{nF}\log\frac{C_{red}}{C_{ox}}$$

where R is the gas constant, T is the temperature, F is the Faraday constant, n is the number of electrons transferred, and E^{o}' is the emf of the electrochemical cell with a AgCl/Ag electrode versus the reference electrode at a chloride activity of 1.0 M. To confirm this relationship experimentally, polymeric membranes with C_{red}/C_{ox} ratios of 5:1, 1:1, and 1:5 were prepared. The emf values were found to depend on log (C_{red}/C_{ox}) with slopes of −56.4 mV/decade and −62.3 mV/decade for carbon based reference electrodes that were conditioned in 0.01 M KCl for 1 h or overnight, respectively. These values are in good agreement with the Nernst equation, which confirms that the phase boundary potential at the interface of the reference membrane and the underlying electron conductor is indeed determined by the ratio of the concentrations of the reduced and oxidized components of the redox buffer.

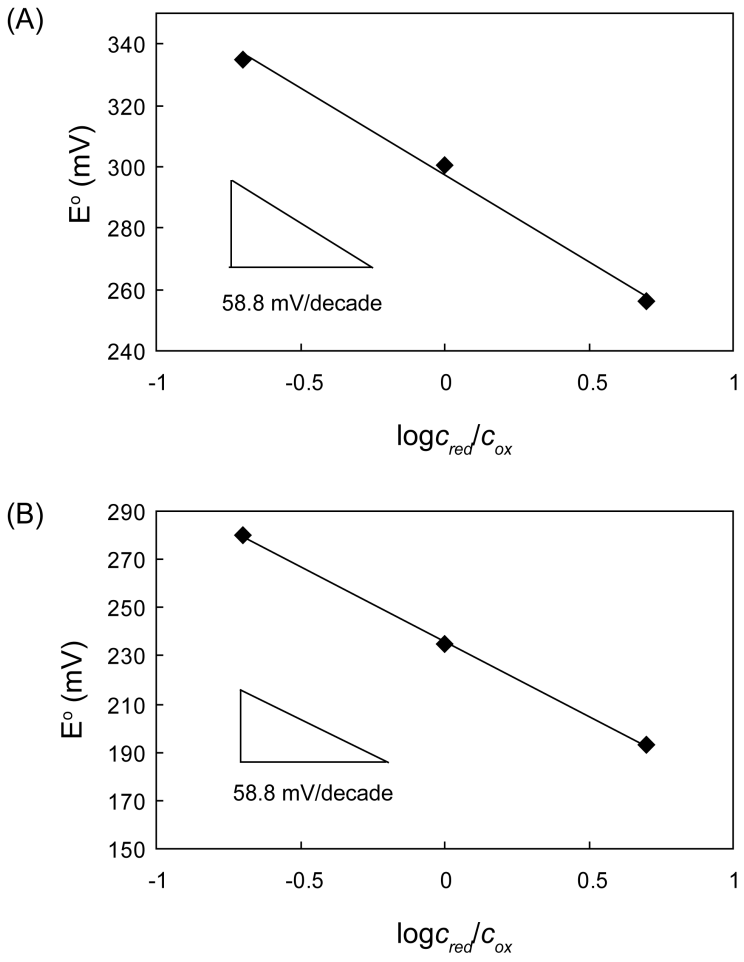

Figure 3. *E*º of the ISE cell of a AgCl/Ag electrode versus the ionic liquid/ Co(II)/Co(III) redox buffer reference electrode, as obtained by extrapolation of the linear section of the response to the Cl^- activity of 1.0 M. The reference electrode was conditioned for (A) 1 hour and (B) 12 hour before measurements.

6.3.3 Long Term Stability of Carbon-based Reference Electrodes with Co(II)/Co(III) Redox Buffer/ Ionic Liquid

The long term stability of the ionic liquid reference electrodes on a carbon rod substrate with a membrane doped with 0.70 mmol/kg of both $[Co(phen)_3]^{3+}$ and

$[Co(phen)_3]^{2+}$ was investigated. The response of these reference electrodes versus a DX200 double-junction reference electrode in 0.01 M KCl solution was monitored for 72 h and the drift was calculated to be 0.30 mV/h, which is about 10 times larger than the drift of the 3DOM carbon/ionic liquid reference electrode.[105] A limited long term stability was also observed in E^o measurements. As shown in Table 2, compared to electrodes conditioned in 50 mL stirred 0.01 M KCl solution for 1 h, the standard deviations of E^o for the carbon-based reference electrodes with membranes doped with ionic liquid and various amount of $[Co(phen)_3](TPFPB)_2$ and $[Co(phen)_3](TPFPB)_3$ improved after conditioning overnight in stirred solution. However, during that time, the absolute values of E^o decreased by about 50 mV. The significant drift and change in E^o was probably caused by the formation of an aqueous layer between the polymeric membrane and the underlying carbon substrate, which changed the interfacial potential, as also suggested by the lack of such a significant drift when carbon contacts were replaced with a modified gold contact (see below). Unfortunately, because of the lack of response of this reference electrode to ions, the hypothesis of water layer formation is not as easy to test with the water layer test[16] as that is possible for ISEs.

6.3.4 Polymeric Membranes Doped with a Redox Couple in Contact with Gold Contacts Modified with a Self-Assembled Alkanethiol Monolayer

To overcome the problem of the water layer formation, gold substrates were chemically modified with a hydrophobic SAM of 1-hexanthiol. A polymeric membrane doped with the $[Co(phen)_3]^{3+/2+}$ couple was then deposited onto the SAM-modified gold, generating a hybrid system with hydrophobicity and redox capacity.

Table 2 shows E^{o} values and standard deviations of the hybrid system when the electrodes were kept in 50 mL 1 mM KCl solution during 4 days. Because of the redox buffer capacity, the standard deviation of E^{o} was only 3.9 mV after one hour of solution exposure, which is comparable to the carbon based reference electrodes with the Co(II)/Co(III) redox buffer. After 24 hours of exposure to 1 mM KCl solutions, the electrodes still showed excellent performance with a standard deviation of 3.5 mV. Interestingly, the initial drift of the emf when these electrodes were first expose to an aqueous solution can be unequivocally explained by uptake of water into the polymeric membrane. To show this and to minimize the initial drift of the electrodes, three SAM-modified gold reference electrodes were stored in a water-saturated atmosphere for 24 h, and the emf response was then recorded from the first moment the electrodes were in direct contact with a 1 mM KCl solution. Figure 4 shows that the emf of the electrodes that had been exposed to humidity changed over a period of 9 h by only 2.4 mV (average of three electrodes), while emf of electrodes that had been stored in ambient air drifted by 32.9 mV. Exposure of the electrodes to humidity also improved the reproducibility of E^{o}, with a standard deviation of 1.8 mV at first contact with the aqueous solution and 0.1 and 4.3 mV after 4 and 9 h, respectively.

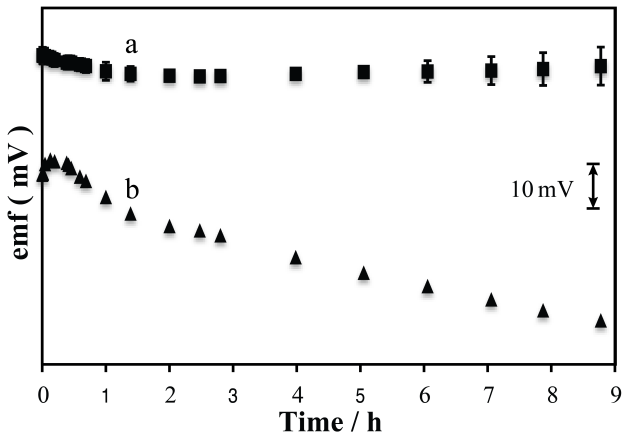

Figure 4. The emf responses of ionic liquid/Co(II)/Co(III) redox buffer reference electrodes based on 1-hexanethiol modified gold electrodes. (a) The reference electrodes were exposed to high humidity for 24 h prior to first contact with aqueous solutions; (b) the reference electrode was stored in ambient air before the measurement.

Table 2. Response of an ISE with a solvent polymeric membrane doped with a redox buffer in contact with a SAM modified gold contact after storage in 1.0 mM KCl for up to 4 days (n=3).

Conditioning time	Slope (mV / decade)	E^o values (mV)
1	61.4 ± 2.4	402.3 ± 3.9
24	60.6 ± 1.2	398.4 ± 3.5
48	60.9 ± 0.8	402.1 ± 23.1
96	60.8 ±1.3	416.9 ±22.7

The standard deviation of E^o for the Co(II)/Co(III) redox buffer/ionic liquid based reference electrode with SAM-modified gold deteriorated after exposure to 1 mM KCl for 48 h or more. It appears likely that transfer of redox couple cations along with the

ionic liquid anion from the polymeric membrane into the aqueous sample resulted in a change in the Co(II)/Co(III) ratio. Where a better long term performance is needed, such problems could be solved by using a more hydrophobic Co(II)/Co(III) redox couple or by attaching the redox couple to the polymer backbone.

6.4 Conclusions

A liquid junction free reference electrode with good E^o reproducibility was developed in this work by combining a polymeric membrane doped with ionic liquid and a Co(II)/Co(III) redox buffer. The thus prepared solid contact reference electrodes demonstrate a standard deviation of E^o as low as 2.1 mV. The reference electrode based on carbon substrates is satisfactory for one-time and short-term use. On the other hand, the reference electrodes with a monolayer-modified gold conductors can be used for up to 24 h as they suffer much less from the formation of a water layer at the membrane/conductor interface. Uptake of water into the polymeric membrane causes a drift of the emf over several hours but can be minimized if the electrode membranes are stored at high humidity prior to the first contact with an aqueous sample. For even longer measurements and for measurements in biological samples, loss of the redox active Co(II)/Co(III) into the sample cause drifts and increased standard deviations of E^o. For such applications, methods to prevent leaching of the Co(II)/Co(III) complexes into the sample are needed, such as the attachment of the $[Co(phen)_3]^{3+/2+}$ complexes onto a polymer backbone or the use of more hydrophobic redox buffer species.

ACKNOWLEDGMENT

This research was supported by the National Science Foundation through grant SBIR 1256626 II-P and OISE CHE-0809328 and Doctoral Dissertation Fellowship from Graduate School, University of Minnesota

CHAPTER SEVEN

Elimination of the Light Sensitivity of Ionophore-Based Ion-Selective Electrodes

In part from:

Xu U. Zou, Li D. Chen, Koichi Nishimura and Philippe Bühlmann, manuscript in preparation

Li D Chen, Xu U Zou, Philippe Buhlmann, *Analytical. Chemistry*. **2012**, 84(21), 9192–9198

Reproduced in part with permission from Analytical Chemistry, 84(21), 9192.

Copyright © 2012 American Chemical Society.

Abstract

Ion-selective electrodes (ISEs) with Zn(II) meso-tetraphenylporphyrin as receptor resulted in significantly improved selectivities for CN^-.[1] However, Zn(II) meso-tetraphenylporphyrin reacts with molecular oxygen upon illumination to give singlet oxygen, a reactive oxidizing species that may initiate the opening of the porphyrin ring. When exposed to light, the Zn(II) meso-tetraphenylporphyrin based CN^--selective electrodes suffered from sub-Nernstian responses to CN^- and decreases in selectivities. However, no decreases in performance were found if the experiments were performed in a dark room. Furthermore, initial results showed that a Nernstian response to CN^- was maintained when the electrodes were protected with a 660 nm high pass filter while a loss of the Nernstian response was observed with 500 nm or 400 nm high pass filters. This observation suggests that the light sensitivity is caused directly by absorption of visible light by Zn(II) meso-tetraphenylporphyrin, that exhibits absorption peaks at 425 nm and 550 nm. A wide variety of light absorbing materials (e.g., graphite, carbon nanotubes, fullerene and different types of organic dyes) were incorporated into ISE membranes to test if the degradation of the Zn(II) meso-tetraphenylporphyrin can be prevented.

7.1 Introduction

Cyanide is used in various industrial applications, including polymer synthesis, electroplating, metallurgy, and mining. For instance, cyanide leaching is a key extraction process for the efficient recovery of gold from complex ores,[177] and cyanide is used in the separation of gold, silver, and copper from platinum.[178] Unfortunately, chronic cyanide exposure induces irritation, pain, and nervous instability, and acute cyanide poisoning can be fatal as it disrupts the mitochondrial electron transport chain by interacting with cytochrome oxidase, inhibiting respiration.[179] Cyanide contamination of the environment through industrial processes is as much a concern as is accidental workplace exposure and poisoning as a result of suicidal, criminal, and terroristic activities. Moreover, cyanide poisoning in residential fires as a result of the combustion of polyurethanes, melamine, and other plastics can be fatal well before victims have inhaled toxic levels of CO, which led the US Food and Drug Administration to approve in 2006 hydroxocobalamin for the prehospital treatment of known or suspected cyanide poisoning.[180]

A variety of methods and techniques were developed for the determination of cyanide, including volumetric titrations,[181] chromatography,[182-184] voltammetry,[185] amperometry,[186] and fluorimetry.[187] Many of these methods require complex sample preparation, such as acidification followed by HCN diffusion through a gas-permeable membrane. Therefore, quick methods that permit selective in-situ determination with high selectivity, such as receptor-based potentiometry,[1, 9,1, 122] have particular promise for medical point-of-care and industrial and environmental on-line monitoring. An ISE with Zn(II) meso-tetraphenylporphyrin as receptor for CN^-, which resulted in improved

selectivities for CN^- as compared to ionophore-free ion-exchanger electrodes has been reported.[188] Particularly noteworthy is the reduction in interference from OH^-. However, when continuously exposed to light from a fluorescent bulb, decreased response slope and worsened detection limit were observed. Also the color of membrane turned from purple to green. The UV-vis spectrum showed a decreased intensity of the peaks at 425 and 550 nm, which indicated that either the ionophore or its complex underwent chemical degradation.

Although it is widely accepted that ion-selective electrodes have limited life times due to the slow leaching of components from the sensing membrane into sample,[189-190] ionophore decomposition has been neglected as a critical factor limiting the usage time.[191-192] However, in the presence of oxygen, some photosensitizers can transfer their energy to molecular oxygen, which converts it into a highly reactive singlet state and regenerates the sensitizer.[193-194] The sensitizer can interact directly with different substrates by H-atom or electron transfer and also with all accessible potential reactants in their close vicinity.[192] Generally speaking, the O-H, N-H and aromatic C-H bonds are considered the most vulnerable towards singlet oxygen in liquid phases.[194] Linder et al. found oxidation of ETH 5294 into a colorless product took place in the presence of anions that could be efficiently oxidized, such as chloride, bromide, iodide, tetraphenyllborate (TPB^-) and tetrakis(4-chlorophenyl)borate ($TpClPB^-$). However, in the case of stable anions, such as nitrate, perchlorate or sulfate, the decomposition of the dye was negligible. Thus, the experimentally observed differences in the color decay in presence of different salts and in the photostability of different chromoionophores can be attributed to the complex result of reactions with singlet oxygen.[192]

Here, we report a detailed study on light sensitivity of Zn(II) meso-tetraphenylporphyrin which exhibits absorption peaks at 425 nm and 550 nm. The light damage is caused directly by absorption of visible light. A wide variety of light absorbing materials (e.g., graphite, carbon nanotubes, fullerene and different types of organic dyes) were incorporated into ISE membranes to test if the degradation of Zn(II) meso-tetraphenylporphyrin can be prevented. Single wall carbon nanotubes (SWCNT) have been found the most effective material to prevent light damage of Zn(II) meso-tetraphenylporphyrin.

7.2 Experimental Section

7.2.1 Materials

All reagents were of the highest commercially available purity and used as received. Deionized and charcoal-treated water (0.18 MΩ m specific resistance) purified with a Milli-Q PLUS reagent grade water system (Millipore, Bedford, MA) was used for preparing all sample solutions. High molecular weight poly(vinyl chloride) (PVC) and 2-nitrophenyl octyl ether (*o*-NPOE) were purchased from Fluka (Buchs, Switzerland), tridodecylmethylammonium chloride (TDDMACl), *N,N′*-bis(4-methoxybenzyl)perylene-3,4:9,10-bis(dicarboximide), Reichardt's dye, single-walled carbon nanotubes (SWCNTs) and multiwalled carbon nanotubes (MWCNTs) from Sigma-Aldrich (St. Louis, MO), Zn(II) meso-tetraphenylporphyrins, Sudan Black B ((2,2-dimethyl-1,3-dihydroperimidin-6-yl)-(4-phenylazo-1-naphthyl)diazene) and Solvent Yellow 56 (4-(diethylamino)azobenzene) was purchased from Alfa Aesar (Ward Hill, MA). Pentacene was purchased from TCI America (Montgomeryville, PA)

7.2.2 Ion-Selective Electrodes

Zn(II) meso-tetraphenylporphyrin-doped membranes were prepared by dissolving the membrane components (66 mg PVC as polymer matrix, 132 mg *o*-NPOE as plasticizer, 1.25 mg Zn(II) meso-tetraphenylporphyrin as ionophore, and 0.75 mg TDDMACl as to provide cationic sites) in tetrahydrofuran (THF). Dyes were soluble in THF and doped into the membrane in various amounts. SWCNT, MWCNT, fullerene, pentacene and *N,N′*-bis(4-methoxybenzyl)perylene-3,4:9,10-bis(dicarboximide) were suspended in THF by sonication first and then mixed with membrane components. The mixed solution was poured into a glass dish (31 mm i.d.), and the THF was allowed to evaporate slowly at room temperature overnight. The molar ratio of cationic sites to ionophore in the resulting membranes was 71:100, and the membrane thickness was approximately 100 μm. The ion-selective membranes were then cut and glued with THF onto the end of a tygon tube (3/16 inches, i.d., and 5/16 inches, o.d.). An outer filling solution containing 1 mM primary anions (typically CN^-) was in direct contact with the backside of the sensing membrane. It was separated by a small cotton plug (tightly packed into a tapered plastic pipette tip) from an inner filling solution (1 mM KCl), into which a AgCl-coated Ag wire was inserted as inner reference electrode. ISEs prepared in this way were used in combination with a double-junction type external reference electrode (DX200, Mettler Toledo, Switzerland; 3.0 M KCl saturated with AgCl as inner-filling solution and 1.0 M LiOAc as bridge electrolyte).

7.2.3 Potentiometric Measurements

Potentials were measured with an EMF 16 potentiometer (input impedance 10 TΩ) controlled with EMF Suite 1.03 software (Lawson Labs, Malvern, PA). Activity coefficients were computed according to a two-parameter Debye-Hückel approximation,[133] and all EMF values were corrected for liquid-junction potentials with the Henderson equation. Selectivity coefficients were determined with the separate solution method (SSM)[195] Using single salt solutions, Nernstian responses to all ions were confirmed in the concentration range where selectivities were determined.

7.2.4 Spectroscopy Experiments

UV-vis absorption spectra were recorded on a JACOB 610 spectrophotometer (BioTek, Winooski, VT). Ionophore-doped membranes were spin-coated onto quartz glass discs for these measurements. ^{1}H NMR spectra were recorded on a Varian Inova 500 spectrometer (Varian, Palo Alto, CA).

7.3 Results and Discussions

7.3.1 Light Sensitivity

Zn(II) meso-tetraphenylporphyrin reacts with molecular oxygen upon illumination to give singlet oxygen, a reactive oxidizing species that may initiate the opening of the porphyrin ring (Figure 1). The product is not a broad mixture of compounds but appears to be one or few distinct decomposition products.

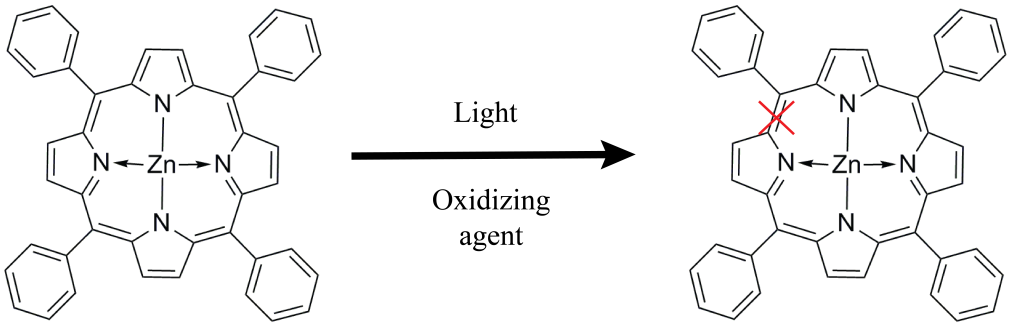

Figure 1. Ring opening of Zn(II) meso-tetraphenylporphyrin upon light illumination.

To study this phenomenon further, ^{1}H NMR spectra were measured of Zn(II) meso-tetraphenylporphyrin in THF-d_8 after equilibration with an equal volume of D_2O solution of 0.1 M KCN for 4 and 8 days. The spectra showed small but distinct peaks not initially present at 7.72, 7.21, 6.82, 6.28 and 5.72 ppm, indicating the dominance of one specific decomposition reaction. These peaks increased in intensity as time progressed (see Figure 2). This observation might be caused by a ring-opening reaction of the Zn(II) meso-tetraphenylporphyrin in the presence of nucleophiles such as OH^- and CN^- and peroxide which might be generated in THF upon exposure to light.[196]

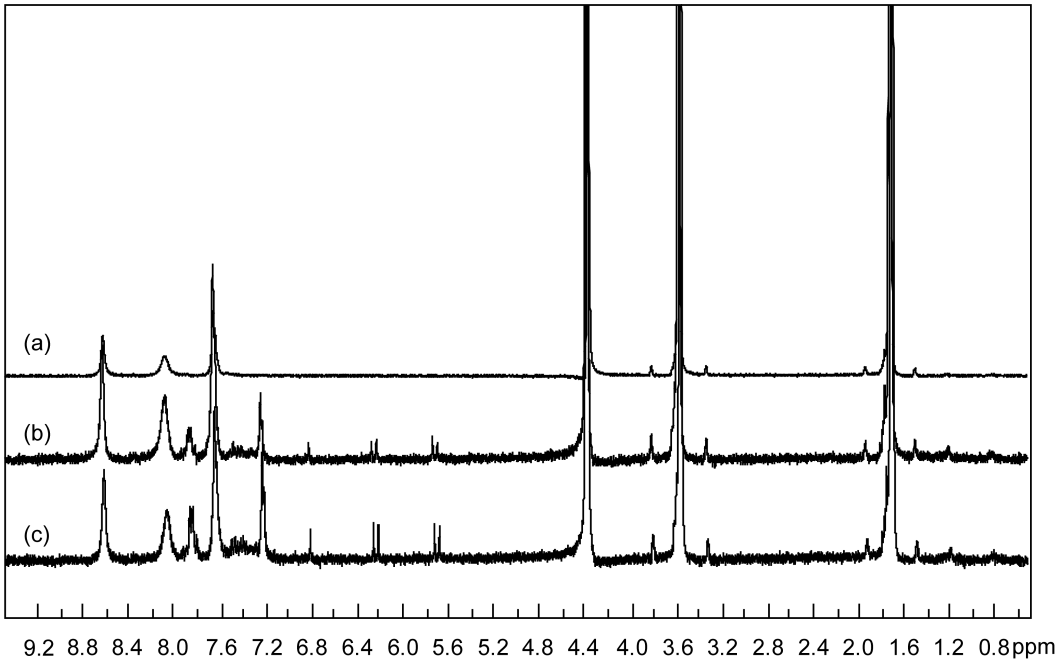

Figure 2. ^{1}H NMR spectra of Zn(II) meso-tetraphenylporphyrin in THF-d_8 after equilibration with an equal volume of D_2O solution of 0.1 M KCN for (a) 0, (b) 4 or (c) 8 days.

By spin coating the membrane on a quartz plate, the decomposition of Zn(II) meso-tetraphenylporphyrin could be observed directly in the membrane phase. No changes in the UV-vis spectrum were observed for the one that was kept in dark. However, for the membrane that was continuously exposed to light from a fluorescent tube, the UV-vis spectrum showed a decreased intensity of the peaks at 425 and 550 nm, and an additional peak at 615 nm (Figure 3). The different results for membranes kept in the dark and membranes exposed to light reveal that light plays a key role in the degradation of membrane performances. The decreased intensity in absorption confirms a reduction in the amount Zn(II) tetraphenylporphyrin due to the chemical degradation.

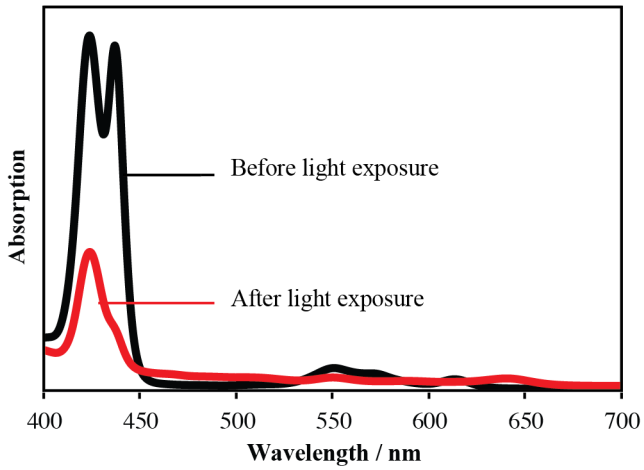

Figure 3. UV-vis spectra of membranes doped with the ionophore Zn(II) meso-tetraphenylporphyrin and 25 mol% cationic sites provided by TDDMACl before and after exposure to light from a fluorescent tube for 3 days.

The degradation of Zn(II) meso-tetraphenylporphyrin was also captured by the potentiometric response to CN^- (Figure 4). When kept in the dark, electrodes exhibited a Nernstian slope of 59.5 mV / decade and a detection limit of 10^{-5} M. After 4 h's light exposure, a 54.5 mV / decade in response slope was observed and the detection limit was $10^{-4.9}$ M. After 24 h's light exposure, significant changes in response slope and detection limit were seen with 43.0 mV / decade and $10^{-4.4}$ M, respectively. The worsened response slope can be attributed to the damage of ionophore, Zn(II) meso-tetraphenylporphyrin in the membrane , resulting in a decreased amount of ionophore and changes in the optimized ionophore-to-sites ratio. Thus, both response slope and detection limit deteriorated probably due to the interference of hydroxide in the solution.

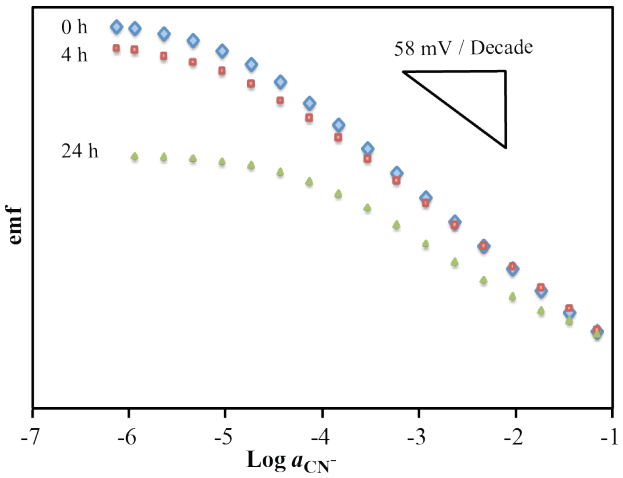

Figure 4. Emf response of a cyanide-selective electrode without light exposure and after 4 and 24 h's exposure to light from a fluorescent tube.

7.3.2 Doping Organic Dyes

Initially, it was hypothesized that only the largest absorption peak was directly related to a serious damaging effect on the ionophore and was therefore responsible for decreasing response slopes and worsened detection limits. As a result, three organic dyes (see Figure 5), which showed strong absorption from 400 nm to 450 nm were doped into the ion-selective membrane in order to absorb the light from that range of wavelengths and prevent the damage. However, the electrodes exhibited a decreased response slope already even before exposed to light. The electron lone pairs on the nitrogen or oxygen atom in these dye molecules (Figure 5) might coordinate with the metal center in the ionophore molecule, which may cause the response change. This proved the doping method was not trivial. According to Lindner et al., upon illumination, some dyes might deteriorate the ISE performance by generating singlet oxygen[197] and damaging the ionophores. [192, 198-199]

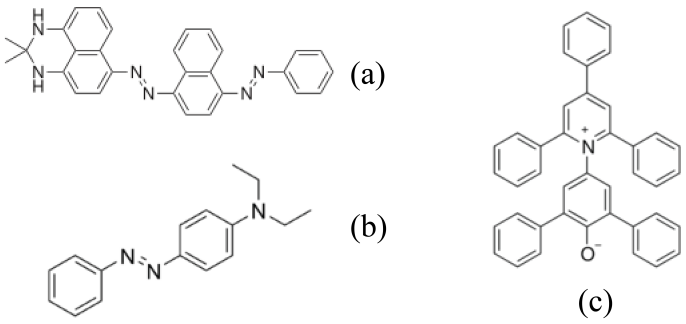

Figure 5. Molecular structure of (a) sudan black B, (b) solvent yellow 56 and (c) Reichardt's dye

7.3.3 Filter Experiment to Determine Damaging Wavelength

The UV-Vis spectrum showed that there were one large absorption peak at 425 nm and two very small peaks at 550 nm and 615 nm. In order to determine which range of wavelengths actually caused the worsening in the performance of the electrodes, three high pass filters with cutoffs at 400 nm, 495 nm, and 665 nm were used, which allowed light beyond the cut-off wavelength to pass. (Figure 6)

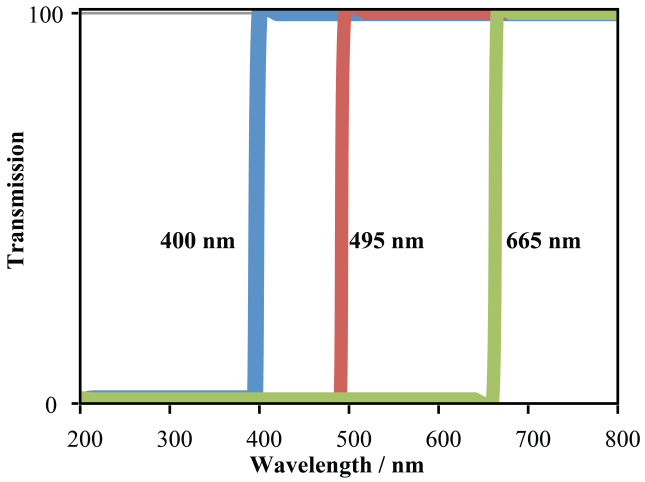

Figure 6. Transmission spectrum of high pass filter of 400 nm, 495 nm and 665 nm.

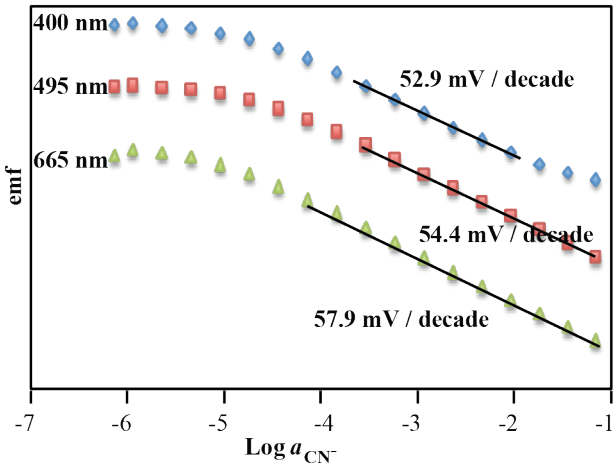

Figure 7. Electrode responses were measured after illumination with a fluorescent bulb above 400, 495 or 665 nm for 4 h.

After exposure to light with wavelength above 400 nm or 495 nm, the electrodes showed sub-Nernstian response with slope of 52.9 or 54.4 mV / decade, respectively. The loss of optimized electrode performances (Nernstian slope and detection limit) were caused by the change of ionophore to ionic sites ratio due to the decrease in amount of intact ionophores. The Nernstian slope was only maintained with the 665 nm filter, with a response slope of 57.9 mV / decade, which showed the light beyond 665 nm has no destructive effect on the ionophore. The results demonstrated that not only would the large absorption at 425 nm damage the ionophore, but also would the small peaks at 550 nm or 615 nm. This complicated the experiment if one would stick to the dye doping method since one dye would probably not suffice the three absorption ranges requirement.

7.3.4 Doping with Other Materials

Alternatively, materials with the characteristics that might absorb the whole range of visible light were selected and incorporated into ISE membranes, which visually made the membranes black and let them absorb all the light, thus protecting the ionophore.

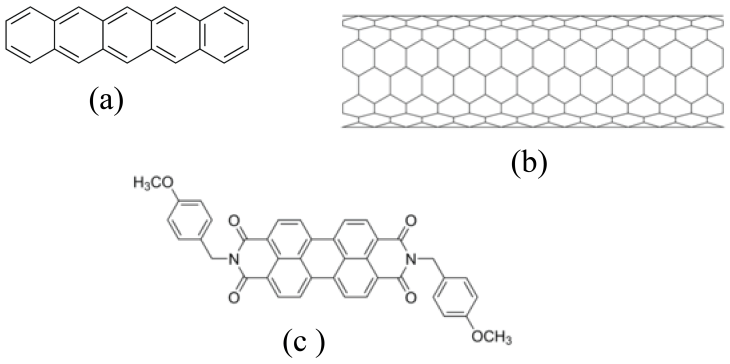

Figure 8. Structure of (a) pentacene, (b) SWCNT and (c) perylene derivative.

All membranes doped with pentacene, SWCNT or perylene derivative showed Nernstian slopes prior being exposed to light. Neither pentacene (doped as 5 wt%) nor the perylene derivative (5 wt%) prevented the light damage successfully as the response slopes decreased to 50.4 mV / decade after 4 h's light exposure and 36.2 mV / decade after 24 h of light exposure for pentacene doped membranes (Figure 9 a), and 51.8 mV / decade after 4 h of light exposure for perylene derivative doped membranes (Figure 9 b). SWCNT doped membrane maintained the Nernstian response of 56.9 mV / decade. Other carbon material such as fullerene soot and carbon black were also tested but the initial response without any light exposure were not Nernstian, probably due to functional groups on their surfaces, resulting in a coordinative interaction with the ionophore. Light absorbing materials like SWCNT showed such a strong absorption of light that photon absorption by the ionophore resulting in ionophore decomposition could be suppressed.

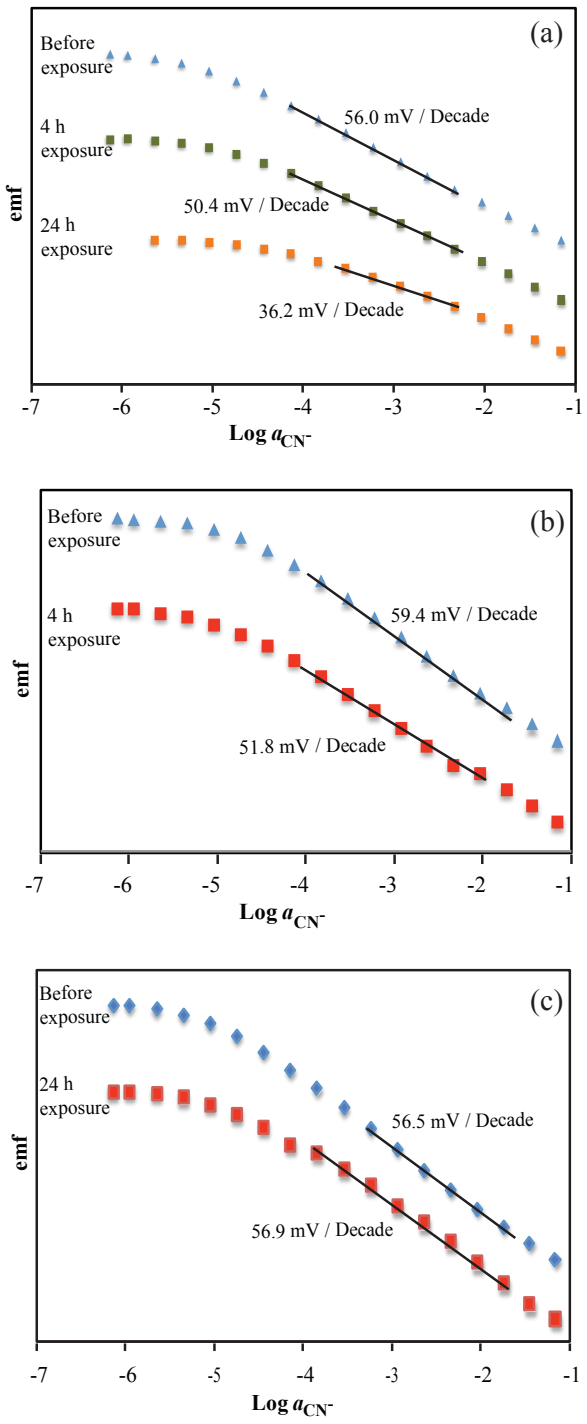

Figure 9. Electrode responses were measured after illumination under a fluorescent bulb. Membranes doped with (a) 5 wt% pentacene, (b) 5 wt % perylene derivative and (c) 7.5 wt% SWCNT.

7.4 Conclusions

This contribution reports a method of doping light absorbing materials to protect light sensitive ionophores from degradation. It has been concluded that the light sensitivity is caused directly by absorption of visible light by Zn(II) meso-tetraphenylporphyrin, which exhibits absorption peaks at 425 nm, 550 nm, or 615 nm. A wide variety of light absorbing materials (e.g., graphite, carbon nanotubes, fullerene and different types of organic dyes) were incorporated into the ISE membranes to test if the degradation of the Zn(II) meso-tetraphenylporphyrin could be prevented. However, only SWCNT did not affect the Nernstian character of the EMF response. This method can be potentially extended to other light sensitive ionophores.

CHAPTER EIGHT

Use of an Electrically Neutral Axial Ligand to Improve the Selectivity of a Cyanide-Selective Electrode With Zn(II) Tetraphenylporphyrin as Ionophore

Abstract

The selectivity is one of the most important characteristics of a sensor, which determines whether a reliable measurement in the target sample is possible. However, improving selectivity for ion-selective electrodes proved to be difficult due to the challenges of synthesizing better ionophores. Here we report a new method to improve the selectivity of Zn(II) meso-tetraphenylporphyrin based cyanide-selective electrode by doping trioctylamine into an ion-selective membrane. Because of the ligand's enhancing effect on the binding constant between Zn(II) meso-tetraphenylporphyrin and anion of interest, the selectivity for anions over nonbinding TPB^- was increased by 1.5 magnitudes. This provides an easy and flexible way to improve the selectivity of ion-selective electrode based on metal porphyrin ionophores.

8.1 Introduction

The selectivity is one of the most important characteristics of a sensor, which determines whether a reliable measurement in the target sample is possible. It is especially critical in clinical applications, such as whole blood or serum measurements.[1] The selectivity of an ion-selective electrode originates from several sources. One is the difference in solvation energy of ions between the aqueous phase (sample solution) and the organic phase (membrane). For example, the selectivity sequence of an ionophore-free cation-exchange electrode is $Cs^+ > Rb^+ > K^+ > Na^+ > Li^+$, which follows the Hofmeister series.[2] With ionophores in the membrane, the selectivity sequence will favor the ions having stronger binding strength with the ionophore that significantly lowers the energy of phase transfer energy of the target ion compared to the effect on other interfering ions, and thus changes the selectivity sequence.

Efforts of improving the selectivity of ion-selective electrodes have been focusing on new ionophores that have a strong binding ability with a target ion. In designing new ionophores, several principles should be applied. Ionophores should be designed to exhibit a sufficient lipophilicity in solvent polymeric membranes for typical flow-through analysers, even for continuous use in whole blood for a whole one month.[1] The ionophores should form stable complexes with the primary ion but complexation also needs to be reversible.[200] The challenge for new ionophores lies in the design and synthesis of new molecules.

Metal porphyrins have been widely used as anion ionophores and their selectivity for a particular ion arises from preferred axial ligation to the central metal ion of the porphyrin complex. Examples include ion-selective electrodes for fluoride,[201]

thiocyanate,[202] acetic acid,[203] diclofenac,[204] cyanide,[120] and chloride.[205]

Here we report a new method to improve the selectivity of Zn(II) meso-tetraphenylporphyrin based cyanide-selective electrode by doping of membranes with neutral ligands. It was previously reported that addition of a pyridine ligand to the fifth coordination site of Zn(II) center enhances ion binding at a sixth coordination site (i.e. the opposite axial binding site) with the association constants increasing by 96 times and 141 times for nitrite and nitrate, respectively.[206] Since higher binding constants will decrease the transfer energy of a target ion from an aqueous phase into the membrane phase and changes the transfer energy for different ions to different extents, binding of neutral ligands has the potential to change the selectivity sequence.

8.2 Experimental Section

8.2.1 Materials

All reagents were of the highest commercially available purity and used as received. Deionized and charcoal treated water (0.18 MΩ m specific resistance) purified with a Milli-Q PLUS reagent grade water system (Millipore, Bedford, MA) was used for preparing all sample solutions. High molecular weight poly(vinyl chloride) (PVC) was purchased from Fluka (Buchs, Switzerland). Tridodecylmethylammonium chloride (TDDMACl), 2-nitrophenyl octyl ether (*o*-NPOE), zinc meso-tetraphenylporphyrins, 4-nonadecylpyridine (Hydrogen ionophore 2), octadecyl isonicotinate (Hydrogen ionophore 4), and trioctylamine were purchased from Sigma-Aldrich (St. Louis, MO).

8.2.2 Ion-Selective Electrodes

Zn(II) meso-tetraphenylporphyrin-doped membranes were prepared by dissolving the membrane components (132 mg PVC as polymer matrix, 264 mg o-NPOE as plasticizer, 2.50 mg Zn(II) meso-tetraphenylporphyrin as ionophore, 1.50 mg TDDMACl to provide cationic sites, and various amount of 4-nonadeclypyridine, octadecyl isonicotinate, or trioctylamine) in 3.0 mL freshly distilled tetrahydrofuran (THF). The purple solution was poured into a glass dish (31 mm i.d.), and the THF was allowed to evaporate slowly at room temperature overnight. The molar ratio of cationic sites to ionophore in the resulting membranes was 71:100, and the membrane thickness was approximately 200 μm. Ion-selective membranes were then cut out from this master membrane using a cork borer and glued with THF onto the end of a Tygon tube (3/16 in. i.d., 5/16 in. o.d.). An outer filling solution containing 1 mM primary anions (typically CN^-) was in direct contact with the backside of the sensing membrane. It was separated by a small cotton plug (tightly packed into a tapered plastic pipet tip) from an inner filling solution (1 mM KCl), into which a AgCl-coated Ag wire was inserted as an inner reference electrode. ISEs prepared in this way were used in combination with a double-junction type external reference electrode (DX200, Mettler Toledo, Switzerland; 3.0 M KCl saturated with AgCl as inner-filling solution and 1.0 M LiOAc as bridge electrolyte).

8.2.3 Potentiometric Measurements

Potentials were measured with an EMF 16 potentiometer (input impedance 10 TΩ) controlled with EMF Suite 1.03 software (Lawson Labs, Malvern, PA). Activity coefficients were computed according to a two-parameter Debye−Hückel

approximation,[133] and all EMF values were corrected for liquid-junction potentials with the Henderson equation.[2] Selectivity coefficients were determined with the separate solution method (SSM). Using single salt solutions, Nernstian responses to all ions were confirmed in the concentration range where selectivities were determined. Reported selectivity values are averages for three or more electrodes.

8.2.4 Spectroscopy Experiment

UV-vis absorption spectra were recorded on JACOB 610 Spectrophotometer (BioTek, Winooski, VT). The solvent (heptane: nitrobenzene=65:35 v/v) was prepared so that the polarity of the mixed solvent is similar to the plasticizer (o-NPOE) used in ion-selective membrane. 4,7,13,16,21,24-Hexaoxa-1,10-diazabicyclo[8.8.8]hexacosane was added to dissolve KCN. Trioctylamine of various concentrations was added into 1 mM Zn(II) tetraphenylporphyrin.

8.3 Results and Discussions

8.3.1 Potentiometric Responses and Selectivities.

To minimize EMF response drifts, 1 mM KCl as outer filling solution of these ISEs was included, in addition to 1 mM KCN and 1 mM NaOH. To prevent the formation of HCN vapors, all KCN sample solutions were prepared in solutions with a 1 mM NaOH background. Calibrations for CN^- and TPB^- were carried out by successive dilution of a 0.1 M KCN/1 mM NaOH solution with 1 mM NaOH, and dilution of a 1 mM NaTPB solution of water except membranes with trioctylamine, respectively. Calibrations for TPB^- of membranes with trioctylamine were carried out by dilution of a 1 mM NaTPB/1

mM NaOH solution with1 mM NaOH. The reason for this is to minimize the effect of hydrogen ions, and to get Nernstian slopes. (When emf measurements of TPB^- were carried out without NaOH, the slopes went up to approximately twice–Nernstian response (data not shown).[207] Trioctylamine, Hydrogen ionophore 2, or Hydrogen ionophore 4 was doped to ISE membranes as modifier with 50 mol% relative to the ionophore.

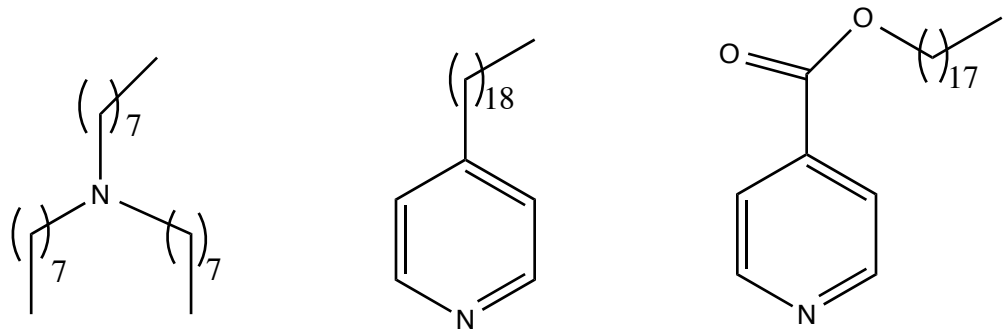

a b c

Figure 1. Molecular structures of ligands. (a) trioctylamine; (b) hydrogen ionophore **2**; (c) hydrogen ionophore **4**

Table 1 Potentiometric responses and selectivities for CN^- over TPB^-

Modifier	Slope (mV/decade)	Selectivity (log K_{CN^-, TPB^-})
(control w/o modifier)	-57.79 ±0.69	8.65 ±0.03
Trioctylamine	-57.72 ±0.17	8.10 ±0.09 *
Hydrogen ionophore 2	-51.53 ±0.34	10.22 ±0.04
Hydrogen ionophore 4	-55.95 ±0.16	9.35 ±0.07

* Background solution: 1 mM NaOH

The potentiometric response and selectivities for CN^- over TPB^- are shown in Table 1. By adding Hydrogen 2 and Hydrogen 4 as modifiers to the ISE membranes, the potentiometric response slope of the ISEs decreased and the CN^- selectivities relative to TPB^- also decreased. These results rendered Hydrogen ionophore 2 and Hydrogen ionophore 4 not suitable for further study. On the other hand, adding trioctylamine to the ISE membranes kept the Nernstian responses to CN^- and the selectivity for CN^- over TPB^- slightly increased. Therefore, trioctylamine doped ISE will be discussed in more details.

8.3.2 Cyanide Selectivity Coefficient

To limit transmembrane ion flux of CN^-, which might bias the selectivity measurement, electrodes with 1 mM KCl as inner filling solution were used in direct contact with the backside of the sensing membrane and an inner reference (AgCl-coated Ag). Table 2 shows the Nernstian response of Zn(II) meso-tetraphenylporphyrin-doped ISEs with trioctylamine as modifier for various ions except hydroxide. This ensures the accuracy of selectivity measurement by separation solution method, which requires Nernstian response for ions in calculations.

Table 2. Response slope of Zn(II) tetraphenylporphyrin-doped ISEs with trioctylamine

Ratio of modifier to ionophore	0%	100%	200%	100%
KCN *	-61.55 ± 0.41	-59.31 ± 1.71	-60.45 ± 0.17	-58.14 ± 0.70
NaTPB *	-58.54 ± 1.51	-58.39 ± 0.85	-57.10 ± 0.64	-53.27 ± 1.00
KSCN	-57.99 ± 0.37	-58.88 ± 0.50	-59.34 ± 0.47	-57.10 ± 2.26
KI	-57.02 ± 0.58	-57.35 ± 0.17	-58.16 ± 0.47	-57.93 ± 1.13
KNO_3	-55.98 ± 0.25	-56.78 ± 0.92	-56.08 ± 0.21	-57.24 ± 0.67
KBr	-54.90 ± 0.12	-56.24 ± 0.60	-55.67 ± 0.14	-56.67 ± 0.51
$NaNO_2$	-55.60 ± 0.16	-56.42 ± 0.33	-55.98 ± 0.18	-56.66 ± 0.31
NaOH	-52.74 ± 3.65	-47.64 ± 5.66	-58.43 ± 1.07	-45.95 ± 0.24
KCl	-50.45 ± 0.29	-52.32 ± 2.42	-49.29 ± 0.13	-53.07 ± 0.46

* Background solution; 1mM NaOH

The selectivities for anions, with respect to tetraphenylborate (TPB^-), were evaluated. Since TPB^- has no binding ability with Zn(II) meso-tetraphenylporphyrin, the binding effect on selectivity can be directly observed when selectivity coefficients are computed with respect to TPB^-. Table 3 shows the logarithm of the selectivity coefficient for different anions with respect to TPB^-. The higher this value is, the more selective the membrane is for TPB^- (notice that these values are negative). The logarithm selectivity coefficient for CN^- over TPB^- increases by 1.34 orders of magnitude with 1000% doped trioctylamine, which means an enhanced response to CN^- with respect to TPB^-. The same trend also applies to other anions. With TPB^- as the primary ion, the logarithm of the selectivity coefficient increases by 1.41 for SCN^-, 1.73 for I^-, 1.72 for NO_3^-, 1.70 for Br^-,

1.59 for NO_2^-, 0.58 for OH^-, 1.61 for Cl^-. Except for OH^-, the selectivity coefficient for all anions increases by over one order of magnitude. The value for OH^- is probably not reliable since the membrane doped with trioctylamine has no Nernstian slope for OH^-. This is consistent with what was observed from ref,[206] which stated that the pyridine ligand increased the stability of the complex of Zn(II) meso-tetraphenylporphyrin and nitrate.

However, the increase in binding ability does not improve the selectivity of CN^- over other interfering anions; it even deteriorates the selectivity slightly, which is shown in Table 4. With CN^- as the primary ion, the logarithm of the selectivity coefficient increases by 0.9 for SCN^-, 0.39 for I^-, 0.38 for NO_3^-, 0.35 for Br^-, 0.24 for NO_2^-, 0.27 for Cl^-. The lower the selectivity value is in Table 4, the more selective the ISE is for CN^-. This is probably due to the fact that the modifier increases the binding constant for all anions to the same extent, which cancels out the enhancing effects.

Table 3. Selectivity coefficients of Zn(II) tetraphenylporphyrin-doped ISEs with trioctylamine with tetraphenylborate (TPB^-) as primary ion

Ratio of modifier to ionophore	0%	100%	200%	1000%
KCN *	-8.54 ± 0.10	-8.12 ± 0.10	-7.83 ± 0.06	-7.20 ± 0.04
KSCN	-8.31 ± 0.10	-7.77 ± 0.19	-7.51 ± 0.04	-6.88 ± 0.07
KI	-9.23 ± 0.08	-8.63 ± 0.18	-8.30 ± 0.04	-7.50 ± 0.06
KNO_3	-10.54 ± 0.09	-9.94 ± 0.20	-9.66 ± 0.03	-8.82 ± 0.09
KBr	-11.36 ± 0.09	-10.76 ± 0.17	-10.47 ± 0.04	-9.66 ± 0.10
$NaNO_2$	-11.62 ± 0.09	-11.08 ± 0.17	-10.80 ± 0.04	-10.03 ± 0.11
NaOH	-12.55 ± 0.11	-12.23 ± 0.29	-11.10 ± 0.15	-11.97 ± 0.10
KCl	-12.74 ± 0.09	-12.18 ± 0.21	-12.00 ± 0.04	-11.13± 0.12

* Background solution: 1mM NaOH

Table 4. Selectivity coefficients of Zn(II) tetraphenylporphyrin-doped ISEs with trioctylamine with CN^- as primary ion

Ratio of modifier to ionophore	0%	100%	200%	1000%
NaTPB *	8.54 ± 0.10	8.12 ± 0.10	7.83 ± 0.06	7.20 ± 0.04
KSCN	0.23 ± 0.01	0.34 ± 0.17	0.32 ± 0.07	0.32 ± 0.07
KI	-0.69 ± 0.03	-0.52 ± 0.15	-0.52 ± 0.15	-0.30 ± 0.03
KNO_3	-2.00 ± 0.02	-1.83 ± 0.18	-1.83 ± 0.18	-1.62 ± 0.06
KBr	-2.82 ± 0.03	-2.65 ± 0.14	-2.65 ± 0.14	-2.47 ± 0.07
$NaNO_2$	-3.08 ± 0.02	-2.96 ± 0.13	-2.97 ± 0.02	-2.84 ± 0.08
NaOH	-4.01 ± 0.16	-4.11 ± 0.22	-4.11 ± 0.22	-4.78 ± 0.07
KCl	-4.20 ± 0.03	-4.06 ± 0.20	-4.06 ± 0.20	-3.93 ± 0.09

* Background solution: 1mM NaOH

8.3.3 UV-Vis Spectroscopy

The ternary system of trioctylamine, CN^- and Zn(II) meso-tetraphenylporphyrin was also observed by UV-Vis spectroscopy. Figure 2 shows the absorbance spectrum between 500 nm and 700 nm of 1 mM Zn(II) meso-tetraphenylporphyrin with addition of trioctylamine in a mixed solvent ((heptane: nitrobenzene=65:35 v/v) that resembles the plasticizer (o-NPOE) used in an ion-selective membrane. Principle component analysis (PCA) (69.6%, 25.5%, 4.9%) indicates there are three species in the system with two species explaining 95.1% of variability of the spectrum. The two major species appear to be Zn(II) meso-tetraphenylporphyrin and the complex of Zn(II) meso-

tetraphenylporphyrin and trioctylamine and the third one might be a weak binding between the complex and another trioctylamine molecule. Figure 2 shows the absorbance spectrum between 500 nm and 700 nm of 1 mM Zn(II) meso-tetraphenylporphyrin, 1 mM KCN and 1 mM 4,7,13,16,21,24-hexaoxa-1,10-diazabicyclo[8.8.8]hexacosane (to dissolve KCN) in a mixed solvent with addition of trioctylamine. PCA analysis reveals that there are at least 4 components in this system (60.2%, 48.6%, 8.35%, 3.05%). As can be seen in Figure 2, there are four possible complexes. Further analysis will be focused on calculating the stability of the complex between Zn(II) tetraphenylporphyrin and CN^- in the presence of trioctylamine.

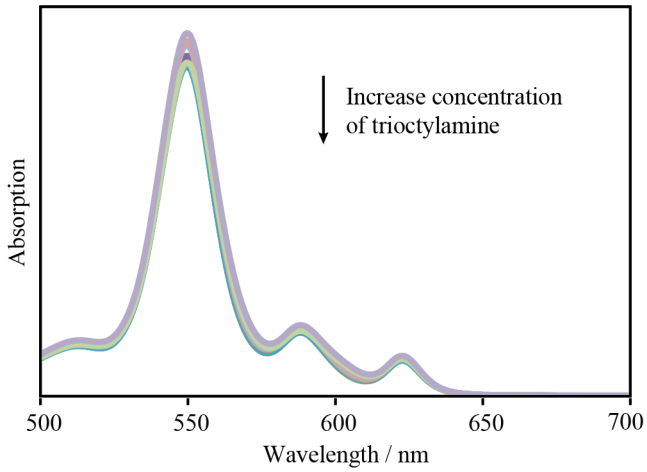

Figure 2. UV-Vis spectrum of 1 mM Zn(II) tetraphenylporphyrin in a mixed solvent (heptane: nitrobenzene=65:35 v/v) with addition of trioctylamine from 0.1 mM to 10 mM.

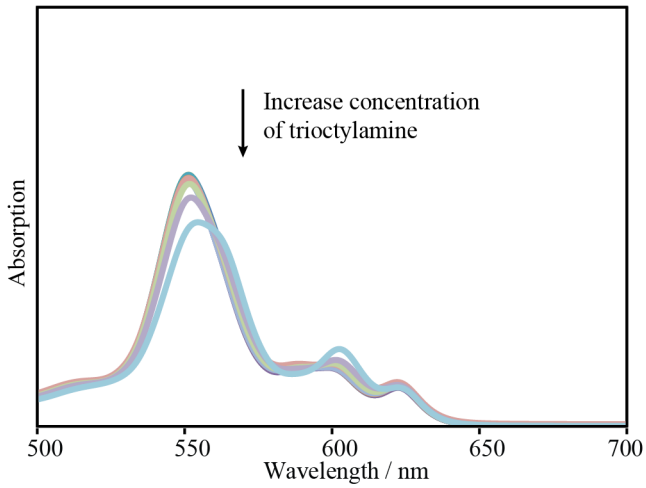

Figure 3. UV-Vis spectrum of 1 mM Zn(II) meso-tetraphenylporphyrin, 1 mM KCN and 1 mM 4,7,13,16,21,24-Hexaoxa-1,10-diazabicyclo[8.8.8]hexacosane in a mixed solvent (heptane: nitrobenzene=65:35 v/v) with addition of trioctylamine from 0.1 mM to 100 mM

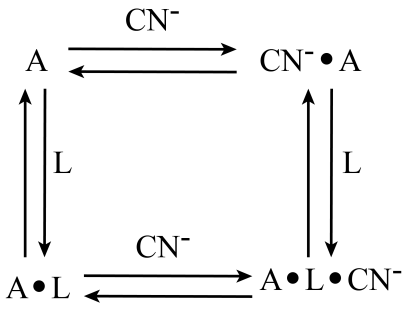

Figure 4. Equilibrium of ions in the solvent. A: Zn(II) tetraphenylporphyrin, L: trioctylamine.

8.4 Conclusions

A new method to improve the selectivity of Zn(II) meso-tetraphenylporphyrin based cyanide-selective electrode was developed by incorporating trioctylamine into ion-selective membranes. The selectivity for anions over the nonbinding TPB^- was increased by 1.5 orders of magnitude. Initial principle component analysis proved such interaction existed. This method provides an easy and flexible way to improve the selectivity of metal porphyrin based ion-selective electrodes. Future work will include calculation of the binding constant of the metal porphyrin-CN^- complex in the presence of ligands.

CHAPTER NINE

Conclusions

9.1 Summary of Results

The primary focus of this work was the development of miniaturizable solid contact electrodes including reference electrodes and ion-selective electrodes for portable, disposable or implantable purposes. The successful development of liquid junction free reference electrodes by a current pulse and their application in real samples not only addresses an industrial challenge in terms of clogging of salt bridge but also facilitates the understanding of ion transfer between two phases. The redox buffer platform based on cobalt (II / III) improves the understanding of redox characteristic of solid contact electrodes and provides high flexibility and compatibility with different systems such as calibration free ionophore based ion-selective electrodes and ionic liquid based solid contact reference electrodes.

As discussed in Chapter 2 and 3, we were able to successfully eliminate the liquid junction that greatly contributes to the shortened life and instability of signals in ISE measurement. A new method of operating reference electrodes with hydrophobic ion-doped polymeric membranes has been proposed. It involves the application of a current pulse to a hydrophobic ion-doped membrane, thereby controlling transmembrane ion fluxes to obtain a sample independent reference electrode potential. The potential of the membrane will be determined by the ions released from the membrane into the sample by the current. It is the external current that controls the constant potential. Thus, if the same current is applied to the membrane every time, a constant potential independent of the sample should be obtained. The concept has been proven with a simple

poly(vinylchloride) plasticized with nitrophenyl octyl ether doped with tetrabutylammonium tetrakis(4-chlorophenylborate). Tetrabutylammonium ions are released to the interface, which determine the potential of the membrane that is independent of the sample. The concentration of the ions released into the sample depends on the current amplitude and length and can be explained quantitatively by diffusion theory. The good stability of the potential exhibited in this study by reference electrodes exposed to serum is particularly promising in view of biological and medical applications that require long term monitoring. This operating mechanism is not limited to ion exchanger membranes and may be applied to ionophore doped membranes. This suggests a high level of flexibility in the design of reference electrodes optimized for specific applications.

As for the redox couple platform, a universal method for a solid contact electrode that is calibration-free, durable, reproducible and inexpensive to fabricate has been developed. A layer containing both cobalt(2+) and cobalt(3+) complexes in a 1:1 mole ratio serves as both a conducting layer and resistive layer to the slight changes within the membrane. Poly(vinylchloride) plasticized with nitrophenyl octyl ether and doped with cobalt(II)$(phen)_3$ and cobalt (III)$(phen)_3$ has been developed as a transducer layer. This layer has shown a very reproducible potential in potassium chloride solutions with a potential with a standard deviation of 0.5 mV and a response slope of 61mV / decade, which is consistent with the theoretical value. This platform shows high flexibility and compatibility with other systems. A liquid junction free all-solid-state reference electrode with good E^o reproducibility was developed by combining a polymeric membrane doped with ionic liquid and a Co(II)$(phen)_3$ / Co(III)$(phen)_3$ redox buffer layer. The thus

prepared solid contact ISEs demonstrate a standard deviation of the E^o values as low as 2.1 mV. The reference electrode based on carbon substrate is good for one time and short term use, and the ones based on monolayer-modified gold conductors can be used for up to 24 h as it suppresses the water layer formation. Further development of the more hydrophobic redox couples of [Co(II) (C_9,C_9-bipy)$_3$] and [Co(III) (C_9,C_9-bipy)$_3$] resulted in the successful application of this concept to K^+, Na^+, Ca^{2+}, H^+ and CO_3^{2-}-selective electrodes, all of which show highly reproducible E^o values while maintaining selectivity over interfering ions.

As for cyanide-selective electrodes, two doping methods were developed. One is doping SWCNT to protect the light sensitive ionophore Zn(II) tetraphenylporphyrin from being damaged by light and improve the life tdime of the sensor. The other one is doping with a neutral ligand, trioctylamine, to enhance the selectivity for anions of interest over nonbinding TPB^- by 1.5 orders of magnitude. This provides an easy and flexible way to improve the selectivity of metal porphyrin based ion-selective electrodes.

9.2 Future Work

For reference electrodes operated in a pulse mode, as discussed in Chapter 2 and Chapter 3, an ion exchanging membrane was taken as proof of concept. The current operating mechanism is not limited to ion exchanging membranes and may also be applied to ionophore doped membranes.[120, 122] This suggests a high level of flexibility in the design of reference electrodes optimized for specific applications. As for conventional salt bridges too, the exact composition of the reference electrode membrane may have to be optimized for samples that pose unusual challenges, such as a very high ionic strength or high concentrations of lipophilic ions. In such cases, ion exchanging membranes

loaded with ions of particularly high hydrophobicity may be used, or reference membranes may be doped with ionophores that exhibit a low selectivity for the sample ions. The good stability of the EMF exhibited by pulse operated reference electrodes exposed to serum is particularly promising in view of biological and medical applications that require long term monitoring. However, it has proven to be not trivial to just dope ionophores into the membrane suggested in Chapter 3 because of the unwanted ion transfer into the membrane. Different membrane compositions and materials will be explored to improve the capacity of membrane operated in this mode. Hydrophilic anion exchanging membranes (FAB) are under study in the Buhlmann lab now. They are loaded with a large amount of anions with a polymeric cationic backbone, which will show strong permselectivity and prevent counter ions from entering the membranes.

The redox couple platform have already been applied to K^+, Na^+, Ca^{2+}, H^+ and CO_3^{2-}-selective solid contact electrodes and ionic liquid based all-solid-state reference electrodes. However, all these electrodes only show limited life times due to the leaching of either the redox couple or the ionic liquid coupled. The goal is to retain the redox couple in the membrane. One route to alleviate this problem would be to develop more hydrophobic redox couples. One disadvantage of cobalt complexes is their high charge, especially the cobalt(3+) complexes, which are relatively hydrophilic. This points to candidates with low charges, which can be obtained by coordinating center metal with charged ligands. Another route will be to directly attach the redox couple onto polymer backbones by covalent binding. It was reported that the Huisgen cycloaddition ("click chemistry") was found to be a simple and efficient method for ferrocene attachment onto PVC. The chemical modification of the PVC backbone does not significantly affect the

ion-selective properties (selectivity, mobility, and solvent casting ability) of potentiometric sensing membranes.[154] This is promising in the application of our redox couple covalent attachment.

As for light protection for Zn(II) meso-tetraphenylporphyrin based cyanide-selective electrodes (Chapter 7), SWCNT doped membrane will be further studied to verify reproducibility. Other metal complex ionophore based ion-selective electrodes will be reevaluated and this doping method will be applied to those systems that also suffer from deteriorating performance upon exposure to light. For selectivity improvements based on neutral ligands (Chapter 8), detailed binding constant calculations will be conducted by UV-Vis spectroscopy and PCA analysis for each chosen ligand.

References

1. Bakker, E.; Bühlmann, P.; Pretsch, E., *Chem. Rev.* **1997,** *97*, 3083-3132.
2. Morf, W. E., *The principles of Ion-selective Electrode and of Membrane Transport*. Elsevier: New York, 1981.
3. Amemiya, S.; Bühlmann, P.; Pretsch, E.; Rusterholz, B.; Umezawa, Y., *Anal. Chem.* **2000,** *72*, 1618-1631.
4. Bobacka, J., *Electroanalysis* **2006,** *18*, 7-18.
5. Michalska, A., *Electroanalysis* **2012,** *24*, 1253-1265.
6. Cattrall, R. W.; Freiser, H., *Anal. Chem.* **1971,** *43*, 1905-1906.
7. Chumbimuni-Torres, K. Y.; Rubinova, N.; Radu, A.; Kubota, L. T.; Bakker, E., *Anal. Chem.* **2006,** *78*, 1318-1322.
8. De Marco, R.; Clarke, G.; Pejcic, B., *Electroanalysis* **2007,** *19*, 1987-2001.
9. Bobacka, J.; Ivaska, A.; Lewenstam, A., *Chem. Rev.* **2008,** *108*, 329-351.
10. Lindner, E.; Buck, R. P., *Anal. Chem.* **2000,** *72*, 336 A-345 A.
11. Sundfors, F.; Bereczki, R.; Bobacka, J.; Tóth, K.; Ivaska, A.; Gyurcsányi, R., *Electroanalysis* **2006,** *18*, 1372-1378.
12. Yin, T.; Qin, W., *TrAC, Trends Anal. Chem.* **2013,** *51*, 79-86.
13. Nikolskii, B. P., *Ion-Selective Electrode Rev.* **1985,** *7*.
14. Cattrall, R. W.; Drew, D. M.; Hamilton, I. C., *Anal. Chim. Acta* **1975,** *76*, 269-277.
15. Cha, G. S.; Liu, D.; Meyerhoff, M. E.; Cantor, H. C.; Midgley, A. R.; Goldberg, H. D.; Brown, R. B., *Anal. Chem.* **1991,** *63*, 1666-1672.
16. Fibbioli, M.; Morf, W. E.; Badertscher, M.; de Rooij, N. F.; Pretsch, E., *Electroanalysis* **2000,** *12*, 1286-1292.
17. James, H. J.; Carmack, G.; Freiser, H., *Anal. Chem.* **1972,** *44*, 856-857.
18. Liu, D.; Meruva, R. K.; Brown, R. B.; Meyerhoff, M. E., *Anal. Chim. Acta* **1996,** *321*, 173-183.
19. Lutze, O.; Meruva, R. K.; Frielich, A.; Ramamurthy, N.; Brown, R. B.; Hower, R.; Meyerhoff, M. E., *Fresenius. J. Anal. Chem.* **1999,** *364*, 41-47.
20. Zielińska, R.; Mulik, E.; Michalska, A.; Achmatowicz, S.; Maj-Żurawska, M., *Anal. Chim. Acta* **2002,** *451*, 243-249.
21. Michalska, A.; Dumańska, J.; Maksymiuk, K., *Anal. Chem.* **2003,** *75*, 4964-4974.
22. Gyurcsányi, R. E.; Rangisetty, N.; Clifton, S.; Pendley, B. D.; Lindner, E., *Talanta* **2004,** *63*, 89-99.
23. Pandey, P. C.; Singh, G.; Srivastava, P. K., *Electroanalysis* **2002,** *14*, 427-432.
24. Han, W.-S.; Yoo, S.-J.; Kim, S.-H.; Hong, T.-K.; Chung, K.-C., *Anal. Sci.* **2003,** *19*, 357-360.
25. Konopka, A.; Sokalski, T.; Michalska, A.; Lewenstam, A.; Maj-Zurawska, M., *Anal. Chem.* **2004,** *76*, 6410-6418.

26. Michalska, A.; Maksymiuk, K., *J. Electroanal. Chem.* **2005,** *576*, 339-352.
27. Michalska, A. J.; Appaih-Kusi, C.; Heng, L. Y.; Walkiewicz, S.; Hall, E. A. H., *Anal. Chem.* **2004,** *76*, 2031-2039.
28. Kaden, H.; Jahn, H.; Berthold, M., *Solid State Ionics* **2004,** *169*, 129-133.
29. Vonau, W.; Gabel, J.; Jahn, H., *Electrochim. Acta* **2005,** *50*, 4981-4987.
30. Kim, I. T.; Lee, S. W.; Elsenbaumer, R. L., *Synth. Met.* **2004,** *141*, 301-306.
31. Song, F.; Ha, J.; Park, B.; Kwak, T. H.; Kim, I. T.; Nam, H.; Cha, G. S., *Talanta* **2002,** *57*, 263-270.
32. Cadogan, A.; Gao, Z.; Lewenstam, A.; Ivaska, A.; Diamond, D., *Anal. Chem.* **1992,** *64*, 2496-2501.
33. Bobacka, J.; Alaviuhkola, T.; Hietapelto, V.; Koskinen, H.; Lewenstam, A.; Lämsä, M.; Pursiainen, J.; Ivaska, A., *Talanta* **2002,** *58*, 341-349.
34. Alaviuhkola, T.; Bobacka, J.; Nissinen, M.; Rissanen, K.; Ivaska, A.; Pursiainen, J., *Chemistry - A European Journal* **2005,** *11*, 2071-2080.
35. Bobacka, J.; Lahtinen, T.; Koskinen, H.; Rissanen, K.; Lewenstam, A.; Ivaska, A., *Electroanalysis* **2002,** *14*, 1353-1357.
36. Bobacka, J.; Väänänen, V.; Lewenstam, A.; Ivaska, A., *Talanta* **2004,** *63*, 135-138.
37. Vázquez, M.; Bobacka, J.; Ivaska, A.; Lewenstam, A., *Sens. Actuators, B* **2002,** *82*, 7-13.
38. Vázquez, M.; Bobacka, J.; Ivaska, A.; Lewenstam, A., *Talanta* **2004,** *62*, 57-63.
39. Vázquez, M.; Danielsson, P.; Bobacka, J.; Lewenstam, A.; Ivaska, A., *Sens. Actuators, B* **2004,** *97*, 182-189.
40. Michalska, A.; Maksymiuk, K., *Anal. Chim. Acta* **2004,** *523*, 97-105.
41. Michalska, A.; Ocypa, M.; Maksymiuk, K., *Electroanalysis* **2005,** *17*, 327-333.
42. Michalska, A.; Konopka, A.; Maj-Zurawska, M., *Anal. Chem.* **2003,** *75*, 141-144.
43. Paciorek, R.; van der Wal, P. D.; de Rooij, N. F.; Maj-Żurawska, M., *Electroanalysis* **2003,** *15*, 1314-1318.
44. Sutter, J.; Radu, A.; Peper, S.; Bakker, E.; Pretsch, E., *Anal. Chim. Acta* **2004,** *523*, 53-59.
45. Bobacka, J., *Anal. Chem.* **1999,** *71*, 4932-4937.
46. Han, W.-S.; Chung, K.-C.; Kim, M.-H.; Ko, H.-B.; Lee, Y.-H.; Hong, T.-K., *Anal. Sci.* **2004,** *20*, 1419-1422.
47. Lindfors, T.; Ivaska, A., *Anal. Chem.* **2004,** *76*, 4387-4394.
48. Kuznetsova, M. V.; Ryasenskii, S. S.; Gorelov, I. P., *Pharm. Chem. J.* **2003,** *37*, 599-601.
49. Gorelov, I. P.; Ryasenskii, S. S.; Kartamyshev, S. V.; Fedorova, M. V., *J. Anal. Chem.* **2005,** *60*, 65-69.
50. Lindfors, T.; Ervelä, S.; Ivaska, A., *J. Electroanal. Chem.* **2003,** *560*, 69-78.
51. Grekovich, A. L.; Markuzina, N. N.; Mikhelson, K. N.; Bochenska, M.; Lewenstam, A., *Electroanalysis* **2002,** *14*, 551-555.
52. Shafiee-Dastjerdi, L.; Alizadeh, N., *Anal. Chim. Acta* **2004,** *505*, 195-200.
53. Zachara, J. E.; Toczyłowska, R.; Pokrop, R.; Zagórska, M.; Dybko, A.; Wróblewski, W., *Sens. Actuators, B* **2004,** *101*, 207-212.
54. Toczyłowska, R.; Pokrop, R.; Dybko, A.; Wróblewski, W., *Anal. Chim. Acta* **2005,** *540*, 167-172.

55. Crespo, G. A.; Macho, S.; Rius, F. X., *Anal. Chem.* **2008,** *80*, 1316-1322.
56. Crespo, G. A.; Macho, S.; Bobacka, J.; Rius, F. X., *Anal. Chem.* **2009,** *81*, 676-681.
57. Hernandez, R.; Riu, J.; Rius, F. X., *Analyst* **2010,** *135*, 1979-1985.
58. Lai, C.-Z.; Fierke, M. A.; Stein, A.; Bühlmann, P., *Anal. Chem.* **2007,** *79*, 4621-4626.
59. Lai, C.-Z.; Joyer, M. M.; Fierke, M. A.; Petkovich, N. D.; Stein, A.; Bühlmann, P., *J. Solid State Electrochem.* **2009,** *13*, 123-128.
60. Fouskaki, M.; Chaniotakis, N., *Analyst* **2008,** *133*, 1072-1075.
61. Li, F.; Ye, J.; Zhou, M.; Gan, S.; Zhang, Q.; Han, D.; Niu, L., *Analyst* **2012,** *137*, 618-623.
62. Ping, J.; Wang, Y.; Wu, J.; Ying, Y., *Electrochem. Commun.* **2013,** *13*, 1529-1532.
63. Jaworska, E.; Kisiel, A.; Maksymiuk, K.; Michalska, A., *Anal. Chem.* **2010,** *83*, 438-445.
64. Jaworska, E.; Wójcik, M.; Kisiel, A.; Mieczkowski, J.; Michalska, A., *Talanta* **2011,** *85*, 1986-1989.
65. Sevilla Iii, F.; Kullick, T.; Scheper, T., *Biosens. Bioelectron.* **1994,** *9*, 275-281.
66. Waleed Shinwari, M.; Jamal Deen, M.; Landheer, D., *Microelectron. Reliab.* **2007,** *47*, 2025-2057.
67. Benjamin, H.; Bhansali, S.; Hoath, S. B.; Pickens, W. L.; Smallwood, R., *Sens. Actuators, B* **2005,** *111-112*, 430-435.
68. Duan; Yvonne, Y.; Millard; Rodney, E.; Tykocinski; Michael; Xuguang, L. U. I.; Clark; Graeme, M.; Cowan; Robert, *Potential applications of a small and high surface area Platinum electrode as an implanted impedance bio-sensor or recording electrode*. Society of Photo-Optical Instrumentation Engineers: Bellingham, WA, ETATS-UNIS, 2001; Vol. 4235, p 8.
69. Shinwari, M. W.; Zhitomirsky, D.; Deen, I. A.; Selvaganapathy, P. R.; Deen, M. J.; Landheer, D., *Sensors* **2010,** *10*, 1679-1715.
70. Dorta-Rodríguez, R.; Barrera-Niebla, M.; González, S.; Hernández-Luis, F., *J. Electroanal. Chem.* **1997,** *436*, 173-188.
71. Elzanowska, H.; Birss, V. I., *J. Appl. Electrochem.* **1993,** *23*, 646-654.
72. Bard, A. J.; Faulkner, L. R., *Eletrochemical Methods: Fundamentals and Applications*. 2nd ed.; John Wiley & Sons, Inc: Hoboken, NJ, 2001.
73. Yu, P.; Dong, S., *Anal. Chim. Acta* **1996,** *330*, 167-174.
74. Guth, U.; Gerlach, F.; Decker, M.; Oelbner, W.; Vonau, W., *J. Solid State Electrochem.* **2009,** *13*, 27-39.
75. Tymecki, Ł.; Zwierkowska, E.; Koncki, R., *Anal. Chim. Acta* **2004,** *526*, 3-11.
76. Gabel, J.; Vonau, W.; Guth, U., *Ionics* **2003,** *9*, 176-181.
77. Gabel, J.; Vonau, W.; Shuk, P.; Guth, U., *Solid State Ionics* **2004,** *169*, 75-80.
78. Vonaua, W.; Oelbnera, W.; Gutha, U.; Henzeb, J., *Sens. Actuators, B* **2010,** *144*, 6.
79. Chen, C. C.; Chou, J. C., *Jpn. J. Appl. Phys.* **2009,** *48*, 111501-111506.
80. Yee, S.; Jin, H.; Lam, L. K. C., *Sens. Actuators* **1988,** *15*, 337-345.
81. van den Berg, A.; Grisel, A.; van den Vlekkert, H. H.; de Rooij, N. F., *Sens. Actuators, B* **1990,** *1*, 425-432.

82. Maminska, R.; Dybko, A.; Wróblewski, W., *Sens. Actuators, B* **2006,** *115*, 552-557.
83. Hashimoto, M.; Upadhyay, S.; Kojima, S.; Suzuki, H.; Hayashi, K.; Sunagawa, K., *J. Electrochem. Soc.* **2006,** *153*, H155-H160.
84. Simonis, A.; Dawgul, M.; Lüth, H.; Schöning, M. J., *Electrochim. Acta* **2005,** *51*, 930-937.
85. Nagy, K.; Eine, K.; Syverud, K.; Aune, O., *J. Electrochem. Soc.* **1997,** *144*, L1-L2.
86. Collins, S. D., *Sens. Actuators, B* **1993,** *10*, 169-178.
87. Huang, I. Y.; Huang, R.-S., *Thin Solid Films* **2002,** *406*, 255-261.
88. Liao, W.-Y.; Chou, T.-C., *Anal. Chem.* **2006,** *78*, 4219-4223.
89. Czaban, J. D.; Rechnitz, G. A., *Anal. Chem.* **1976,** *48*, 277-281.
90. Jin, X.; Lu, J.; Liu, P.; Tong, H., *J. Electroanal. Chem.* **2003,** *542*, 85-96.
91. Rius-Ruiz, F. X.; Kisiel, A.; Michalska, A.; Maksymiuk, K.; Riu, J.; Rius, F. X., *Anal. Bioanal. Chem.* **2011,** *399*, 3613-3622.
92. Rius-Ruiz, F. X.; Crespo, G. A.; Bejarano-Nosas, D.; Blondeau, P.; Riu, J.; Rius, F. X., *Anal. Chem.* **2011,** *83*, 8810-8815.
93. Kisiel, A.; Michalska, A.; Maksymiuk, K.; Hall, E. A. H., *Electroanalysis* **2008,** *20*, 318-323.
94. Kisiel, A.; Mazur, M.; Kuśnieruk, S.; Kijewska, K.; Krysiński, P.; Michalska, A., *Electrochem. Commun.* **2010,** *12*, 1568-1571.
95. Kijewska, K.; Blanchard, G. J.; Szlachetko , J.; Stolarski, J.; Kisiel, A.; Michalska, A.; Maksymiuk, K.; Pisarek, M.; Majewski, P.; Krysiński, P.; Mazur, M., *Chem. Eur. J.* **2012,** *18*, 310-320.
96. Kisiel, A.; Kijewska, K.; Mazur, M.; Maksymiuk, K.; Michalska, A., *Electroanalysis* **2012,** *24*, 165-172.
97. Payne, R. B.; Buckley, B. M.; Rawson, K. M., *Ann. Clin. Biochem* **1991,** *28*, 68-72.
98. D'Orazio, P., *Ann. Clin. Biochem* **1991,** *28*, 628-629.
99. Pedrotti, J. J.; Angnes, L.; Gutz, I. G. R., *Electroanalysis* **1996,** *8*, 673-675.
100. Lee, H. J.; Hong, U. S.; Lee, D. K.; Shin, J. H.; Nam, H.; Cha, G. S., *Anal. Chem.* **1998,** *70*, 3377-3383.
101. Bakker, E., *Electroanalysis* **1999,** *11*, 788-792.
102. Mi, Y.; Mathison, S.; Bakker, E., *Electrochem. Solid-State Lett.* **1999,** *2*, 198-200.
103. Yoshimatsu, T.; Kakuichi, T., *Anal. Sci.* **2007,** *23*, 1049-1052.
104. Shibata, M.; Yamanuki, M.; Iwamoto, Y.; Nomura, S.; Kakuichi, T., *Anal. Sci.* **2010,** *26*, 1203-1206.
105. Zhang, T.; Lai, C.-Z.; Fierke, M. A.; Stein, A.; Bühlmann, P., *Anal. Chem.* **2012,** *84*, 7771-7778.
106. Shibata, M.; Sakaida, H.; Kakiuchi, T., *Anal. Chem.* **2011,** *83*, 164-168.
107. Kakuichi, T.; Yoshimatsu, T.; Nishi, N., *Anal. Chem.* **2007,** *79*, 7187-7191.
108. Mattinen, U.; Bobacka, J.; Lewenstam, A., *Electroanalysis* **2009,** *21*, 1955-1960.
109. Kisiel, A.; Michalska, A.; Maksymiuk, K., *Bioelectrochemistry* **2007,** *71*, 75-80.
110. Galster, H., pH Measurement: Fnadamentals, Methods, Applications, Instrumentation. Wiley-VCH: New York, 1991; p 33.

111. Hung, L. Q., *J. Electroanal. Chem. Interfacial Electrochem.* **1980,** *115*, 159-174.
112. Fogh-Andersen N.; Christiansen T. F. ; Komarmy L.; O., S.-A., *Clin. Chem.* **1978,** *24*, 1545-1552.
113. U., O.; D., A.; W., S., *Clin. Chem.* **1986,** *32*, 1448-1459.
114. Rumpf, G.; Spichiger-Keller, U.; Bühler, H.; Simon, W., *Anal. Sci.* **1992,** *8*, 553-559.
115. Bhakthavatsalam, V.; Shvarev, A.; Bakker, E., *Analyst* **2006,** *131*, 895-900.
116. Fibbioli, M.; Bandyopadhyay, K.; Liu, S.-G.; Echegoyen, L.; Enger, O.; Diederich, F.; Bühlmann, P.; Pretsch, E., *Chem. Commun.* **2000,** *0*, 339-340.
117. Zhou, M.; Gan, S.; Cai, B.; Li, F.; Ma, W.; Han, D.; Niu, L., *Anal. Chem.* **2012,** *84*, 3480-3483.
118. Vanamo, U.; Bobacka, J., *Electrochim. Acta* **2013,** *122*, 316-321.
119. Bjerum, N., *Z. Physik. Chem.* **1905,** *53*, 428-440.
120. Bühlmann, P.; Chen, L. D., Ion-Selective Electrodes With Ionophore-Doped Sensing Membranes. In *Supramolecular Chemistry: From Molecules to Nanomaterials*, Gale, P. A.; Steed, J. W., Eds. John Wiley & Sons, Ltd.: Hoboken, NJ, 2012; Vol. 5.
121. Bakker, E.; Pretsch, E., Advances in Potentiometry. In *Electroanalytical Chemistry: A Series of Advances*, Bard, A. J.; Zoski, C. G., Eds. CRC Press, Taylor & Francis Group: Boca Raton, FL, 2012; Vol. 24.
122. Bühlmann, P.; Pretsch, E.; Bakker, E., *Chem. Rev.* **1998,** *98*, 1593-1688.
123. Dohner, R. E.; Wegmann, D.; Morf, W. E.; Simon, W., *Anal. Chem.* **1986,** *58*, 2585-2589.
124. Lindner, E.; Gyurcsányi, R. E.; Buck, R. P., *Electroanalysis* **1999,** *11*, 695-702.
125. Bakker, E.; Pretsch, E., *Anal. Chem.* **2002,** *74*, 420 A-426 A.
126. Morf, W. E.; Badertscher, M.; Zwickl, T.; de Rooij, N. F.; Pretsch, E., *J. Electroanal. Chem.* **2002,** *526*, 19-28.
127. Shvarev, A.; Bakker, E., *Anal. Chem.* **2003,** *75*, 4541-4550.
128. Gemene, K. L.; Meyerhoff, M. E., *Anal. Chem.* **2010,** *82*, 1612-1615.
129. Kim, Y.; Rodgers, P. J.; Ishimatsu, R.; Amemiya, S., *Anal. Chem.* **2009,** *81*, 7262-7270.
130. Kim, Y.; Amemiya, S., *Anal. Chem.* **2008,** *80*, 6056-6065.
131. Ding, J.; Qin, W., *J. Am. Chem. Soc.* **2009,** *131*, 14640-14641.
132. Henderson, L. J., *J. Biol. Chem.* **1921,** *46*, 411-419.
133. Meier, P. C., *Anal. Chim. Acta* **1982,** *136*, 363-368.
134. Sokalski, T.; Ceresa, A.; Zwickl, T.; Pretsch, E., *J. Am. Chem. Soc.* **1997,** *119*, 11347-11348.
135. Samec, Z.; Trojánek, A.; Langmaier, J.; Samcová, E., *J. Electroanal. Chem.* **2000,** *481*, 1-6.
136. Samec, Z.; Trojánek, A.; Langmaier, J.; Samcová, E., *Electrochem. Commun.* **2003,** *5*, 867-870.
137. Florido, A.; Daunert, S.; Bachas, L. G., *Electroanalysis* **1991,** *3*, 177-182.
138. Gemene, K. L.; Meyerhoff, M. E., *Electroanalysis* **2012,** *24*, 643-648.
139. Shvarev, A.; Bakker, E., *Talanta* **2004,** *63*, 195-200.
140. Makarychev-Mikhailov, S.; Shvarev, A.; Bakker, E., *J. Am. Chem. Soc.* **2004,** *126*, 10548-10549.
141. Zou, X. U.; Bühlmann, P., *Anal. Chem.* **2013,** *85*, 3817-3821.

142. Armstrong, R. D.; Lockhart, J. C.; Todd, M., *Electrochim. Acta* **1986,** *31*, 591-594.
143. Ishimatsu, R.; Izadyar, A.; Kabagambe, B.; Kim, Y.; Kim, J.; Amemiya, S., *J. Am. Chem. Soc.* **2011,** *133*, 16300-16308.
144. Taky, M.; Pourcelly, G.; Lebon, F.; Gavach, C., *J. Electroanal. Chem.* **1992,** *336*, 171-194.
145. Taky, M.; Pourcelly, G.; Gavach, C., *J. Electroanal. Chem.* **1992,** *336*, 195-212.
146. Bodor, S.; Zook, J.; Lindner, E.; Tóth, K.; Gyurcsányi, R., *J. Solid State Electrochem.* **2009,** *13*, 171-179.
147. Larchet, C.; Nouri, S.; Auclair, B.; Dammak, L.; Nikonenko, V., *Adv. Colloid Interface Sci.* **2008,** *139*, 45-61.
148. Johnson, R. D.; Bachas, L. G., *Anal. Bioanal. Chem.* **2003,** *376*, 328-341.
149. Lindner, E.; Gyurcsányi, R. E., *J. Solid State Electrochem.* **2009,** *13*, 51-68.
150. Sundfors, F.; Höfler, L.; Gyurcsányi, R. E.; Lindfors, T., *Electroanalysis* **2011,** *23*, 1769-1772.
151. Veder, J.-P.; De Marco, R.; Clarke, G.; Chester, R.; Nelson, A.; Prince, K.; Pretsch, E.; Bakker, E., *Anal. Chem.* **2008,** *80*, 6731-6740.
152. Buck, R. P., *Ion-Selective Electrodes in Analytical Chemistry*. Plenum: New York, 1980; p p 58.
153. de Levie, R., *J. Chem. Educ.* **1999,** *76*, 574.
154. Pawlak, M.; Grygolowicz-Pawlak, E.; Bakker, E., *Anal. Chem.* **2010,** *82*, 6887-6894.
155. Sohail, M.; De Marco, R.; Alam, M. T.; Pawlak, M.; Bakker, E., *Analyst* **2013,** *138*, 4266-4269.
156. Hurvois, J. P.; Moinet, C., *J. Organomet. Chem.* **2005,** *690*, 1829-1839.
157. Meruva, R. K.; Meyerhoff, M. E., *Electroanalysis* **1995,** *7*, 1020-1026.
158. Veder, J.-P.; De Marco, R.; Patel, K.; Si, P.; Grygolowicz-Pawlak, E.; James, M.; Alam, M. T.; Sohail, M.; Lee, J.; Pretsch, E.; Bakker, E., *Anal. Chem.* **2013,** *85*, 10495-10502.
159. Maric, M.; Sohail, M.; De Marco, R., *Electrochem. Commun.* **2014,** *41*, 27-30.
160. Zou, X. U.; Cheong, J. H.; Taitt, B. J.; Bühlmann, P., *Anal. Chem.* **2013,** *85*, 9350-9355.
161. Sapp, S. A.; Elliott, C. M.; Contado, C.; Caramori, S.; Bignozzi, C. A., *J. Am. Chem. Soc.* **2002,** *124*, 11215-11222.
162. Barton, J. K.; Raphael, A. L., *J. Am. Chem. Soc.* **1984,** *106*, 2466-2468.
163. Herman, H. B.; Rechnitz, G. A., *Science* **1974,** *184*, 1074-1075.
164. Jung-Chuan Chou; Ya-Ping Huang; Chen, C.-C. Method for sodium ion selective electrode, sodium ion selective electrode therefrom and sodium ion sensing device. US7994546 B2, 2009.
165. Sokalski, T.; Ceresa, A.; Fibbioli, M.; Zwickl, T.; Bakker, E.; Pretsch, E., *Anal. Chem.* **1999,** *71*, 1210-1214.
166. Oesch, U.; Brzózka, Z.; Xu, A.; Simon, W., *Med. Biol. Eng. Comput.* **1987,** *25*, 414-419.
167. Behringer, C.; Lehmann, B.; Haug, J.-P.; Seiler, K.; Morf, W. E.; Hartman, K.; Simon, W., *Anal. Chim. Acta* **1990,** *233*, 41-47.
168. Qin, Y.; Mi, Y.; Bakker, E., *Anal. Chim. Acta* **2000,** *421*, 207-220.

169. Palade, D. M.; Ishkov, B. V.; Gannova, Y. N., *Russ. J. Coord. Chem.* **2003,** *29*, 110-114.
170. Pawlak, M.; Bakker, E., *Electroanalysis, In press* **2014**.
171. Amemiya, S., Potentiometric Ion-Selective Electrodes. In *Handbook of Electrochemistry*, Zoski, C. G., Ed. Elsevier: Oxford, UK, 2007; Vol. 7, pp 261-294.
172. Michalska, A.; Konopka, A.; Maj-Zurawska, M., *Anal. Chem.* **2002,** *75*, 141-144.
173. Lai, C.-Z.; Fierke, M. A.; Stein, A.; Bühlmann, P., *Anal. Chem.* **2007,** *79*, 4621-4626.
174. Lai, C.-Z.; Joyer, M. M.; Fierke, M. A.; Petkovich, N. D.; Stein, A.; Bühlmann, P., *J. Solid State Electrochem.* **2009,** *13*, 123-128.
175. Oesch U.; Ammann D.; W., S., *Clinical Chemistry* **1986,** *32*, 1448-1459.
176. Zou, X. U.; Cheong, J. H.; Taitt, B. J.; Bühlmann, P., *Anal. Chem.* **2013,** *85*, 9350-9355.
177. Marsden, J. O.; House, C. I., The Chemistry of Gold Extraction. In *Society of Mining Metallurgy and Exploration*, Littleton, CO, 2006.
178. Pesce, L. D., *In Kirk-Othmer Encyclopedia of Chemical Technology*. John Wiley & Sons, Inc.: 2000.
179. Vennesland, B.; Comm, E. E.; Knownles, C. J.; Westly, J.; Wissing, F., *Cyanide in biology*. Academic Press: London, 1981.
180. F.D.A., U. S. http://www.fda.gov/NewsEvents/Newsroom/PressAnnouncements/2006/ucm108807.htm?utm_campaign=Google2&utm_source=fdaSearch&utm_medium=website&utm_term=cyanide&utm_content=1 (accessed March 2014).
181. John, W. W., *Handbook of Anion Determination*. 1st ed.; Butterworth: London, UK, 1979.
182. Sumiyoshi, K.; Yagi, T.; Nakamura, H., *J. Chromatogr. A* **1995,** *690*, 77-82.
183. Sano, A.; Takezawa, M.; Takitani, S., *Biomed. Chromatogr.* **1989,** *3*, 209-212.
184. Fagan, P. A.; Haddad, P. R., *J. Chromatogr. A* **1991,** *550*, 559-571.
185. Sousa, M. d. F. B.; Godinho, O. E. S.; Aleixo, L. M., *Electroanalysis* **1995,** *7*, 1095-1097.
186. Polta, J. A.; Johnson, D. C., *Anal. Chem.* **1985,** *57*, 1373-1376.
187. Miralles, E.; Prat, D.; Compano, R.; Granados, M., *Analyst* **1997,** *122*, 553-558.
188. Chen, L. D.; Zou, X. U.; Bühlmann, P., *Anal. Chem.* **2012,** *84*, 9192-9198.
189. Dinten, O.; Spichiger, U. E.; Chaniotakis, N.; Gehrig, P.; Rusterholz, B.; Morf, W. E.; Simon, W., *Anal. Chem.* **1991,** *63*, 596-603.
190. Oesch, U.; Simon, W., *Anal. Chem.* **1980,** *52*, 692-700.
191. Tsagkatakis, I.; Peper, S.; Retter, R.; Bell, M.; Bakker, E., *Anal. Chem.* **2001,** *73*, 6083-6087.
192. Langmaier, J.; Lindner, E., *Anal. Chim. Acta* **2005,** *543*, 156-166.
193. Kearns, D. R., *Chem. Rev.* **1971,** *71*, 395-427.
194. Schweitzer, C.; Schmidt, R., *Chem. Rev.* **2003,** *103*, 1685-1758.
195. Bakker, E.; Pretsch, E.; Bühlmann, P., *Anal. Chem.* **2000,** *72*, 1127-1133.
196. Johnson, J. A.; Olmstead, M. M.; Stolzenberg, A. M.; Balch, A. L., *Inorg. Chem.* **2001,** *40*, 5585-5595.
197. Gegiou, D.; Huber, J. R.; Weiss, K., *J. Am. Chem. Soc.* **1970,** *92*, 5058-5062.
198. Rosenthal, I.; Bercovici, T.; Frimer, A., *J. Heterocycl. Chem.* **1977,** *14*, 355-357.

199. Lin, T. S.; Retsky, J., *J. Phys. Chem.* **1986,** *90*, 2687-2689.
200. Erno Pretsch; Martin Badertscher; Martin Welti; Takuya Maruizumilf; Werner E. Morf; Simon, W., *Pure & Appl. Chem.* **1988,** *60*, 567-574.
201. Mitchell-Koch, J. T.; Pietrzak, M.; Malinowska, E.; Meyerhoff, M. E., *Electroanalysis* **2006,** *18*, 551-557.
202. Daunert, S.; Wallace, S.; Florido, A.; Bachas, L. G., *Anal. Chem.* **1991,** *63*, 1676-1679.
203. Hattori, H.; Komiya, S.; Yuchi, A., *Proceedings of IUPAC International Congress on Analytical Sciences 2001 (ICAS 2001)* **2001**, i1353-i1356.
204. Santos, E. M. G.; Araújo, A. N.; Couto, C. M. C. M.; Montenegro, M. C. B. S. M., *J. Pharm. Biomed. Anal.* **2006,** *42*, 535-542.
205. Bakker, E.; Malinowska, E.; Schiller, R. D.; Meyerhoff, M. E., *Talanta* **1994,** *41*, 881-890.
206. Whittington, C. L.; Maza, W. A.; Woodcock, H. L.; Larsen, R. W., *Inorg. Chem.* **2012,** *51*, 4756-4762.
207. Bühlmann, P.; Umezawa, Y., *Electroanalysis* **1999,** *11*, 687-693.